COPY NO. 230

NATIONAL ADVISORY COMMITTEE FOR AERONAUTICS

Vol. 2

NACA CONFERENCE ON AIRCRAFT PROPULSION SYSTEMS

Lewis Flight Propulsion Laboratory
Cleveland, Ohio

December 8, 1955

NACA

[redacted]

[redacted]

3982

NACA CONFERENCE
ON
AIRCRAFT PROPULSION SYSTEMS

Lewis Flight Propulsion Laboratory
Cleveland, Ohio

December 8, 1955

[redacted]

[redacted]

[redacted]

~~SECRET~~

NACA CONFERENCE ON AIRCRAFT PROPULSION SYSTEMS

December 8, 1955

ADVANCED CONCEPTS

Morning Technical Sessions — Bruce T. Lundin, Chairman

Afternoon Technical Sessions — Walter T. Olson, Chairman

[redacted]

INTRODUCTION

Walter T. Olson and Bruce T. Lundin

The papers on ADVANCED CONCEPTS examine the contribution that advanced engines and high-energy fuels may make toward broadening the spectrum of speed, altitude, and range of future aircraft. Of the wide variety of powerplant types that would be pertinent to the subject, only the turbojet and ram-jet systems were discussed. These four papers comprise the material presented in panel discussions on the subject. The information in the papers is closely related; each paper presents a successive phase in the development of the central theme.

The introductory paper reviews the difficulties that must be overcome to achieve flight at higher speeds and altitudes and for longer ranges. It also introduces some of the new concepts and approaches that are more fully developed in the succeeding papers.

The second paper is a study directed toward efficient turbojet engines with very high thrust for their weight at the more severe flight requirements of the future. The paper examines in detail the relations among the aerodynamic, thermodynamic, and structural considerations of turbojet engines. Advantage is taken of the heat-sink capabilities and high combustion rates of the fuel. Recent research data that support the analyses are included.

Proper evaluation of the effectiveness of an advanced turbojet engine and a high-energy fuel requires an integration of engine, fuel, fuel system, and aircraft, and a study of the resulting performance of the complete aircraft. Engine performance alone is not enough. Two further steps in the story are therefore taken in the third paper. First, because high-energy fuels have properties so dissimilar to the familiar hydrocarbons, the special problems of tankage and fuel systems are examined. This discussion is intended to provide some insight and understanding of the principles involved, rather than recommendations on specific designs of fuel-system equipment. Second, performance estimates of aircraft based on these advanced propulsion systems are presented. Several types of aircraft and flight mission were considered to provide general results and to reveal the main trends.

The fourth paper presents the application of advanced ram-jet engines and high-energy fuels to long-range missiles. Its scope somewhat parallels that of the second and third papers. First, some of the aerodynamic, structural, and propulsion considerations that establish the altitude and flight speed for the missile are reviewed. Then follows a discussion of the various components of the engine and the missile fuel system. The paper concludes with a presentation of the speed, altitude, and range capabilities of the complete missile system utilizing various high-energy fuels.

The papers presented are considered to supplement, rather than to substitute for, the reports in which the NACA customarily releases its work. Information regarding the NACA's regular reports may be obtained from the Division of Research Information, NACA, 1512 H Street N. W., Washington 25, D. C.

NATIONAL ADVISORY COMMITTEE FOR AERONAUTICS
LEWIS FLIGHT PROPULSION LABORATORY
Cleveland, Ohio

LIST OF CONFEREES

The following conferees were registered at the NACA Conference on Aircraft Propulsion Systems, December 7 and 8, 1955.

Name	Affiliation
Abbott, I. H.	NACA - Washington
Achter, M. R.	Naval Research Laboratory
Alexander, J. D.	Boeing
Alexander, W. D.	Convair
Alford, J. S.	General Electric
Alsobrook, B. R.	Rohr Aircraft
Altis, H. D.	McDonnell Aircraft
Anderson, Maj. P. B.	WADC - WPAFB, Ohio
Anderson, R. J.	Thompson Products
Ashby, J. W. (1)	Surface Combustion
Ascher, Pvt. W.	Redstone Arsenal
Attinello, J. S.	Fairchild Engine
Avery, W. H.	Johns-Hopkins University
Bachle, C. F. (2)	Continental Aviation
Badger, W. L.	General Electric
Bailey, B. M.	Arthur D. Little, Inc.
Barfield, H. P.	WADC - WPAFB, Ohio
Barlow, Capt. J. W. B.	WADC - WPAFB, Ohio
Barnard, D. P. (2)	Standard Oil
Barnes, T. G.	Grumman Aircraft
Bartlett, J. L.	Garrett Corp.
Baxter, J. W.	Ryan Aeronautical
Beach, W. C.	North American
Beard, M. G.	American Airlines
Beck, N. J.	Douglas Aircraft
Beck, W. A.	Dow Chemical
Beckelman, B. F.	Boeing
Bell, E. B. (2)	WADC - WPAFB, Ohio
Bellman, D. R.	NACA - Edwards
Berkey, D. C.	General Electric

(1) Attended December 7th only.
(2) Attended December 8th only.

Berteling, Lt. Col. J. B.	Chief, Naval Operations
Biles, Maj. M. B.	Atomic Energy Commission
Blackburne, E. F.	Detroit Arsenal
Blatz, W. J.	McDonnell Aircraft
Bleich, L. A.	Lear, Inc.
Bliss, Comdr. L. K.	Office of Naval Research
Blom, T.	WADC - WPAFB, Ohio
Bolster, Rear Adm. C. M. (Ret.)(2)	General Tire & Rubber
Bond, F. D.	Fredric Flader
Bower, W. S.	Curtiss-Wright
Bowman, R. G.	Republic
Boyer, R. P.	Arnold Engineering
Boyum, Comdr. J. H.	Naval Air Test Center
Bradley, F. B.	North American
Bridgeforth, R. M.	Boeing
Brill, Capt. J. R.	WADC - WPAFB, Ohio
Brown, E. D. (2)	Pratt & Whitney
Brown, R. R.	Bureau of Aeronautics
Bubb, Capt. J. E.	ATIC - WPAFB, Ohio
Bucher, Lt. Col. O. B., Jr.	USAF, Washington
Burdick, D. G.	Aerojet
Calderbank, Col. J. J. B.	WADC - WPAFB, Ohio
Caldwell, F. R.	National Bureau of Standards
Campbell, G. W.	North American
Campbell, L. F.	Naval Research Laboratory
Campbell, K.	Curtiss-Wright
Carlson, P. G.	Solar Aircraft
Carr, B. B. (2)	Callery Chemical
Cesaro, R. S.	NACA - Washington
Chandler, M. E.	Chandler-Evans
Chapman, C. E.	Convair
Charlamb, A. (1)	Studebaker-Packard
Charshafian, J. O.	Curtiss-Wright
Chell, Capt. P. L.	ARDC, Baltimore
Chickering, Capt. J. B.	Maxwell Air Force Base
Clark, J. R.	Chance-Vought
Clay, Lt. J. T.	WADC - WPAFB, Ohio
Clousing, L. A.	NACA - Ames
Cochran, D. (2)	General Electric
Collins, W. (2)	Continental Aviation
Collman, J.	GMC, Centerline, Michigan
Cooley, J. L.	Calif. Research Corp.
Cooper, F. M.	General Electric

(1) Attended December 7th only.
(2) Attended December 8th only.

Crowley, J. W.	NACA - Washington
Culbertson, Col. A. T. (1)	Deputy Chief of Staff
Daley, J. A.	Naval Air Materials Center
Dallenbach, F.	AiResearch
Daniels, A. J.	Boeing
Dankhoff, W. F. (2)	General Electric
Davis, W. F.	NACA - Ames
DeCrescente, C. A.	Bureau of Aeronautics
Demeritte, F. J.	Naval Ordnance Laboratory
DenHartog, J. P. (1)	Mass. Inst. of Tech.
Dibble, C. G.	General Electric
Diehl, Capt. W. S.	Bureau of Aeronautics
Diels, M. F.	Minneapolis-Honeywell
Dietz, R. O.	ARO, Inc.
Doll, Capt. R. E.	David Taylor Model Basin
Dougherty, F. G.	Allison
Downs, W. D.	Deputy Chief of Staff
Drake, J. A.	Marquardt Aircraft
Drell, H.	Lockheed
Droegemueller, E. A.	Pratt & Whitney
Dryden, H. L.	NACA - Washington
DuBois, Maj. J. M.	ARDC - Cleveland
Duncan, Cmdr. R. L.	Naval Air Test Center
Dunnam, M. P.	WADC - WPAFB, Ohio
Eaton, R. H.	University of Michigan
Eddy, E. A. (2)	Republic
Elder, D. L.	Douglas
Emmons, P. C.	Bell Aircraft
Erwin, J. R.	NACA - Langley
Faget, M.	NACA - Langley
Fedenia, J. N.	Naval Ordnance Laboratory
Fehrman, Capt. A. L.	USAF, Inst. of Tech.
Fejer, A. J.	University of Toledo
Fisher, R. E.	Marquardt Aircraft
Fitzpatrick, J. S.	Boeing
Fletcher, J. L.	Douglas
Fliedner, C. S.	Bureau of Aeronautics
Folsom, R. G.	University of Michigan
Ford, A. R.	Naval Air Development Center
Fortune, Capt. W. C.	Office of Naval Research
Francois, G. L.	Studebaker-Packard

(1) Attended December 7th only.
(2) Attended December 8th only.

Franz, A.	Avco Mfg. Company
Frazer, A. C.	Northrop Aircraft
Freeman, W. B.	Temco Aircraft
Frick, C. W.	NACA - Ames
Furgerson, W. T.	Oak Ridge National Lab.
Gangl, A. H.	WADC - WPAFB, Ohio
Gareri, Maj. D. J.	ATIC - WPAFB, Ohio
Gebhardt, W. A.	Bendix Aviation
Geehring, Lcdr. D. R.	Bureau of Aeronautics
Gibbons, H. B.	Chance-Vought
Gibson, J. O.	Goodyear Aircraft
Gilmer, W. N.	Experiment, Inc.
Glass, M. D.	Boeing
Goddard, F. E.	Calif. Inst. of Tech.
Godfrey, P. W.	McDonnell Aircraft
Goethert, B. H.	ARO, Inc.
Grandfield, J. P.	Curtiss-Wright
Gray, W. A.	Glenn L. Martin
Greenlaw, A. L.	Glenn L. Martin
Gregory, A. T.	Fairchild Engine
Grey, J.	Princeton University
Gruber, A. R. (2)	Nuclear Dev. Assoc.
Gunther, F. C.	Calif. Inst. of Tech.
Haines, Maj. C. E.	USAF, Baltimore
Hairston, G.	USAF, Washington
Haley, Capt. T. B.	Bureau of Aeronautics
Hand, W. H. (2)	North American
Hasel, L.	NACA - Langley
Haugen, Brig. Gen. V. B. (2)	WADC - WPAFB, Ohio
Hausmann, G. F.	United Aircraft
Hayes, R. V.	Bureau of Aeronautics
Hazert, C. N.	USAF, Washington
Heaton, Col. D. H.	Deputy Chief of Staff
Heckel, Lt. J. L.	WADC - WPAFB, Ohio
Hedrick, I. G.	Grumman Aircraft Corp.
Heilig, L. F.	Northrop Aircraft
Helfrich, Capt. G. F.	Atomic Energy Commission
Hemsley, Lt. Col. R. T.	USAF, Baltimore
Hesse, W. J.	Bureau of Aeronautics
Hill, J. F.	Surface Combustion
Hoadley, H. H.	United Aircraft
Holaday, W. M.	Socony-Mobile Lab.
Holden, F. R.	Naval Air Development Center

(2) Attended December 8th only.

Holmquist, Cdr. C. O.	Naval Air Test Center
Huff, G. F. (2)	Callery Chemical
Hulbert, J. K.	Fredric Flader Co.
Hurley, W. V.	Ass't. Sec. of Air Force
Huntsberger, R. F.	NACA - Ames
Igou, D. T. (2)	Surface Combustion
Ingham, Maj. J. S.	Arnold Engineering
Isbell, E. G.	Douglas Aircraft
Jaquis, R. E.	Bureau of Aeronautics
Jenny, R. B.	Douglas Aircraft
Johns, F. R.	Naval Air Development Center
Johnson, C. L.	Lockheed
Kassner, R. F. (1)	Avco Manufacturing Co.
Keith, B. C.	WADC - WPAFB, Ohio
Keller, G. H.	Curtiss-Wright
Kelly, R. D.	United Airlines
Kelso, Maj. W. R.	Ass't. Sec. of Air Force
Kerr, J. A.	Convair
Kirkpatrick, Mrs. E.	Garrett Corp.
Klein, Lt. E. L.	AMC - WPAFB, Ohio
Klein, H.	Douglas Aircraft
Knoernschild, E. M.	Garrett Corp.
Knott, J. E.	Allison
Kotcher, E.	WADC - WPAFB, Ohio
Krug, E. H. (1)	Lear, Inc.
Kuhrt, W. A.	United Aircraft
Kunz, W. J. (1)	Bendix Aviation
Kupelian, V. S.	Naval Ordnance Lab.
Kurrle, C.	USAF - Research & Dev.
Kuzmitz, F. V. (2)	Bendix Aviation
Lankford, J. L.	Experiment, Inc.
Laucher, R. G.	Marquardt Aircraft
Lawler, J. A.	Radioplane Company
Lawton, Lt. Col. T. O.	AMC - WPAFB, Ohio
Lee, J. G.	United Aircraft
Leibold, E. P.	Lockheed
Levitt, B. B. (2)	Northrop Aircraft
Lifton, H. D.	North American
Littlewood, W.	American Airlines
Logan J. W. (2)	Cambridge Corporation
Long, J. V.	Solar Aircraft

(1) Attended December 7th only.
(2) Attended December 8th only.

Lott, M. A.	Nav. Air Turb. Test Sta.
Lucas, Maj. R. E.	ARDC - USAF, Baltimore
Lucas, V. E. (2)	Firestone Tire & Rubber
Lundquist, W. G.	Curtiss-Wright
Luther, J. M.	Convair
Lutz, R. J.	Rand Corporation
McCarthy, J. F.	Strategic Air Command
McClellan, H. J.	Boeing
McCreery, F. E.	Rohr Aircraft
McDowall, C. J.	Allison
McMurtrey, L. J.	Boeing
MacFee, F. E., Jr.	General Electric
Mackley, E. E.	NACA - Langley
Maloney, J. G.	Convair
Martin, Maj. W. W.	USAF, Baltimore
Maske, E. B.	Convair
Maskey, H. (1)	Continental Aviation
Maurer, R. J.	Bureau of Aeronautics
Mertaugh, L. J., Jr.	USAF, Kirtland AFB
Mezger, B. J.	Curtiss-Wright
Mock, F. C. (2)	Bendix Aviation
Monts, L. F.	Beech Aircraft
Moore, C. C.	Union Oil Co.
Morrison, J. A.	Boeing
Muse, T. C.	Dept. of Defense
Napier, B. A.	Lear, Inc.
Nash, J. O.	Pratt & Whitney
Nay, H. O.	Douglas Aircraft
Nelson, H. J.	Bendix Aviation
Nesbitt, W.	Borg-Warner Corporation
Neumann, G. (2)	General Electric
Newton, G. W.	ARO, Inc.
Nichols, F. A.	Bureau of Aeronautics
Nichols, L. W.	Nav. Ord. Test Sta.
Nichols, M. R.	NACA - Langley
Noeggerath, W. C.	Lockheed
Norton, W. J.	Hydrocarbon Research
O'Donnell, W. J.	Republic
O'Hare, W. S.	Douglas Aircraft

(1) Attended December 7th only.
(2) Attended December 8th only.

Olson, G. A.	North American
Ormsby, R. B.	Lockheed
Passman, R. A.	Bell Aircraft
Patella, F.	WADC - WPAFB, Ohio
Paul, C. H.	AiResearch Mfg.
Pearce, R. B.	North American
Pearch, Col. L. D.	Deputy Chief of Staff
Pedersen, G. H.	Curtiss-Wright
Petroff, A. N. (1)	Cessna Aircraft
Phillips, E. C. (2)	WADC - WPAFB, Ohio
Pierce, E. F.	Curtiss-Wright
Pinnes, R. W.	Bureau of Aeronautics
Piry, M.	Fairchild Engine
Pouchot, W. D.	Westinghouse
Powell, W. V.	North American
Pratt, P. W.	Pratt & Whitney
Rains, D. A.	Propulsion Res. Corp.
Rall, F. T.	WADC - WPAFB, Ohio
Rapp, G. C. (1)	General Electric
Rathbun, K. C.	Experiment, Inc.
Ray, G. D.	Bell Aircraft
Reagan, J. F.	Beech Aircraft
Redding, A. H.	Westinghouse
Reeder, J. P.	NACA - Langley
Reid, H. J. E.	NACA - Langley
Reinhardt, W.	Reaction Motors
Rex, Lt. Col. E. M.	USAF, Inst. of Tech.
Rhode, R. V. (2)	NACA - Washington
Rich, B. R.	Lockheed
Robbins, Lt. Col. H. W.	USAF - ARDC, Baltimore
Robertshaw, F. C. (1)	General Electric
Robinson, R. G.	NACA - Ames
Ross, R. S.	Goodyear Aircraft
Rostkowski, Capt. F. J. (1)	ARDC - Cleveland
Rothrock, A. M.	NACA - Washington
Rothrock, Col. J. H.	WADC - WPAFB, Ohio
Rummel, R. W.	Trans-World Airlines
Ryder, B. J.	Bendix Aviation
Sadler, C. E.	McDonnell Aircraft Corp.
Sanders, J. E.	Curtiss-Wright
Sanwald, G. L.	Naval Air Material Center
Sarginson, F.	Fredric Flader

(1) Attended December 7th only.
(2) Attended December 8th only.

Savage, C. A.	Convair
Scalia, M. E.	Glenn L. Martin
Schamberg, R.	Rand Corporation
Schechter, W. H. (2)	Callery Chemical
Scheller, K.	WADC - WPAFB, Ohio
Schmidt, H.	Borg-Warner
Schmidt, R. D.	Minneapolis-Honeywell
Schumacher, P. W. J.	WADC - WPAFB, Ohio
Schwartz, W.	WADC - WPAFB, Ohio
Schwoerer, F.	Westinghouse
Sells, B. E.	General Electric
Selmer, Cdr. R. J. (Alt.)	Nav. Air Test Center
Sen, W. J.	WADC - WPAFB, Ohio
Sens, W. H.	Pratt & Whitney
Shattuck, B. F. (1)	General Electric
Sheldon, Z. D. (2)	General Electric
Shippen, W. B.	Johns-Hopkins University
Silvern, D. (2)	Continental Aviation
Simmers, R.	Lockheed
Simpson, G. R.	Nav. Air Turb. Test Sta.
Slaughter, J. D. (2)	Surface Combustion
Smith, C. B. (1)	Pratt & Whitney
Smith, Capt. C. O.	WADC - WPAFB, Ohio
Smith, Capt. R.	Kirtland Air Force Base
Smith, Lt. Col. R. O.	AFDRD-AN, Washington
Smull, T. L. K.	NACA - Washington
Snyder, W. E.	GMC, Centerline
Soderberg, C. R.	Mass. Inst. of Tech.
Sorgen, C. C.	Off. of Ass't. Sec. of Def.
Spier, Lt. Col. F.	Detroit Arsenal
Standahar, R. M.	General Electric
Steen, Maj. C. H.	WADC - WPAFB, Ohio
Steffens, S. G.	WADC - WPAFB, Ohio
Stephens, Maj. W. R.	WADC - WPAFB, Ohio
Stack, J.	NACA - Langley
Stickle, G. W.	Tactical Air Command
Stranges, P. A.	Olin Mathieson Chem. Co.
Stroud, J. F.	Lockheed
Sweet, Lt. Col. F. J.	USAF - Washington
Taylor, E. B.	Douglas Aircraft
Taylor, E. S.	Mass. Inst. of Tech.
Taylor, F. C.	Radioplane Company

(1) Attended December 7th only.
(2) Attended December 8th only.

Taylor, J. E. (2)	Thompson Prod.
Tesch, Col. W. A.	ARDC - WPAFB, Ohio
Theodorsen, T.	Republic
Thomas, A. N.	Marquardt Aircraft
Thompson, F. L.	NACA - Langley
Thoren, T. R.	Thompson Prod.
Thurman, G. R. (1)	Firestone Tire & Rubber
Tilgner, C.	Grumman Aircraft
Todd, D. (1)	Continental Aviation
Torrell, B. N. (1)	Pratt & Whitney
Towle, H. C.	Republic
Townsend, S. J. C.	Chance-Vought
Trent, W. C.	Chance-Vought
Trimble, J. I. (1)	Surface Combustion
Underwood, A. F. (2)	GMC, Detroit
Underwood, W. J.	NACA-Wright-Patterson AFB
Van Thielen, P. R.	Detroit Arsenal
Van Voorhis, S. N. (2)	Lincoln Laboratories
Von Ohain, H.	WADC - WPAFB, Ohio
Vyvyan, W. W. (1)	Ryan Aero.
Walker, C. J.	General Electric
Walker, C. L.	NACA - Washington
Walker, J. H.	Johns-Hopkins University
Walter, D. L.	Marquardt Aircraft
Warner, R. S.	Cambridge Corp.
Watson, Brig. Gen. H. E. (2)	ATIC - WPAFB, Ohio
Watton, A.	WADC - WPAFB, Ohio
Weeks, L. M.	McDonnell Aircraft
Weeks, N. E.	Westinghouse
Weidhuner, D. D.	Off. of Chief of Trans.
Wendling, J. H.	ATIC - WPAFB, Ohio
Wetzler, J. M.	Allison Division
White, R. S.	CAA - Washington
Whitten, J. P.	NACA - Langley
Wilson, W. B.	Edwards Air Force Base
Wise, J. C.	Thompson Prod.
Wislicenus, G. F. (2)	Penn. State Univ.
Witbeck, N. C. (2)	Fairchild
Woods, R. J.	Bell Aircraft
Woodward, W. H.	NACA - Washington
Woodworth, L. R.	Rand Corporation

(1) Attended December 7th only.
(2) Attended December 8th only.

Worley, W. E.	Bendix Avia.
Worth, W.	WADC - WPAFB, Ohio
Wosika, L. R.	Solar Aircraft
Wright, A. M.	Pratt & Whitney
Young, G. B. W.	Rand Corporation
Zambon, L. B.	General Electric
Zarkowsky, W. M.	Grumman Aircraft
Zipkin, M. A.	Goodyear Aircraft
Zwemer, H. A.	Lockheed Aircraft

1. INTRODUCTORY CONCEPTS AND PROBLEMS

DeMarquis D. Wyatt, Chairman
Roland Breitwieser
Edmund R. Jonash
Roger W. Luidens
Arthur D. Zimmerman

1. INTRODUCTORY CONCEPTS AND PROBLEMS

INTRODUCTION

Successful flight with man-carrying airplanes powered by air-breathing engines has been achieved, or is on the verge of being achieved, in the altitude and Mach number range shown by the shaded limits in the lower left of figure 1. Future progress will be measured by the extension of these boundaries and by the concurrent improvement in flight ranges over those currently possible.

The probable directions of future flight progress are indicated in figure 1 by the arrow. In general, it may be anticipated that significant increases in flight speed will be accompanied by increasing flight altitudes, so that aerodynamic configurations having high lift-drag ratios can be maintained. The obstacles that must be overcome in developing suitable air-breathing propulsion systems for these future aircraft are examined in this paper. Although it is difficult to isolate speed, range, and altitude considerations for separate discussions, this approach is used for clarity.

The power-plant problems that will be obstacles to higher-speed flight are examined first. These problems are primarily associated with temperature effects, in one form or another. Problems associated with higher-altitude flight are then considered. In this area engine weight and combustion are the principal difficulties encountered. Finally, analysis of the aircraft range problem indicates the desirability of making marked improvements in engine weight, engine efficiency, and fuel type. Special attention is devoted to high-energy fuels.

SPEED PROBLEMS

Temperatures that may be expected to be encountered in flight on various parts of an aircraft are indicated in figure 2. The solid curve represents the stagnation temperature. The dashed curve indicates a representative skin temperature that an external surface might feel at an altitude of 70,000 feet. Because of the boundary-layer recovery factor and radiation, this temperature will be lower than the stagnation temperature by several hundred degrees at the higher flight speeds. The engine inlet, on the other hand, will have a recovery factor of essentially unity and almost no radiation, so that the engine will feel the full stagnation temperature. Structural problems, such as reductions in material strength, differential expansions, and the like, may therefore be expected to be more severe in the engine than in the airframe as flight speeds are increased.

Power-plant installations have already encountered temperature-associated problems at subsonic flight speeds that will be aggravated by higher stagnation temperatures. One of these is a fuel stability problem. Figure 3 shows the temperature as a function of time in hours at which two undesirable changes in fuel properties take place. The lower curve illustrates the tendency for excessive gum to form in JP fuels. The upper curve indicates the temperatures at which the first traces of thermal cracking (with resulting coke formation) have been observed in relatively stable pure hydrocarbons. The solids formed by either reaction tend to clog lines, filters, and injection nozzles.

Several current engines have experienced fuel-system gumming difficulties at flight speeds where the stagnation temperature is not an important factor. For example, the data point at 400° F and a time of 10 seconds corresponds to conditions in an oil-cooler heat exchanger where excessive gum formation in the fuel used as a coolant has been observed. The duration times at the right of the curve correspond to fuel-storage conditions.

As flight speeds are increased, the high stagnation temperatures shown in figure 2 will be felt in the accessory regions adjacent to the engine. In addition, the fuel tanks will, unless insulated, tend to stabilize at the skin-temperature levels indicated in figure 2. From a comparison of the flight temperatures with the critical temperatures of figure 3, it is apparent that the already troublesome fuel problems will be aggravated at higher flight speeds unless elaborate protection not only of the fuel tanks but of all the transmission lines and pumping system is provided.

The turbojet engine encounters another temperature-associated problem at moderate supersonic Mach numbers. Because the compressor inlet feels the high stagnation temperatures associated with increasing flight speed, the compressor performance can be considerably compromised. It can be shown that the aerodynamic performance characteristics of a compressor are a function of the compressor equivalent rotational speed rather than of the true mechanical speed. In conventional operation the mechanical speed N is maintained at a constant value over the supersonic flight speed range of the airplane. The corresponding variation in equivalent speed is shown in figure 4. The increasing stagnation temperatures cause the equivalent speed to reduce as flight speed is increased. Thus, at a flight Mach number of 2 the compressor equivalent speed has fallen to 80 percent of its maximum value. At a Mach number of 4.0, the equivalent speed is down to 53 percent of the maximum.

Some of the consequences of operating the compressor over this wide range can be deduced from figure 5, which is a representation of a typical compressor map. There are several undesirable operating regions that limit the useful portion of the compressor map. For example, the maximum

pressure rise that the compressor can deliver is bounded by the stall-limit line. At this condition the compressor blade rows go into complete stall. An unstable flow results that makes it impossible to operate the compressor at higher pressure ratios.

The stall-limit line is a boundary of useful compressor operation over the whole range of equivalent speeds. Another type of stall occurs at reduced equivalent speeds that further limits the useful range of the compressor. As the equivalent speed is reduced the compressor blades steadily depart from design operating conditions until, finally, some of the blades partially stall. The resultant stall zones rotate relative to the blade row and hence are called rotating stalls. The shaded region of figure 5 illustrates the typical range of compressor operating conditions in which rotating stalls are encountered.

An engine operating line is included in figure 5. This line is determined by a balance of work, mass flow, and speed between the compressor and turbine. From the selected take-off operating point the equivalent speed increases as altitude is increased into the stratosphere at subsonic speeds. At the cruise Mach number in the stratosphere the engine equivalent speed is a maximum. With further increases in flight speed, however, the increasing stagnation temperatures move the engine operating point down the operating line to lower values of compressor equivalent speed. For the particular example illustrated, the engine operating point would fall in the rotating-stall region of the compressor at Mach numbers greater than about 2.2.

Compressor operation in a rotating-stall condition is generally not permissible because of the possibilities of blade failures induced by the blade vibrations that are excited by the rotating stalls. Up to the present time rotating stalls have been encountered for the most part only during transient operation while the engine is being accelerated to rated mechanical speed. Thrust is not a major requirement during this operation; and, therefore, several compressor fixes have been stalled at the expense of thrust, to alleviate rotating-stall problems. Such fixes will not be suitable for sustained high-speed flight where full thrust is a primary requisite. Thus, rotating stall remains as a primary obstacle that must be overcome before turbojets can be used as successful power plants at speeds greatly in excess of current values. At the present time there appear to be only two possible solutions. First, compressors might be designed that are free of rotating stall in the desired operating region. Second, the engine operating schedule might be altered from the present constant-mechanical-speed type of schedule so that the operating line would not enter the rotating-stall region of the compressor.

Even if the first solution to the rotating-stall problem is possible, there would still remain other problems associated with the compressor operation at low equivalent speeds. Near the take-off operating point the

compressor efficiency is near its maximum, about 85 percent. At the low equivalent speeds corresponding to flight Mach numbers of 3 to 3.5 the efficiency of current compressors may drop as low as 60 percent on the operating line. These low compressor efficiencies would be reflected as high specific fuel consumptions.

There is still another disadvantage of operating in this lower speed region. The engine air-flow rate at the operating point is greatly reduced below the ultimate compressor capability. In the example of figure 5, for instance, the corrected air flow $w_a\sqrt{\theta}/\delta$ at Mach 3.5 is less than 40 percent of the maximum value. Since thrust has a one-to-one relation to air flow, this engine would be delivering only about 40 percent of its potential thrust.

The temperature effect on the compressor equivalent speed creates a number of problems that must be overcome before the turbojet engine can be used for substantially higher speeds than those now being attained. These higher speeds are within the capabilities of the ram-jet engine, however, inasmuch as it has no compressor and the attendant problems. In fact, the most desirable speed for the ram jet lies somewhat above that considered for the turbojet, as illustrated by the engine efficiency curves of figure 6.

As is well known, the ram-jet engine produces very little thrust and has a low cycle efficiency at subsonic and low supersonic speeds. As flight speed is increased, the efficiency increases rapidly. If the combustion temperature is increased as flight speed is increased, the engine efficiency continues to rise. As shown by figure 6, an engine efficiency of about 45 percent can be attained at flight Mach numbers near 5. This compares favorably with the best efficiencies obtained with any heat engines.

Of course, the ram-jet engine does not show an indefinitely improving performance as flight speed and cycle temperature are raised. Figure 7 shows the decreasing heat-release margin as Mach number is increased. These curves were calculated assuming stoichiometric combustion of JP-4 fuel. At low combustor-inlet temperatures, corresponding to low flight speeds, a temperature rise of about 3800° F can be achieved across the combustor. As combustor-inlet temperature is raised, the amount of temperature rise that can be obtained across the combustor decreases. This is a result of dissociation of the constituent elements in the combustion process. (Air itself begins to dissociate at temperatures above about 3500° F; hence the reflex in the combustor-inlet temperature curve.) The dissociation proceeds to the point that, at flight Mach numbers near 10, no effective total-temperature rise can be discerned in the heat-addition process.

Whether or not any thrust can be produced near Mach 10 depends upon the flow process in the exhaust nozzle. If recombination of the elements occurs as the temperature of the expanding gases decreases, some thrust could be realized even though the apparent total-temperature rise across the combustor was zero. The amount of thrust would be small in any case, however, and in general it may be concluded that hydrocarbon fuels are incapable of producing thrust much above Mach 10. Thus, a definite speed restriction may be ultimately placed upon the ram jet burning conventional fuels.

ALTITUDE PROBLEMS

In contrast to the temperature problems which must be solved to permit higher flight speeds, altitude limitations are predominantly a function of engine weight. Figure 8 shows the specific-weight variation for a typical current turbojet engine.

As flight altitude is increased, the reduction in air density causes a decrease in the air flow through the engine. The thrust is correspondingly reduced, and the specific weight (weight per lb of thrust) increases for a given engine. The specific-weight curves have the same trends but are displaced as operating conditions are changed. At a fixed Mach number, for example, turning on the afterburner increases the thrust for a given engine weight. The specific weight of the engine at that altitude is therefore reduced. The inlet ram experienced as flight speed is increased increases the weight flow and thus increases the engine thrust and reduces the engine specific weight still more.

The significance of engine specific weight on flight altitude is qualitatively illustrated by the hypothetical airplane models of figures 9 and 10. Figure 9 represents the proportions of an airplane designed to fly at a 60,000-foot altitude and a Mach number of 2.5, using two engines. (The engines are shown on the wing tips to facilitate size comparisons.) As indicated in figure 8, the engine specific weight for this altitude would be 0.5 pound per pound thrust. For the assumed lift-drag ratio of the airplane the total engine weight would therefore amount to about 18 percent of the gross weight. Normally, such a configuration would be able to carry an appreciable fuel load and would have good range.

At a design altitude of 90,000 feet the engine specific weight would be about 2.0 pounds per pound thrust. Translated into total engine weight, the engines for this high-altitude aircraft (fig. 10) would be about 55 percent of the airplane gross weight. The rest of the gross weight would be comprised of structure and pay load, so that practically no range would be possible. This latter airplane must therefore be considered to be impractical as long as engine specific weights remain near the values of those currently in operation.

Decreases in the engine specific weight for the assumed airplanes would directly reduce the installed engine weight by the same proportion. The reduced engine weight could be replaced with a corresponding fuel load and hence increase the aircraft range at a given altitude. The maximum altitude for a given range could be increased about 15,000 feet for each 50-percent reduction in engine specific weight.

The engine specific weight can be reduced through three approaches. Improvements in structural efficiency can reduce the engine structural weight for a given thrust. Improvements in the aerodynamic efficiency to increase the amount of air flow through an engine of a given weight can cause corresponding improvements in engine thrust. Finally, improvements can be made in the thermodynamic cycle to increase the amount of thrust per unit air flow.

The specific-weight problem of turbojet engines at high altitudes is further complicated by undesirable shifts in the compressor map under high-altitude operating conditions. Figure 11 shows changes that are experimentally observed in compressor efficiency and air-flow rate w_a at the operating point as the Reynolds number of the air flow entering the compressor is reduced. These Reynolds number changes occur in flight as altitude is increased and air density decreases. The values shown are based on the velocity relative to the rotor row and the chord length of the first stage. As the Reynolds number is reduced, the boundary-layer thickness increases on the blades, the drag increases, and the general airfoil efficiency of the blade falls off. Little effect is noted until the Reynolds number is reduced to between 200,000 and 400,000, depending on the compressor. Further reductions in Reynolds number, however, result in marked decreases in both compressor efficiency and air flow. The data of figure 11 show that this behavior is a general characteristic of all compressors.

The relation between Reynolds number, flight Mach number, and altitude is illustrated by figure 12. The Reynolds numbers shown on this figure are based on chord lengths of 0.2 foot and a velocity relative to the blade of Mach 0.8. These conditions are comparable to the data conditions of figure 11. The altitude at which the Reynolds number effects on the compressor become significant varies with flight Mach number. At subsonic speeds the effect would first become noticeable at about 40,000 feet. At Mach 3, on the other hand, the effects would not be apparent until an 80,000-foot altitude is reached. Compressor performance would deteriorate rapidly at higher altitudes.

Presumably, similitude will hold, so that the undesirable compressor effects of figure 11 will occur at constant Reynolds number regardless of the size of the compressor. The altitudes at which the critical Reynolds number will occur (fig. 12) will, however, depend upon the chord lengths. If, for example, chord lengths are increased twofold to 0.4 foot, the

altitude for a given Reynolds number would increase by approximately 15,000 feet. It has previously been demonstrated that increases in flight altitude will either require larger engines or more engines. As a solution to the Reynolds number problem, it is obvious that larger engines should be adopted for higher flight altitudes, since the compressor deterioration for geometrically similar engines would thereby be postponed.

Another engine problem that must be solved if flight is to be attained at higher altitudes is the combustion problem. Many current turbojet combustors operate at reduced combustion efficiencies at altitudes greater than 55,000 to 60,000 feet at subsonic flight speeds. The problem is mainly one of the low pressures and temperatures existing under those flight conditions. Increases in flight speed can, of course, be expected to relieve these difficulties at a given altitude.

Much research has been conducted on the problems of turbojet combustion. Experimental burners that are considerably better than most of the current combustors have undergone considerable evaluation. Yet even these advanced burners show deficiencies when considered in the light of future flight requirements. Efficiency contours for one such combustor specifically designed for high combustion efficiency at high altitude are shown on figure 13 as a function of altitude and flight Mach number. It is assumed that the combustor is operating with a compressor having a take-off pressure ratio of 7 and current values of air flow per unit frontal area.

The maximum altitude at which 100-percent combustion efficiency could be maintained varies from 60,000 feet at Mach 1 to 95,000 feet at Mach 3. At altitudes roughly 30,000 feet higher, the combustion efficiency would fall off about 15 percent. These values seem to be acceptably high in terms of current flight experience; however, engine specific weights must be reduced below the values of currently flying engines if these high flight altitudes are to be practical. One of the solutions will probably be to increase the air-flow weight per unit frontal area through the adoption of advanced compressor designs. The increased air-flow rates will mean higher velocities through the burner. From tests of many experimental and production burners, it has been established that increases in velocity will generally reduce combustion efficiency for a given altitude - flight-speed condition. Thus, in advanced engines it may be anticipated that combustion problems will be much more severe than indicated by figure 13.

Another method of reducing engine specific weight is through the use of an afterburner. For any given altitude-speed condition, afterburner pressures are considerably lower than those in the primary combustor. The velocities are also higher. As a consequence, afterburner combustion efficiencies are considerably lower than those in the primary combustor.

[redacted]

Efficiency contours for an advanced experimental afterburner are shown on figure 14 as a function of flight Mach number and altitude for the same engine assumed in figure 13. The levels of combustion efficiency are generally superior to those obtained with currently flying engines. Even so, the efficiency levels are well below those for the primary combustor. The peak efficiencies are only 88 percent, and these cannot be attained at altitudes higher than about 50,000 feet at Mach 1 and 80,000 feet at Mach 3. As in the case of the primary combustor, the use of high-air-flow compressors would increase the velocities through the afterburner above the levels used for these data, and greatly reduced combustion efficiencies can be anticipated.

The combustion problem can thus be summarized as satisfactory for present engine operating limits when advanced, but known, combustor design techniques are employed; the necessary engine modifications to permit higher altitudes will, however, create new combustor problems as a result of higher burner velocities.

RANGE CONSIDERATIONS

Thus far, the discussion of future power-plant problems has not directly considered aircraft range. Obviously, range will also be an important measure of future progress. As the speed-altitude spectrum is extended, present range capabilities should at least be maintained and, if possible, extended.

A sufficient preliminary evaluation of aircraft range considerations can be made from a treatment of only the cruise portion of the flight path as represented by the Breguet equation. While this approach neglects the take-off, acceleration, maneuver, and holding problems of actual aircraft flight, it does suffice to indicate the first-order influence of the quantities predominantly affecting range.

The Breguet range equation can be written in the form

$$\text{Range} = h_c \eta_e \frac{L}{D} \ln \frac{W_g}{W_g - W_f} \qquad (1)$$

where h_c is the heating value of the fuel; η_e is the engine efficiency, defined as the work output of the engine, thrust times velocity, divided by the mechanical equivalent of the input fuel energy; and L/D is the lift-drag ratio of the configuration. The Breguet equation is completed by a log term involving component weights. As written in equation (1), this term includes the gross weight of the aircraft at the start of the Breguet path W_g and the fuel weight available for cruise flight W_f.

[redacted]

Obviously, increases in the amount of fuel in a given gross weight airplane will increase the aircraft range. The amount of fuel that can be carried in the airplane can be viewed as the residual weight after provision is made for the necessary fixed weights. Thus, the range equation may also be written in the form

$$\text{Range} = h_c \eta_e \frac{L}{D} \ln \frac{1}{\frac{W_e}{W_g} + \frac{W_s}{W_g} + \frac{W_p}{W_g}} \qquad (2)$$

The log term of equation (1) has now been replaced by an equivalent term containing the sum of the engine weight W_e, the structural weight W_s, and the pay-load weight W_p, each being expressed as a fraction of the gross weight at the start of the cruise path. Flight range can be increased over a given reference value only if reductions can be made in one or more of these quantities.

The pay-load weight is fixed by military tactical considerations and will not be considered as a variable within the control of the designer. With regard to propulsion, the structural weights will be affected by the fuel-tank weights, which will vary with the properties of various fuels. This variation must be accounted for in a thorough evaluation of range capabilities using different fuels but will not be treated in this discussion.

Engine weight has previously been shown to be a critical factor in the attainment of higher flight altitudes. As indicated by equation (2), the range is also favorably influenced by any reductions in engine weight. As far as range is concerned, however, the engine weight cannot be considered independently of the engine efficiency. In fact, engine weight, engine efficiency, and airplane lift-drag ratio must be concurrently evaluated to determine desirable engine design trends.

The lift-drag ratio has a predominant influence in the selection of optimum cruise flight speed of the aircraft. This choice of flight speed in turn strongly affects the engine operating point at which the engine designer attempts to optimize performance. Thus, the aerodynamic capabilities of aircraft configurations strongly influence advanced engine design concepts.

A comparative evaluation of airplanes having fixed-speed missions shows clearly that maximum flight ranges would occur at subsonic speeds. A well-designed subsonic bomber may have lift-drag ratios 5 or more times greater than an all-supersonic bomber. All-subsonic missions are becoming less important, however, and there is an increasingly evident necessity for supersonic over-the-target capabilities. When airplane designs are compromised to satisfy the dual-speed requirements of long cruise radius

[redacted]

at subsonic speeds and supersonic dash, the lift-drag margin between subsonic and supersonic speeds decreases. Instead of a 5:1 ratio, subsonic lift-drag ratios tend to reduce to values only $2\frac{1}{2}$ to 3 times those possible at supersonic speeds.

Now, if aircraft range were solely a function of L/D, a preponderance of flight at subsonic speeds would still be desirable, even for the dual-speed mission. The engine-efficiency term that appears in the range equation tends to modify this conclusion, however. As previously shown for the ram-jet engine (fig. 6), engine efficiency tends to increase as flight speed is increased. The amount that the efficiency increases depends upon the type of engine cycle used over the flight Mach number range.

The variation of engine efficiency with flight Mach number is shown in figure 15 for afterburning and nonafterburning engines having turbine-inlet temperatures of 1500° F, about the level of current practice. At a Mach number of 0.9 the nonafterburning engine has an efficiency of 19 percent. Supersonic flight is not presently feasible with nonafterburning engines of the weight levels that are currently in flight; consequently, current modes of operation require the use of afterburners for supersonic speeds. At a Mach number of 2.5 the efficiency of the afterburning engine is only 25 percent, or about 1.3 times the level of efficiency at subsonic speeds. This small increase in efficiency is not sufficient to overcome the $2\frac{1}{2}$ or 3 to 1 reduction in L/D, and the longest over-all ranges are obtained with the shortest possible supersonic dash.

If the specific weight of the nonafterburning engine can be reduced, the relative efficiency of supersonic flight can be increased markedly. Several engines in advanced design stages give promise of specific weights only about half of the values of currently flying engines. These weight reductions will be accomplished through increases in the air flow per unit frontal area by adoption of advanced compressor designs, and by reduction in the engine structural weight through advanced structural practices.

If the engine weight can be reduced to a point that Mach 2.5 flight is possible without afterburning, an engine efficiency of 40 percent could be achieved. This efficiency value would be about twice that currently possible at subsonic speeds and would go a long way towards compensating for the loss in L/D in going from subsonic to supersonic speeds. All-supersonic flight would thus begin to look competitive on a range basis with the present dual-speed type of mission.

The desirability of conducting entire flight missions at supersonic speeds is even greater if the use of higher turbine-inlet temperature

[redacted]

cycles is considered. The efficiency of an engine having a 2500° F turbine-inlet temperature T_t and no afterburner is compared in figure 16 with that of the 1500° F afterburning engine. The efficiency of the lower-temperature nonafterburning engine at Mach 0.9 is also shown for comparison. At subsonic and low supersonic speeds the nonafterburning-engine efficiency is reduced when the turbine-inlet temperature is increased. At higher supersonic speeds, however, this efficiency loss is erased. At Mach 2.5, for example, the efficiency of the 2500° F engine is about the same as that of the 1500° F engine. In addition, the higher-temperature engine will be lighter, as indicated by the engine specific-weight curves of figure 17.

The curves of figure 17 assume engine air-flow rates per unit frontal area corresponding to the values of currently flying engines. The decrease in specific weight between the 1500° and 2500° F nonafterburning engines is therefore the direct result of the greater thrust per pound of air delivered by the higher cycle temperature. The higher-temperature engine has a specific weight comparable to that presently associated with low-temperature nonafterburning engines.

As previously mentioned, 1500° F nonafterburning engines having lower specific weights than those indicated in figure 17 are now in advanced design stages. Presumably, the same weight-reduction programs could be applied to the 2500° F engine, so that it would continue to have a weight advantage. The greater permissible fuel load would thus continue to favor the higher cycle temperature at higher supersonic speeds.

Having considered the interrelated effects of lift-drag ratio and engine weight and efficiency on range, the only factor in the Breguet equation that has not been considered is the heating value of the fuel. The sorts of fuels that might be expected to give heats of combustion higher than those obtained from conventional hydrocarbon fuels can be determined from figure 18, where the heat of combustion is plotted as a function of the atomic number.

A periodic variation in heating value is obtained, with hydrogen leading the elements with a heat of combustion of 51,500 Btu per pound as compared with 18,500 for JP-5. Other elements that contain interesting heats of combustion are lithium, beryllium, and boron. The heat of combustion of lithium is about the same as that of JP-5, so that not much improvement is indicated from that source. Beryllium is not considered a likely prospect, since it is scarce and has an extremely toxic oxide. There remain for consideration, therefore, hydrogen, boron, and compounds of these elements.

Two boron hydride compounds have been under investigation as jet-engine fuels for some time. They are diborane and pentaborane, with heating values of 31,300 and 29,100 Btu per pound, respectively. Diborane

is a gas under normal atmospheric conditions. Pentaborane is a liquid that boils at temperatures slightly above ambient.

Under the auspices of the Bureau of Aeronautics, and more recently the Air Force, a concerted effort is underway to make new boron fuels with heating values similar to pentaborane but with more desirable physical properties. The technique employed has been to attach a methyl or ethyl group to the somewhat unstable boron hydrides. A commercial grade of ethyldecaborane (EDB) having a heating value of about 25,000 Btu per pound shows promise, although only laboratory quantities of the fuel have been made to date.

The various fuels should more properly be compared on the basis of thrust rather than on the basis of heating values alone, since the specific heats of molecular weights of combustion products change with changes in molecular composition accompanying combustion. Fuels containing boron further complicate the transfer of heat energy to thrust, since the exhaust gases may undergo a change of phase of one of the products, boron oxide. Boron oxide exists as a glassy liquid up to temperatures of about 2900° F and then vaporizes. The heat of vaporization of the liquid boron oxide is about 2000 Btu per pound, which amounts to about 7 percent of the heat of combustion of pentaborane.

The effective heating values of pentaborane and hydrogen, relative to JP-5 fuel, are shown in figure 19 for a range of combustion temperatures and thrusts. The combustion temperature shown is that for the JP-5. Effective heating value is defined as that part of the heat of combustion that produces thrust. Since it is necessary to index the comparison at some inlet temperature and pressure and at some nozzle expansion ratio, the example chosen for figure 19 is a ram jet flying at Mach 3 and an altitude of 80,000 feet.

The combustion products for hydrogen and JP-5 are assumed to be in chemical equilibrium in the expansion process through the nozzle. Two curves are shown for pentaborane, one for equilibrium and one for frozen composition. This latter process assumes that the molecular and phase compositions existing at the end of combustion are retained as the gas expands through the nozzle.

At low levels of thrust, corresponding to low combustion temperatures, the effective heating values are the same as the chemical heating values. As the temperature is increased, the effective heating-value ratio for hydrogen remains essentially constant. For pentaborane, however, less heat energy goes into the production of thrust as the combustion temperature is increased. The break in the curve for frozen expansion is at the temperature where much of the heat energy goes into the vaporization of boron oxide. In equilibrium expansion, the break in the curve is postponed to higher temperatures, because recondensation of the boron oxide is assumed to occur in the expansion process.

There are other fuel properties that influence their relative desirability. One of these properties that must be considered is the density. A comparison of the relative fuel volumes per unit of heat energy of hydrogen, JP-5, pentaborane, and EDB is shown in figure 20. Hydrogen has the highest effective heating value of these fuels, but it is quite bulky. Hydrogen occupies roughly 4 times the volume of JP-5, and over 5 times the volume of EDB.

If the various fuels are assumed to be operating in the same engine cycles, so that engine efficiencies are the same, the relative range capabilities will depend upon the comparative lift-drag ratios attainable with the fuels and upon the amount of fuel weight that can be stored in the airplane as well as upon the comparative effective heating values. For a supersonic airplane having thin wings, the majority of the fuel will be contained in the fuselage. The fuel volume will therefore affect the airplane lift-drag ratio through the required size of the fuselage.

Potential lift-drag ratios are plotted in figure 21 as a function of flight altitude at Mach 2.5 for airplanes using hydrogen, EDB, and JP-5 fuels. Each point on the curves corresponds to a different design point. In general, the lift-drag ratios increase with increases in flight altitude, since the wings become larger and the fuselage drags become a smaller proportion of the total drag. The limiting L/D would correspond to an all-wing configuration. JP-5 and EDB fuels have about the same volumes per Btu and hence are represented by a single configuration analysis.

A JP-5 or EDB airplane designed for flight at 60,000 feet would have the wing-fuselage proportions indicated in figure 21 at that point. Because of the lower density, a hydrogen airplane designed for the same weight of fuel load at the same altitude would have a much larger fuselage relative to the wing. The size of the wing on the hydrogen airplane would be increased if the design altitude were higher. As shown, the hydrogen airplane proportions at 80,000 feet would be about the same as those of the JP-5 airplane at 60,000 feet. Hence, the same L/D could be attained. With respect to lift-drag ratio, therefore, it would be desirable to fly an airplane using hydrogen fuel at a higher altitude than an airplane using either JP-5 or EDB.

As previously shown, the engine size must increase as altitude is increased. The amount of fuel that can be carried in a given gross weight airplane therefore reduces as altitude is increased. This factor must be considered in evaluating a desirable flight altitude for a hydrogen-fueled airplane. Figure 22 presents engine weights required for the various fuels as a function of altitude. The engine weight is here expressed as a fraction of the airplane gross weight.

At any altitude larger engines would be required for the hydrogen airplane than for the other two fuels because the L/D is lower. For a given gross weight the lower L/D produces a higher required thrust and hence a larger engine for a given cycle. At 60,000 feet, engines totaling 7.5 percent of the gross weight would suffice for the JP-5 or EDB airplanes. (The engines assumed in these calculations are advanced cycles having lower specific weights than those currently flying.) At the same altitude the engines for the hydrogen airplane would amount to about 11 percent of the gross weight. At the higher altitude of 80,000 feet, shown by figure 21 to be required to attain the same L/D, the engines for the hydrogen airplane would be 20 percent of the gross weight. Thus the desirability of higher altitudes to improve the hydrogen-airplane lift-drag ratios tends to be offset by the higher engine weights and consequently lower fuel loads that can be carried.

A first-order evaluation of the comparative range capabilities of aircraft using the three fuels is shown in figure 23. In addition to the variations in L/D and engine weight shown in figures 21 and 22, a schedule of structural-weight variation with altitude is included in these calculations. The maximum range of the JP-5 airplane is taken as unity. At low altitudes, range increases as altitude is increased for all the aircraft because of the improving lift-drag ratios as wing size is increased. At altitudes above that for maximum range for each aircraft, increasing engine weight is a predominant factor, which, together with the increasing structural weight, reduces the fuel load more rapidly than compensated for by increasing L/D.

The increased range of the EDB airplane over the JP-5 airplane directly reflects the increased heating value of the fuel, since the two airplanes are assumed to have comparable lift-drag ratios and engine weights. The increased range of the hydrogen airplane is less than that corresponding to the heating-value advantage of the fuel, thus showing the disadvantages stemming from the lower lift-drag ratios and increased engine weights. The greatly increased heating value overcompensates for these disadvantages, however.

The importance of L/D is illustrated by the higher altitudes at which maximum range is attained with the hydrogen airplane as compared with the other two. If the range advantage of hydrogen is entirely removed by increased altitudes, the hydrogen airplane could fly at the same range as the JP-5 airplane at altitudes over 30,000 feet higher.

In this simplified analysis, the zero-range maximum ceiling is the same for all the fuels. This occurs because maximum altitude would be reached when all the fuel weight is converted to engine weight. With no fuel in the airplane, the fuel type is unimportant.

It was shown earlier that combustion problems arise with present fuels at the extreme altitudes that the calculations of figure 23 show to be attainable with EDB or hydrogen. An indication of the combustion

quality that might be expected with these high-energy fuels can be obtained from an examination of some of the fundamental combustion properties that have been found to be indicative of their performance in jet-engine combustors. Comparative flame speeds measured in laboratory burners at ambient conditions are shown as a function of equivalence ratio in figure 24. These data were obtained by Drs. Berl and Olsen and Captain Gayhart at the Applied Physics Laboratory of The Johns Hopkins University.

It has been established that fuels with higher flame speeds burn with higher combustion efficiencies to lower pressures in engine combustors. At an equivalence ratio of 1.0 (stoichiometric fuel-air ratio), hydrogen has a flame speed about 7 times that of JP-5. Pentaborane has a flame speed almost 15 times that of JP-5. Only meager data are available for diborane and none for EDB; however, it is expected that they will have flame speeds comparable to that of pentaborane.

Another measure of the combustion performance of a fuel is its flammability limit. Comparative flammability limits of JP-4, hydrogen, and several boron fuels are shown in figure 25. These data were obtained in combustion experiments using a 2-inch-diameter glass tube. The various fuels could be ignited over the range of equivalence ratios and pressures within the loops. JP-4 fuel could only be ignited at fuel-air mixtures between 0.4 and 3.0 times the stoichiometric value. Hydrogen could be ignited to both leaner and richer limits and at considerably lower pressures. The data on the boron fuels are limited. It is evident, nevertheless, that flammability limits with these fuels are considerably broader than with the hydrocarbon fuels.

Both the flame-speed data and the flammability-limit data indicate that fuels such as hydrogen and the boron hydrides are more reactive and will burn under more severe operating conditions than do current hydrocarbon fuels. Improved high-altitude combustor performance should therefore be possible with these fuels.

It was shown earlier that a succession of temperature problems arises as higher aircraft flight speeds are considered. The use of fuel to cool various airframe and power-plant components would help overcome some of these problems. The relative heat-absorptive capacities of the various fuels are therefore of interest. The comparative cooling capacities of the fuels under discussion are shown in figure 26 as a function of the final fuel temperature. The cooling capacity is here expressed as the ratio of the heat absorbed by the fuel to the heating value. The comparisons of the relative cooling capacities are therefore valid for conditions where all the fuel being used as a coolant is burned in the engine to provide a given temperature rise.

In the calculation of this figure, hydrogen was assumed to be initially liquid at its boiling temperature. The normally liquid fuels, JP-5, pentaborane, EDB, and the pure hydrocarbon mixture of isohexane and

n-heptane, were considered to be solids at their freezing points. All the fuels were considered to be vaporized at their atmospheric boiling temperatures.

The heat capacity of JP-5 fuel is limited by the permissible temperatures before excessive gum formation is encountered, as shown by figure 3. Some JP-type fuels have been heated to temperatures approaching 1000° F in laboratory equipment, but this is not at present a practical thing for the kinds of fuels that would be available in large quantities. Limiting temperatures presently appear to be about 300° F. Pure hydrocarbon mixtures, such as the isohexane, n-heptane mixture shown in figure 26, might be stable up to 800° to 900° F and would therefore represent a better heat sink.

The boron hydride fuels are seriously limited in their heat-absorption capacities by decomposition at relatively low temperatures. Of the fuels indicated, hydrogen has by far the best heat-capacity characteristics, with a high specific heat and the capability of being heated to extremely high temperatures that are only limited by the heat exchanger. Even with a relatively low final temperature of 500° F, hydrogen will absorb almost 3 times as much heat as JP-5.

CONCLUDING REMARKS

This brief examination of the future problems of air-breathing power plants has indicated the concepts that must be considered if substantial progress is to be made in the altitude, flight speed, and range of this class of aircraft. In addition to a series of problems associated with higher inlet temperatures, the analysis has indicated the desirability of reducing engine weights, improving engine efficiencies through cycle changes, and utilizing high-energy fuels.

A number of potential merits of hydrogen and boron hydride fuels have been shown. These fuels are not without their disadvantages, however. Pentaborane, for example, has the penalties of limited availability, high manufacturing cost, complex storage and handling problems, and undesirable products of combustion. Pentaborane is toxic and decomposes at relatively low temperatures. Boron oxide is formed in the combustion process and has a melting point of about 1000° F. As a result, the oxide tends to deposit on combustion-chamber walls and on turbine nozzles and blades. Means for reducing this deposition are currently being studied.

Fuels having heats of combustion approaching that of pentaborane, but with more desirable physical properties, are under development. One of these fuels is ethyldecaborane (EDB). Because of its reduced volatility, EDB is less hazardous than pentaborane. Its heat of combustion is still about 40 percent better than that of JP-5 fuel.

The use of hydrogen fuel will also bring some disadvantages. One of these is its high manufacturing cost. In addition, use of hydrogen requires storage of the fuel in the aircraft as a liquid. The development of lightweight, well-insulated tanks to retain the fuel at a temperature of -423° F will be necessary. While the handling of liquid hydrogen is not new to many industries, application to aircraft propulsion will require considerable development.

PROBABLE FUTURE FLIGHT TRENDS

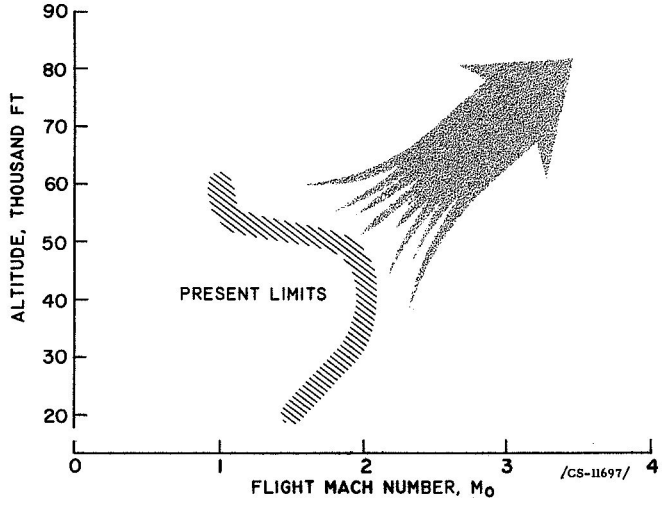

Figure 1

FLIGHT STAGNATION TEMPERATURES

STANDARD ATMOSPHERE

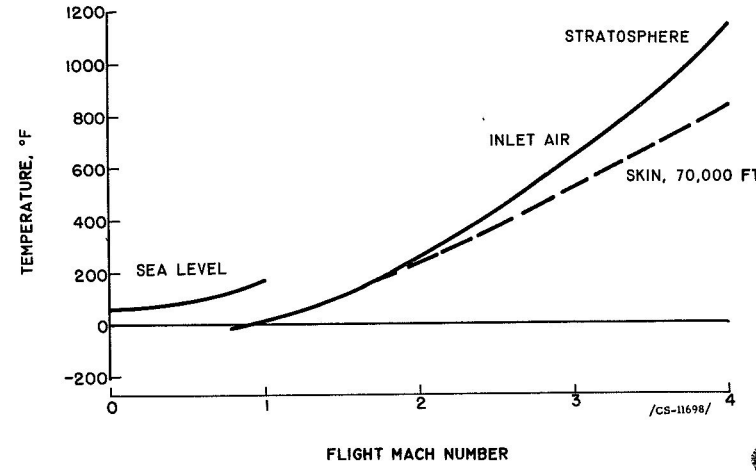

Figure 2

TEMPERATURE-TIME EFFECTS ON HYDROCARBON REACTIONS

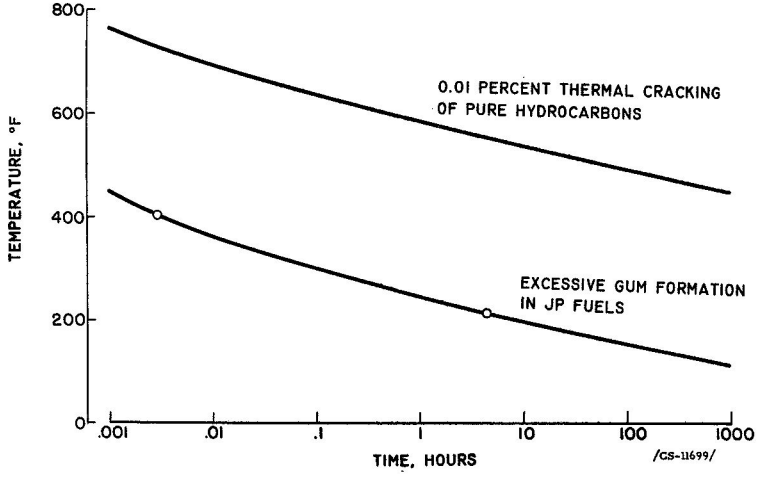

Figure 3

EQUIVALENT-SPEED SCHEDULE OF TURBOJET ENGINE

STANDARD ATMOSPHERE N, CONSTANT

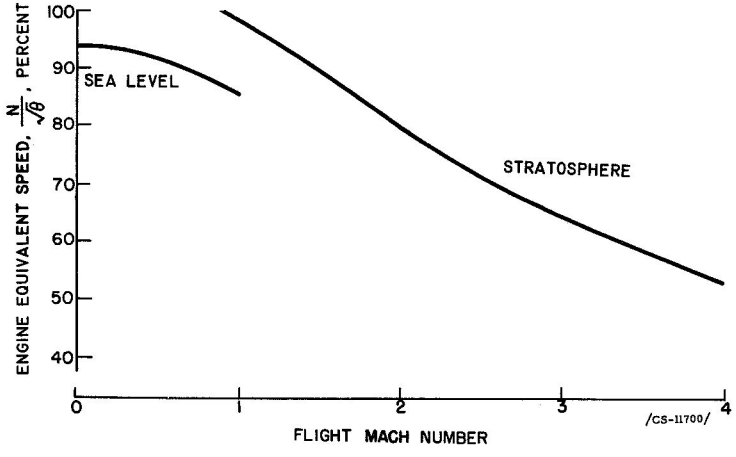

Figure 4

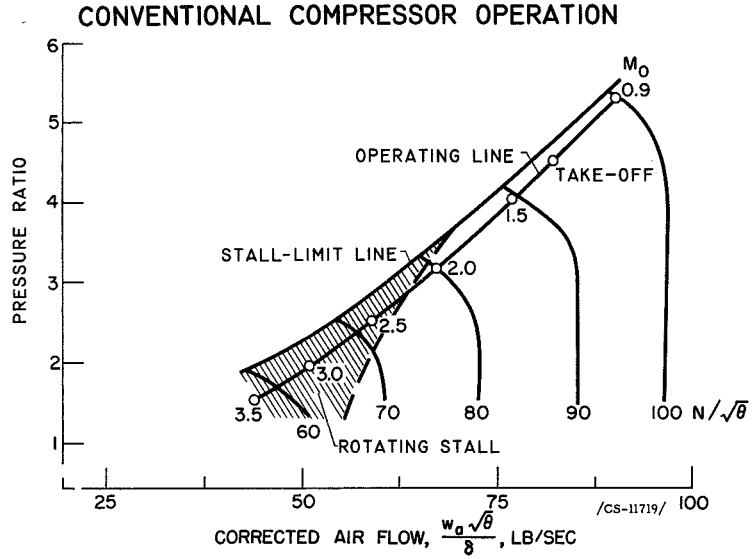

Figure 5

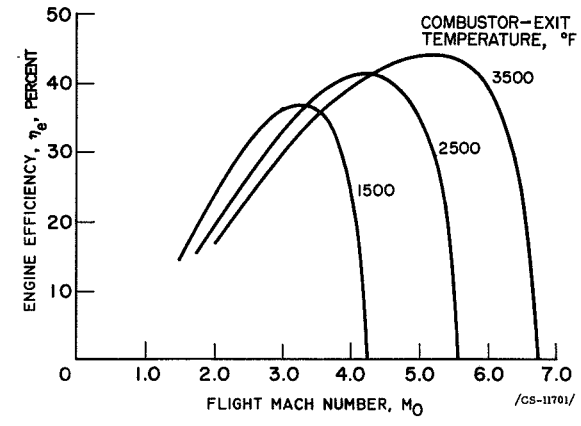

Figure 6

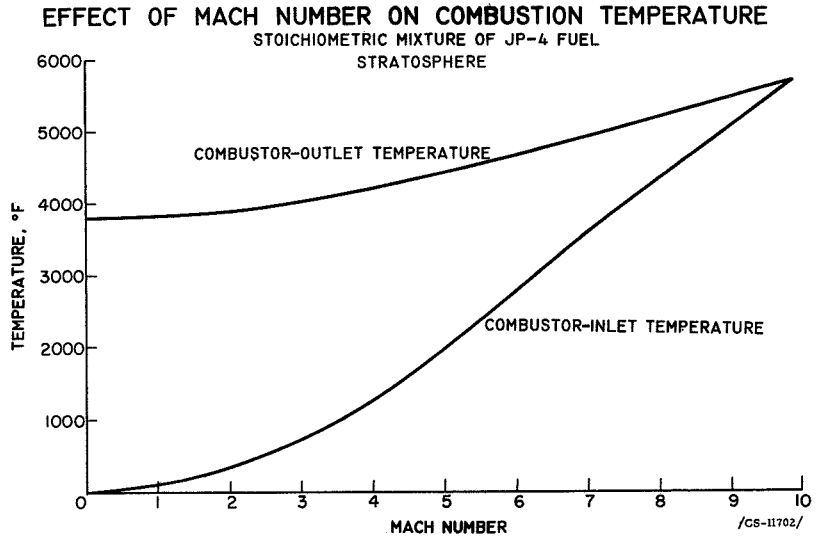

Figure 7

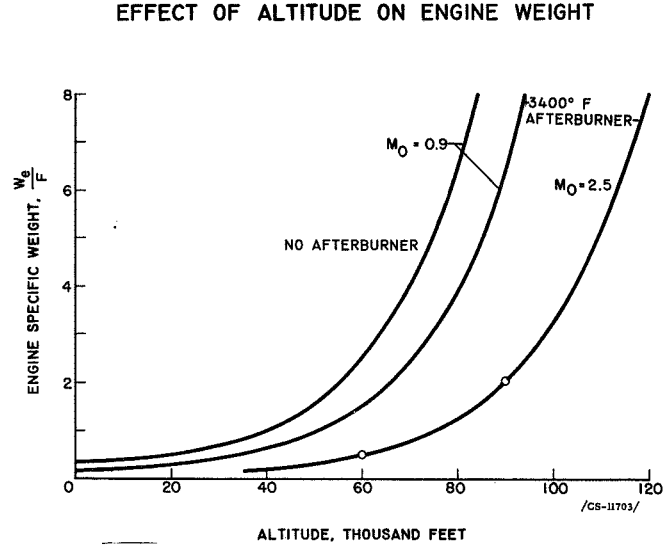

Figure 8

MACH 2.5 INTERCEPTOR DESIGNED FOR
60,000 FEET ALTITUDE

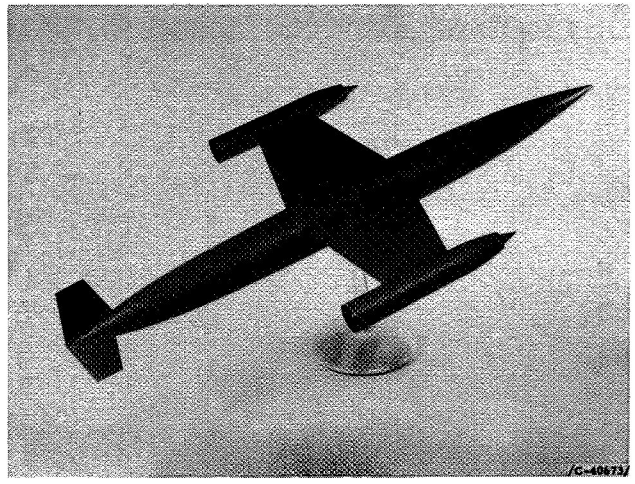

Figure 9

MACH 2.5 INTERCEPTOR DESIGNED FOR
90,000 FEET ALTITUDE

Figure 10

EFFECT OF REYNOLDS NUMBER ON COMPRESSOR PERFORMANCE

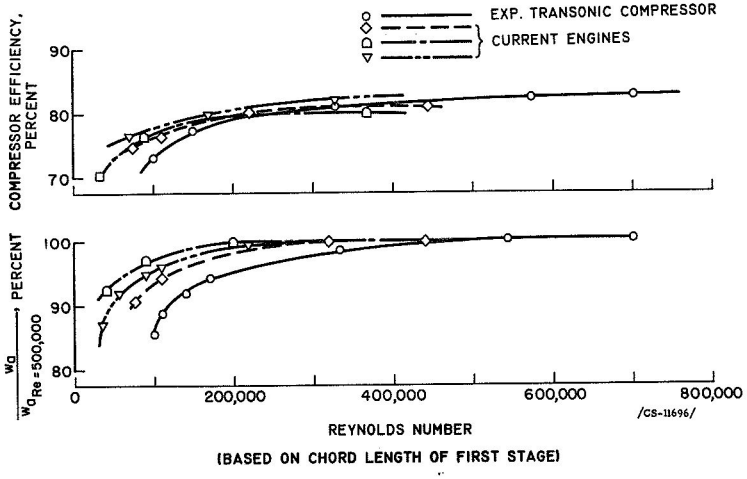

Figure 11

EFFECT OF ALTITUDE AND MACH NUMBER ON COMPRESSOR-INLET REYNOLDS NUMBER

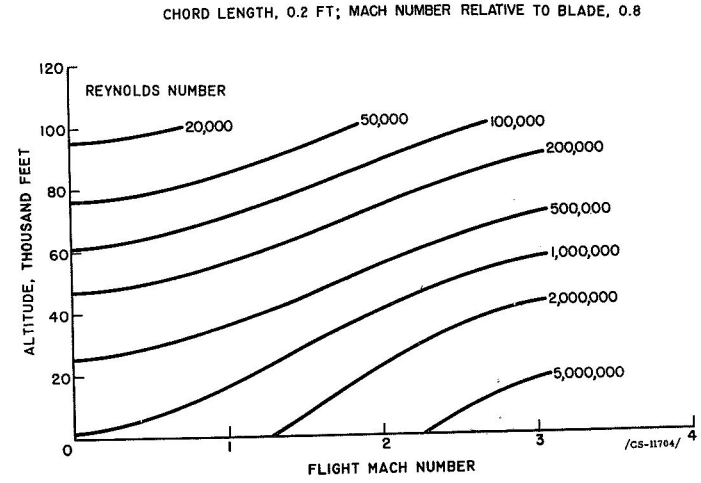

Figure 12

EFFICIENCIES FOR AN EXPERIMENTAL TURBOJET BURNER

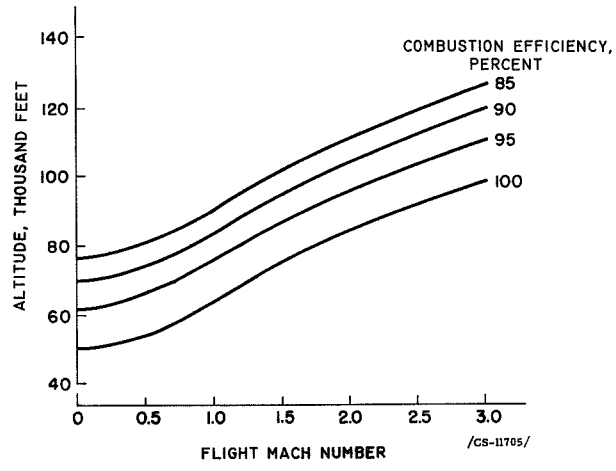

Figure 13

EFFICIENCIES FOR AN EXPERIMENTAL AFTERBURNER

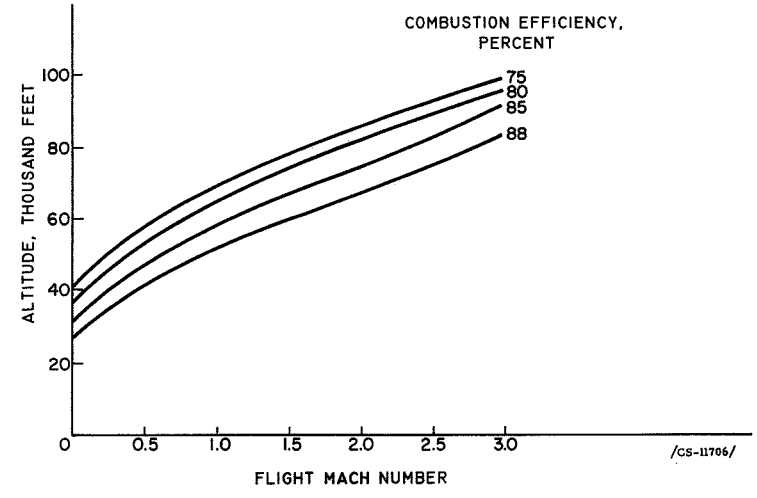

Figure 14

FLIGHT-SPEED EFFECT ON TURBOJET EFFICIENCY

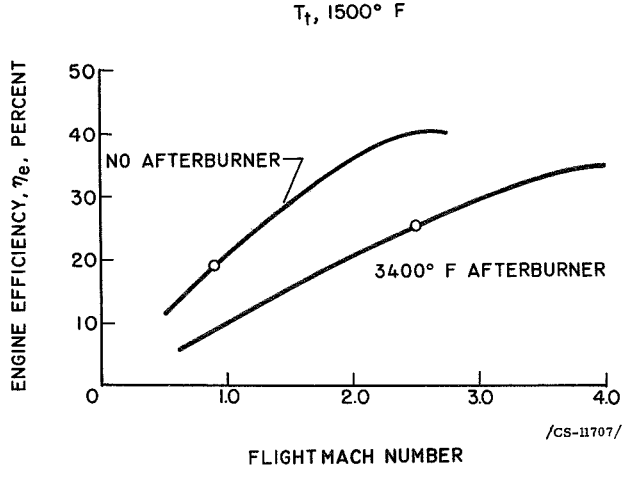

Figure 15

EFFECT OF CYCLE TEMPERATURE ON TURBOJET EFFICIENCY

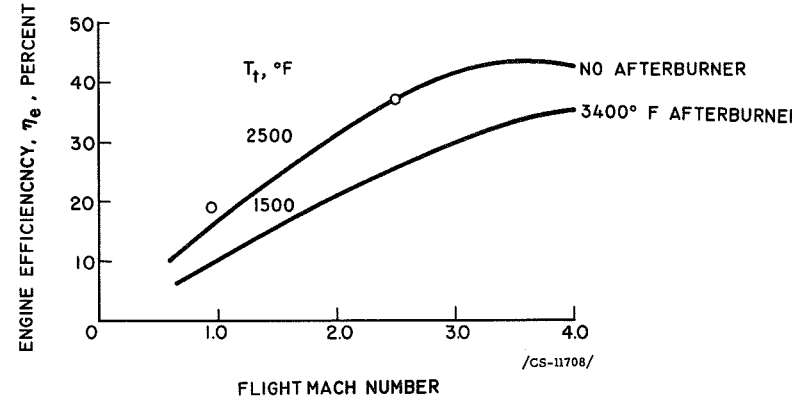

Figure 16

EFFECT OF CYCLE TEMPERATURE ON TURBOJET SPECIFIC ENGINE WEIGHT

ALTITUDE, 60,000 FEET

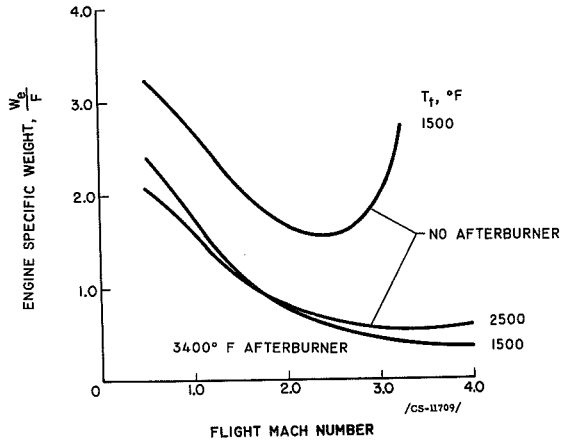

Figure 17

HEATS OF COMBUSTION

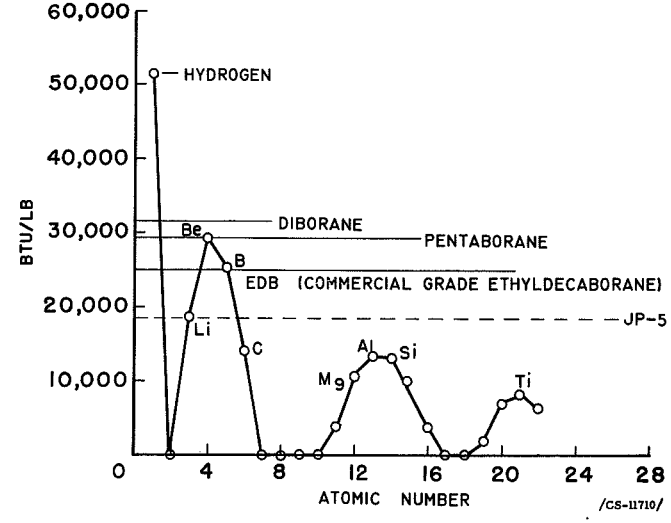

Figure 18

EFFECTIVE HEATING VALUE OF HYDROGEN AND PENTABORANE COMPARED TO JP-5

BASED ON PERFORMANCE IN A RAM JET AT M_0 = 3.0

ALTITUDE, 80,000 FT

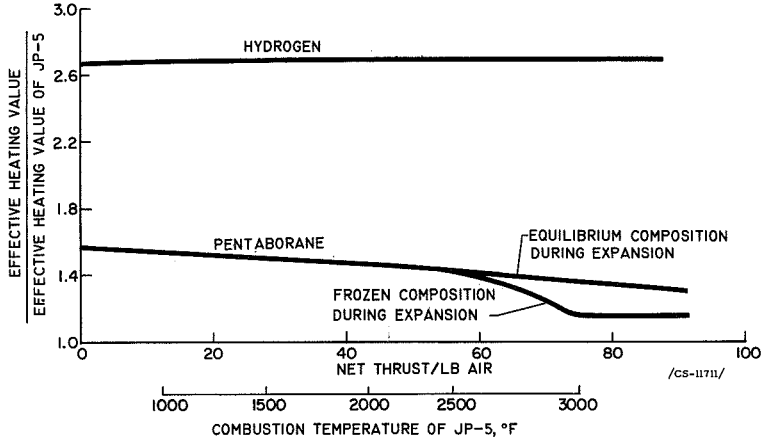

Figure 19

COMPARATIVE FUEL VOLUMES

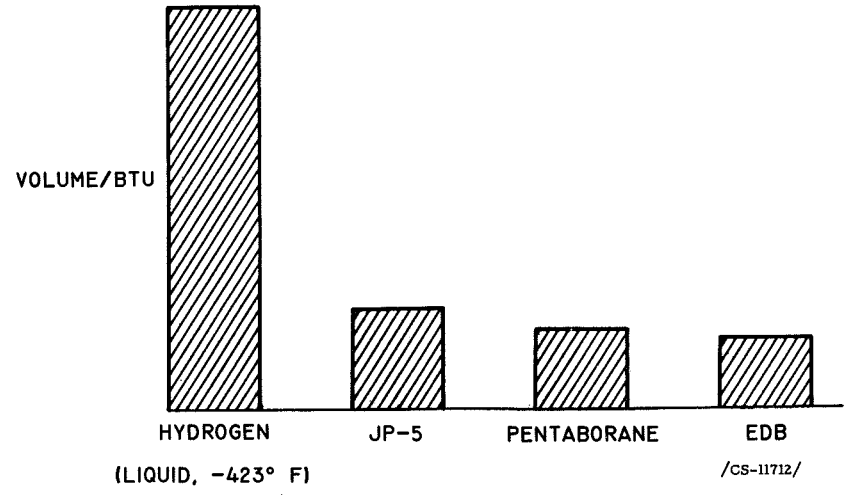

Figure 20

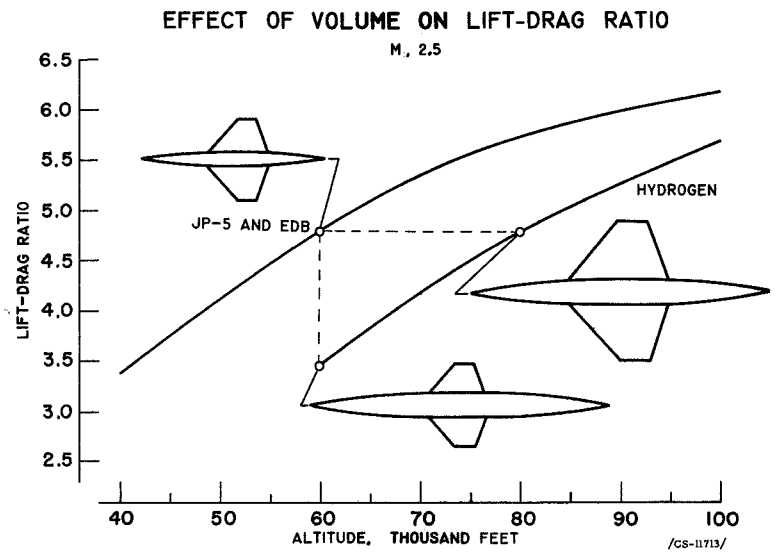

Figure 21

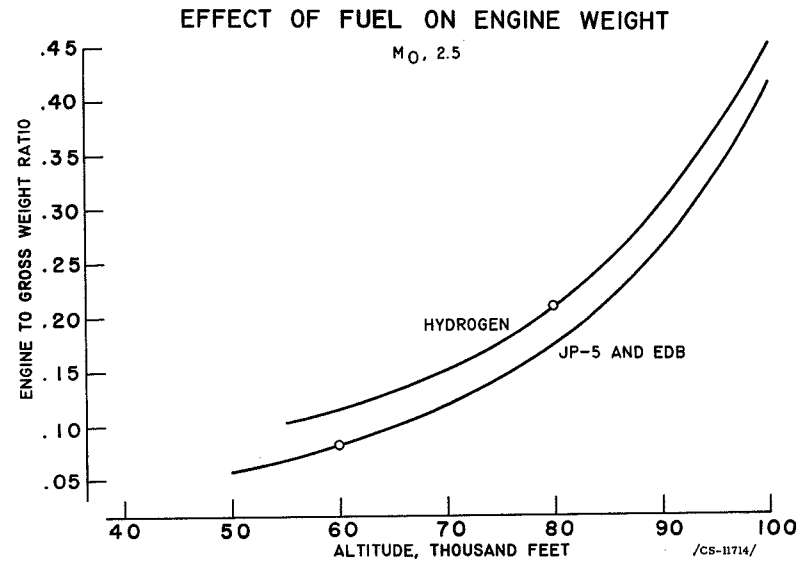

Figure 22

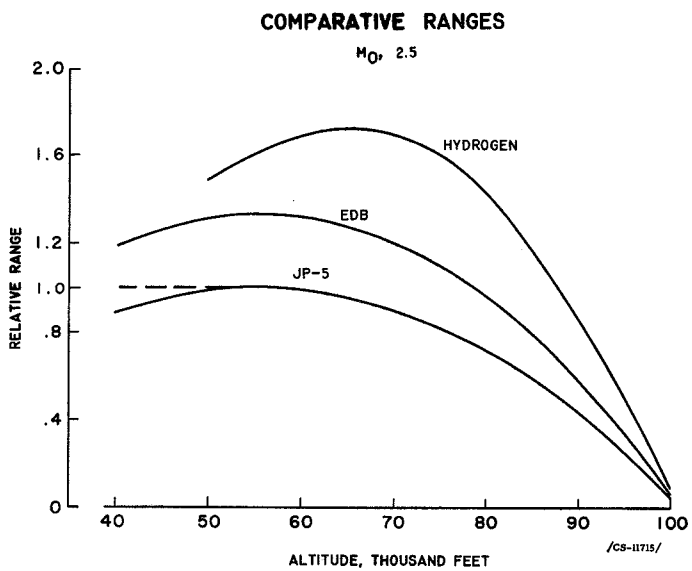

Figure 23

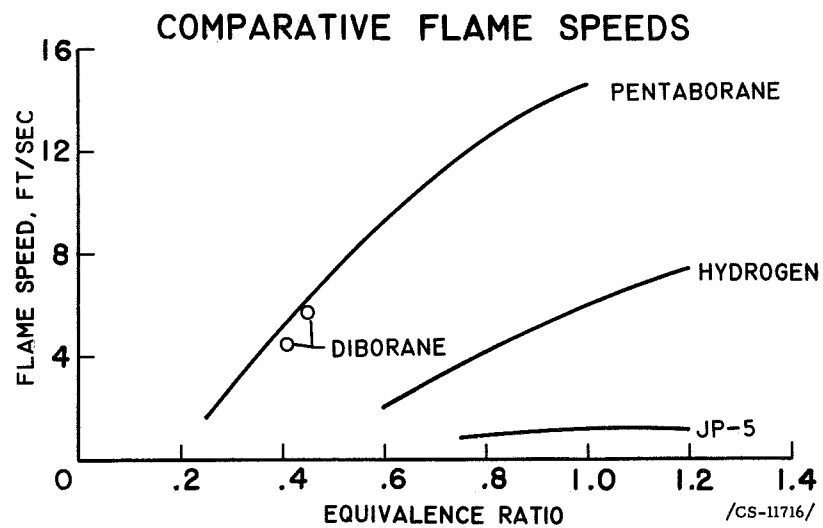

Figure 24

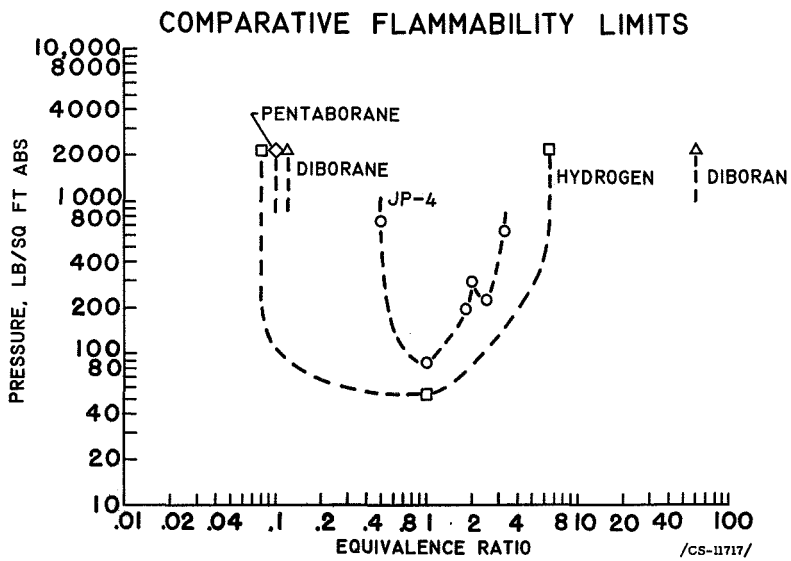

Figure 25

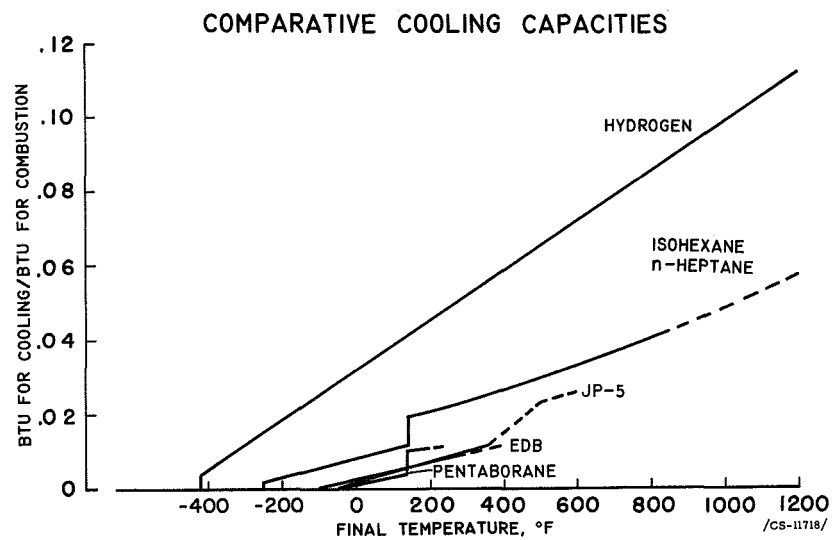

Figure 26

2. TURBOJET ENGINES FOR HIGH-SPEED AND HIGH-ALTITUDE APPLICATIONS

David Gabriel, Chairman
Charles H. Voit
Wilfred E. Scull
Robert E. English
Robert R. Ziemer
Robert J. Lubick

2. TURBOJET ENGINES FOR HIGH-SPEED AND HIGH-ALTITUDE APPLICATIONS

INTRODUCTION

Engine weight is one of the most important parameters determining the performance of airplanes designed to fly at altitudes of 80,000 feet or higher and at flight Mach numbers up to 3.0 or 3.5. Current production engines, which are designed essentially for high take-off thrust and low subsonic fuel consumption, are so heavy that flight with a useful range at these extreme conditions of altitude and speed is not possible if these engines are used.

It is the purpose of this paper to describe methods of minimizing the weight of turbojet engines for high-speed, high-altitude applications. Minimum engine weight may be realized by incorporating into the design of an engine all the advanced components and potential advantages of high-energy fuels that research has made available to the engine designer. In order to realize the full advantage of these advanced features, the engine design point should be at a high-speed condition where the thrust requirements are greatest.

An example of the kind of engine that will typically result from these design practices is shown in figure 1. This photograph illustrates the arrangement and compatibility of the various advanced components, but no particular significance is attached to the details of the design.

The transonic compressor supplies a very high air flow per unit of frontal area and produces about twice the pressure ratio per stage as current subsonic compressors. This type of compressor is therefore the smallest, most compact compressor available in the near future.

The annular combustor was designed to operate on high-energy fuel. The use of high-energy fuel in the combustor permits the attainment of very high combustion efficiencies at extremely high altitudes and, in addition, results in a short, high throughput combustor. The combustor will supply outlet gas temperatures or turbine-inlet temperatures as high as 2500° F.

To illustrate the possible compactness that can be achieved, a one-stage turbine was used. The turbine was designed to operate at its limiting aerodynamic and structural conditions at the design point. At this point the exit axial Mach number is 0.7, and the rotor-inlet relative Mach number at the hub is 0.8. High blade speed was maintained by designing for a turbine rotor-blade root stress of 50,000 pounds per square inch. This results in a one-stage turbine only slightly larger in diameter than the compressor. Of course, additional turbine stages could be used with some reduction in turbine diameter.

An essential feature in the design of a compact lightweight engine is the turbine cooling system. The turbine in figure 1 is cooled by a secondary fluid which flows in a closed system between the turbine and the heat exchanger. This secondary fluid is cooled, in turn, by the engine fuel.

For efficient operation at very high speeds, a divergent-ejector exhaust nozzle is shown. The performance of this nozzle is approximately equivalent to that of a variable-area convergent-divergent nozzle. The nozzle-outlet diameter was chosen as a reasonable compromise between internal performance and external drag. Because of the very high gas temperatures involved, the entire aft end of the engine is cooled by a suitable combination of air and fuel.

It is evident that a number of advanced components are combined into this type of engine. The realization of the potential advantages of these advanced components requires the proper combination of several basic factors in engine design.

BASIC DESIGN CONSIDERATIONS

The detailed design of an engine is, of course, a complex procedure which involves the well-known process of compromises among a large number of interrelated factors. Although it is outside the scope of this paper to explore the design process in detail, a simplified discussion will aid in establishing several very desirable aspects of high-speed engine design.

Three factors of primary importance in design are as follows:

(1) Selection of proper components

(2) Selection of proper design point

(3) Consideration of off-design operation

Selection of proper components involves choosing a compressor, combustor, and turbine whose combined characteristics provide good over-all performance. Individual characteristics of the components which are most useful in achieving this good performance are high flow per unit of frontal area, short length, and the ability to operate at high temperatures and high stresses.

The flight condition for which the engine is primarily designed (the design point) is chosen, of course, to produce maximum performance at the most important flight condition. However, the engine must provide adequate performance at other flight conditions so that the selection of the design point must be tempered by the third requirement, proper consideration of off-design operation.

In subsequent sections these three factors and the relations between them will be examined in order to indicate desirable design practice for high-speed engines.

SELECTION OF COMPONENTS

The air-handling capacity of axial-flow compressors is shown in figure 2. The maximum air flow per unit compressor frontal area W_a/A_c is a function of the compressor-inlet axial Mach number and the hub-to-tip radius ratio. As indicated by the shaded areas, the transonic compressor with its higher axial Mach number and lower hub-tip ratio produces a higher flow than current subsonic compressors. The transonic compressor is capable of delivering air flows up to 37 or 38 pounds per second per square foot of compressor frontal area. In addition, as previously mentioned, the transonic compressor delivers approximately twice the pressure ratio per stage as the subsonic compressor or, in other words, requires only half the number of compressor stages.

The maximum air-handling capacity is only one of many factors to be considered in the selection of a compressor. Some additional considerations are shown in the typical transonic compressor map in figure 3. The range of useful operation of a compressor is restricted by the stall-limit line and engine surge at high pressure ratios, by the rotating-stall region at low speeds, and by the relative Mach number (or air flow) limit at high speeds. Although it is possible to operate the compressor at both lower and higher speeds than shown by these limits, this type of operation is not desirable. Operation at low speeds within the rotating-stall regions may introduce prohibitively high blade stresses, and operation at speeds above the relative Mach number limit results in low compressor efficiencies and negligible gains in air flow. As indicated by the efficiency contours and the shaded region, operation at very low pressure ratios is undesirable because of low compressor efficiencies. Thus, the range of useful compressor operation is restricted to a small region boxed in on all sides by limits or undesirable regions of operation.

The operating limits shown in figure 3 are for uniform inlet-flow conditions. Experience has shown that engines installed in airplanes are subjected to nonuniform inlet-pressure distributions which appreciably reduce the region of useful compressor operation, as shown in figure 4. The effects of these inlet-pressure distortions are to lower the stall-limit line and extend the region of rotating stall to higher rotative speeds. The exact magnitude of these changes will depend on the detailed compressor design and on the magnitude of the air distortion. Figure 4 shows an example of typical variations in stall limits that might be encountered in a high-speed airplane. As a consequence of the shifts in the stall limits, the useful range of engine operation is reduced to about 20 percent in engine speed. Operation in this reduced range will be considered in the subsequent discussion.

METHODS OF ENGINE OPERATION

The compressor map of figure 4 is reproduced in figure 5 with a dashed line superimposed on it showing the conventional engine operating line described in the first paper. For the constant rotational speed of the conventional operating line, equilibrium operation of the compressor with the other engine components results in reduced compressor equivalent speed as flight speed increases. As flight Mach number increases from 0.9 to 3.5, the compressor equivalent speed is reduced from 100 percent to less than 60 percent. As a result the air flow is decreased more than 50 percent, and the compressor is required to operate in the rotating-stall region. In fact, at all flight Mach numbers above about 1.6 the compressor operates in the rotating-stall region.

An obvious way to avoid these problems is to increase the compressor equivalent speed $N/\sqrt{\theta}$. This can be done, of course, by increasing the rotational speed. If, for example, the rotational speed is increased from 10,000 rpm at a flight Mach number of 0.9 to 17,000 rpm at a Mach number of 3.5, the equivalent compressor speed will remain constant. The equilibrium operating line will fall along the 100-percent equivalent speed line as indicated by the series of circled points. This type of operation, of course, results in a very large increase in air flow compared with the conventional constant-speed line but requires very high centrifugal blade stresses. The stress at the roots of the turbine blades would be over 140,000 psi. Obviously, some compromise between constant rotational speed and constant equivalent speed is required.

A possible compromise is illustrated in figure 6, which is the same as figure 5 except for the addition of the compromise operating line. For the compromise operating line the engine rotational speed is increased as flight speed is increased until a turbine rotor-blade root stress of 50,000 psi is reached (flight Mach number, 1.87). As flight Mach number is further increased, the engine rotational speed is held constant in order to avoid higher blade stresses and therefore the equivalent speed decreases. This compromise operation results in an increase in air flow of about 40 percent at flight Mach numbers of 2.5 to 3.0 compared with the conventional constant-rotating-speed case. In addition, the range of stall-free operation is extended to a flight Mach number of 2.8 compared with 1.6 for the constant-speed operating line.

This compromise method of operation is equivalent to choosing a design point at a flight Mach number of 1.87, because it is at this flight condition that the turbine is operating at its stress limit and the compressor is operating at its flow limit. In addition, a method of operation off-design is chosen so that the compressor operates at its flow limit at all flight speeds below 1.87, which results in adequate low-speed and take-off performance for most applications.

ENGINE AIR-HANDLING CAPACITY

If the high-flow transonic compressor is combined with a one-stage turbine, the turbine will have a larger frontal area than the compressor. The air flows per unit of frontal area (defined in this case as turbine frontal area) that can be obtained for the compromise operating line and the conventional operating line are compared in figure 7. For the constant-speed engine, the air-flow line is terminated at a flight Mach number of 1.6, because it is at this flight condition that rotating stall occurs. Similarly, the air-flow line for the high-stress compromise operating line is terminated at a flight Mach number of 2.8. Throughout the entire range of supersonic Mach numbers, the engine with the compromise operating line has a higher air-handling capacity than the engine with the conventional operating line.

The maximum Mach number limitation imposed on both engines by rotating stall may be circumvented by the use of special devices to reduce the angle of attack on the inlet compressor stages. Two of these devices are shown in figure 8. Indicated in the sketch are adjustable compressor stator vanes and interstage compressor bleed. These two devices are currently in use on production engines and have been demonstrated to have a favorable effect on rotating-stall limits. Both devices, however, add weight and complexity to the engines and may introduce other performance penalties. Another way to provide stall-free operation is to use a compressor designed to operate stall-free at the highest flight speed desired by properly setting the blade angles, compressor flow areas, and number of compressor stages. In such a design, however, some penalties must be taken in take-off performance and compressor weight.

An example of the relative effects of these stall-preventive measures is shown in figure 9. Air flow per unit of engine or turbine frontal area is again plotted against flight Mach number for the compromise operating line and for the conventional constant-speed operating line. The solid portions of the curve are reproduced from figure 8, and the dashed portions of the curves indicate the flow obtained if rotating stall is eliminated. In the case of the constant-speed engine, it is assumed that stall is avoided by the use of compressor bleed; and in the case of the compromise or high-stress engine, it is assumed that stall is avoided by use of a compressor designed to be stall-free at a flight Mach number of 3.5. The effect of using a compressor (with the compromise operating line) designed to be stall-free over this wide range of flight speeds is a reduction in the air flow at flight Mach numbers less than 2.5. Compared with the flow that can be obtained if operation at flight Mach numbers above 2.8 is not required (upper solid line), a flow reduction of 20 percent at low speeds must be taken in an engine which operates stall-free up to a flight Mach number of 3.5. Even with this penalty the air-handling capacity of the engine with the compromise operating line is nearly the

same as that of the engine with the conventional operating line at low flight speeds; at high flight speeds where high thrust is of paramount importance, the compromise engine has about a 40-percent advantage in flow.

METHODS OF REDUCING TURBINE FRONTAL AREA

In figures 7 and 9 the engine air-handling capacity was limited by the frontal area of the one-stage turbine. As shown in figure 10, increasing the turbine blade root stresses or the number of turbine stages increases the air flow per unit of engine frontal area. At a flight Mach number of 2.8, where the one-stage-turbine engine with a blade stress of 50,000 psi has a flow of only 23 pounds per second per square foot of frontal area, an increase in air flow of 25 percent may be obtained at the same stress by using a two-stage turbine. A one-and-one-half-stage turbine (one stage with an outlet stator) will provide about a 12-percent increase in air flow over the one-stage turbine. The leveling off of the air-flow curve at a stress of 30,000 psi for the two-stage turbine is the result of limiting the turbine hub-tip ratio to a value of 0.5 for structural reasons. Although, as shown in figure 10, increasing the blade stress of a two-stage turbine to values higher than 30,000 psi does not increase the air-flow capacity, higher stresses are desirable because they permit the use of higher engine rotating speeds, which results in the use of a smaller and lighter compressor.

The beneficial effect on air-handling capacity of increasing the turbine-inlet temperatures is shown in figure 11. The flow through the turbine is limited by the Mach number of the gases leaving the turbine. At high turbine-inlet temperatures the temperature and pressure drop required across the turbine to drive the compressor decrease. Consequently, for the same turbine-exit Mach number, the high density and velocity of the gases at high turbine-inlet temperatures result in a greater turbine air-handling capacity. As shown in figure 11, at a compressor pressure ratio of about 3.0, which is in the range of interest at flight Mach numbers of 2.8, the air flow per unit of engine frontal area may be increased about 20 percent if the turbine-inlet temperature is increased from 1500° to 2500° F.

It is evident that, by the combination of one or more of these three design considerations, choice of a high flight Mach number design point (1.87 in the example shown) with an appropriate method of off-design operation, use of a high-flow turbine and compressor, and use of a high turbine-inlet temperature, the air flow per unit of engine (or turbine) frontal area may be increased from 50 to 80 percent compared with that of current-production engines. The principal advantage of such an increase in air flow is that it will result in a comparable reduction in engine weight for a given thrust requirement.

In order to achieve this weight advantage, it is necessary to operate the turbine at rotor-blade root stresses higher than those of current engines. Blade stresses as high as 50,000 psi will be required to provide the high air flows shown in the previous examples.

EFFECT OF TURBINE COOLING ON ALLOWABLE STRESSES

As shown in figure 12, the most promising method of providing for the necessary high turbine blade stresses is to cool the turbine blades. In this figure, the 100-hour rupture stress and yield stress are plotted against blade temperature for two typical materials, S-816 and Inconel X. Present-day turbojet engines have blade stresses of about 18,000 to 25,000 psi at blade temperatures of 1450° to 1500° F. In these engines the turbine blades are operated at conditions that leave little margin of safety even when good high-temperature blade materials are used. If the turbine blade temperatures are reduced to approximately 1200° F by some suitable cooling method, blade stresses of 50,000 psi can be tolerated with a good margin of safety.

A few experimental air-cooled blades have been run at high stresses by keeping the blade metal temperatures in the 1200° F range. Figure 13 shows one of these air-cooled turbine rotor blades made of a material similar to Inconel X. The cooling air flows from the blade root through an annulus formed by the blade shell and an insert and then is discharged at the rotor tips. This annular space is occupied by corrugated fin-like metal sheets. Extensive experimental research has been carried out on this type of blade, and it appears to be one of the best types of force-convention cooled blades. The particular blade shown was tested in a high-stress, single-stage, 2000° F inlet-temperature turbine. As indicated in the table on the figure, the blades were operated for approximately 40 hours at a root stress of over 40,000 psi. At the conclusion of the tests, the blade was removed from the engine in an undamaged condition.

From these experiences with the operation of turbine blades at high stresses and from the previously discussed analytical studies of engine design and component matching, it appears to be entirely feasible to design and build engines with an air-handling capacity well over 50 percent greater than that of our current-production engines.

COMBUSTOR DESIGN CONSIDERATIONS

Combustors designed to operate in these high-flow engines must provide efficient combustion under conditions of inlet pressure and velocity more severe than those in our current engines.

An example of the pressure and velocity environments is shown in figure 14. The reference velocity for combustors which will fit within the envelope of the compressor and turbine is plotted against flight Mach number for high-flow engines having one-, one-and-one-half-, and two-stage turbines. The reference velocity is defined as the volume flow per unit of combustor cross-sectional flow area. Also shown is a table listing some of the conditions of combustor-inlet temperature and pressure.

The required velocities vary from around 150 feet per second at low flight speeds to over 300 feet per second at high flight speeds. As indicated in the table, at flight conditions where the velocity is high, the pressure and temperature are also high; and where the pressure and temperature are low, the velocity is also low. To some extent, therefore, the pressure and velocity effects offset each other, but the combustor-inlet conditions are still extreme compared with current practice.

The performance of a JP-fueled combustor at inlet conditions corresponding to those for the high-flow, one-stage turbine engines in figure 14 is shown in figure 15. Although the combustor-outlet temperature in the experimental combustor was only 2000° F, the combustor temperature rise during the tests corresponded to that required for a 2500° F outlet temperature; and there is no reason to believe that similar performance could not be obtained at combustor-outlet temperatures of 2500° F. Even though the combustor tested was the culmination of a considerable development effort, adequate performance was obtained only at conditions simulating the very high flight speeds. At intermediate Mach numbers, the combustor efficiency fell off very rapidly. It may be concluded that at flight Mach numbers around 2.0 to 2.5 a more reactive fuel would be very beneficial.

A comparison of the performance of a combustor using the highly reactive hydrogen fuel with the JP-fueled combustor of figure 15 is shown in figure 16. With the hydrogen-fueled combustor the highly efficient range of operation is extended to flight Mach numbers of less than 1.5 at an altitude of 80,000 feet compared with a minimum Mach number for reasonable performance of about 2.5 for the JP-fueled combustor. In addition, the length of the hydrogen-fueled combustor is 30 to 40 percent less than that of the JP-fueled combustor. The hydrogen-fueled combustor, therefore, not only provides substantial improvements in combustion efficieny at the extreme combustor-inlet conditions required for advanced high-flow engines, but also permits the use of a shorter, lighter combustor with attendant weight savings in the combustor and throughout the rest of the engine due to shorter drive shafts, and so forth. In addition to these experiments with special combustors, a total of 60 hours of operation with hydrogen fuel was obtained on two engines, the J65 and the J71. Only minor modifications were made to the combustors and fuel systems. It was found that the combustor altitude limits were extended

from about 75,000 feet at a flight Mach number of 0.8 with JP fuel to over 90,000 feet (the facility limit) with hydrogen fuel. All other combustor characteristics such as ignition limits and acceleration characteristics were also improved. No major problems were encountered with the use of hydrogen fuel.

At some flight conditions, there may be problems associated with the flow of hydrogen from the fuel tanks to the combustor. These problems, which will be discussed in more detail in the following paper, lead to the question of whether the hydrogen-fueled combustor will be limited to the use of hydrogen alone. The hydrogen combustor shown in figure 16 has also been operated on propane. The efficiencies obtained were lower than those for hydrogen but would probably be adequate for relatively low-altitude use such as take-off and climb or training missions.

At the high combustor-outlet temperatures under consideration, adequate life of the combustor liner may be an important problem. A special structural design was developed for the hydrogen-fueled combustor to provide adequate liner cooling and strength. These features are illustrated in figure 17. The upstream end of the liner is constructed of independently supported channels that increase the liner rigidity and aid in directing the secondary air through slots in the sloping downstream walls of the liner. The slots in the liner are formed by the use of individual channels. In order to cool the downstream transition section, a small portion of the secondary air is bled behind a sloping shield placed about 1/4 inch from the housing walls. The combustor operated satisfactorily throughout the test program.

Pentaborane-Fueled Combustors

In addition to hydrogen there are other highly reactive fuels which may provide adequate combustor performance in these high-flow engines. Among these fuels are pentaborane, diborane, and ethyldecaborane. Some engine operating experience has been obtained with pentaborane as the fuel.

A J47 engine with modified combustors has been operated for short periods of time for the past few years with pentaborane fuel. It has been found that a disadvantage of using pentaborane is the formation of boron oxide, a product of combustion. The boron oxide forms as a viscous liquid which flows through the turbine and out along the tail pipe. A movie was taken during a typical run showing the boron oxide flow in the turbine and engine tail pipe. An artist's sketch of a typical scene from this movie is shown in figure 18. Streams of liquid boron oxide are shown flowing past the turbine tips and along the tail-pipe walls. At the conclusion of the tests, the walls of the tail pipe and exhaust nozzle were coated with a layer of glass-like solidified boron oxide, and some powdery deposits remained on the turbine blades.

The continual flow of liquid through the turbine is detrimental to turbine performance, as shown in figure 19. The solid point shows the turbine efficiency at the beginning of the run with JP-4 fuel. After the fuel system was switched over to pentaborane, the turbine efficiency decreased continually until after about 22 minutes of operation a drop in turbine efficiency of 4 percent had resulted. This decrease in efficiency, coupled with increased tail-pipe losses, resulted in an over-all loss in specific fuel consumption of 12 percent for the 22-minute run.

In contrast to the problems encountered when using pentaborane as a fuel in the main combustors, the use of pentaborane as an afterburner fuel may not introduce large problems. Limited experience with afterburners indicates that there is little if any deterioration in afterburner performance with time.

A total of about 1 hour of operating experience with pentaborane as an engine fuel has been accumulated, together with 10 or 15 hours with other boron-containing fuels (principally trimethylborate). Throughout this experience the liquid products of combustion have produced troublesome performance losses in the engine. The problems with application of pentaborane, however, do not appear insurmountable. It is entirely possible that as more fuel becomes available continued research with ingenuous combustor or engine designs or operation at higher turbine-inlet temperatures where the boron oxide liquid is less viscous may go a long way toward solving these problems.

Hydrogen-Fueled Afterburners

Advanced, high-air-flow engines will introduce extreme afterburner-inlet velocities as well as primary combustor velocities. A comparison of the performance of two afterburners at the inlet conditions required for high-flow engines operating at 80,000 feet is shown in figure 20. The JP-fueled afterburner is the culmination of about 10 years of afterburner research and represents about the best performance currently available. The hydrogen-fueled afterburner is the first experimental hydrogen-fueled afterburner investigated at the NACA Lewis laboratory. Both afterburners are large enough in diameter to largely eliminate consideration of scale effects in the performance comparison.

The hydrogen-fueled afterburner has about 10-percent higher combustion efficiency over the entire range of flight conditions investigated. In addition, the hydrogen afterburner has a lower internal pressure loss because no flameholders were used. One of the most significant results is that the hydrogen afterburner has higher performance with a reduction in afterburner length (and hence weight) of as much as 75 percent.

The improvement in performance of both the hydrogen-fueled afterburner and the primary combustor is, of course, due to the very high chemical reactivity of the fuel. It is conceivable that continued research will provide even higher combustion efficiencies and even shorter lengths.

EFFECT OF TURBINE-INLET TEMPERATURE ON PERFORMANCE

Previously it was shown that high turbine-inlet gas temperatures are beneficial in producing high air flows per unit of engine frontal area. In figure 21 the effect of turbine-inlet temperature on engine thrust and fuel consumption is shown at a flight Mach number of 3.0 for both afterburning and nonafterburning engines.

Comparison of the afterburning to the nonafterburning engine shows the thrust level of the afterburning engine to be higher over the entire range of turbine-inlet temperature. Associated with this increased thrust, however, is a higher specific fuel consumption. Increasing the turbine-inlet temperature for the afterburning engine from 1500° to 2500° F results in an 8-percent increase in thrust and a 10-percent decrease in specific fuel consumption. These gains can lead to a substantial improvement in airplane range.

At a turbine-inlet temperature of 2500° F, the thrust of the afterburning engine is still higher than that of the nonafterburning engine. This increase in thrust, however, is at the expense of a somewhat higher specific fuel consumption and also an increase in weight and system complexity due to the afterburner. At this value of turbine-inlet temperature, then, a choice of the two designs would depend on consideration of a particular engine, the airplane installation, and the flight mission.

It is evident that there is a considerable performance advantage to be gained for either the afterburning or nonafterburning engines by the use of turbine-inlet temperatures in the range from 2000° to 2500° F. In order to permit the turbine to operate at these high temperatures, there are several possible turbine-cooling methods.

TURBINE-COOLING METHODS

The cooling method most commonly used is to cool the turbine with compressor bleed air which, in turn, is cooled in a ram-air heat exchanger.

The manner in which the cooling temperatures vary with flight Mach number at both compressor inlet and exit is shown in figure 22. The shaded area represents the allowable blade metal temperatures for a stress of 50,000 psi. Turbine blade cooling with air bled at the compressor exit

becomes increasingly difficult as flight Mach number increases because of the rise in temperature of the cooling air. At a flight Mach number of 3.5, the air temperature is nearly as high as the allowable metal temperature. Such air can thus do little cooling.

The temperature of the compressor-discharge air can be lowered by rejecting heat to the ram air. But even the temperature of the ram air approaches the allowable blade temperature. Thus, use of a heat exchanger to cool the compressor bleed air to a value near ram temperature is seen to be of limited value for a flight Mach number near 3.5.

The amount of air required to cool both the turbine rotor and stator blades is shown in figure 23. The coolant is compressor bleed air that has been cooled in a heat exchanger by ram air. The coolant flow is expressed as a function of the engine air flow w_c/w_a. Two engines were considered; one has a turbine-inlet gas temperature of 2500° F and a one-stage turbine, and the other has a turbine-inlet temperature of 2000° F and a two-stage turbine. These temperatures are from 300° to 900° above those currently used. For these calculations the assumed average rotor-blade temperature was constant at 1250° F. A climb to 80,000 feet at a flight Mach number of 2 was assumed; the flight Mach number was then increased at constant altitude to a Mach number of 3. At a Mach number of 2, the coolant flows are 6 and 9 percent of engine air flow. At a Mach number of 3, the coolant flows are 12 to 14 percent and are rising rapidly. If the turbine is to be cooled by reasonable amounts of compressor bleed air above a flight Mach number of 2.5, some means must be provided for cooling this air that is more effective than a ram-air heat exchanger.

Use of Fuel as a Heat Sink

As discussed in the first paper, refrigerated JP-5, light hydrocarbons, and hydrogen all show promise as a good heat sink. One of the largest heat loads of the entire airplane will be that for cooling the turbine. It is, therefore, logical to make use of the fuel for this purpose, prior to burning it in the combustion chamber. As an example, figure 24 shows schematically a method of using hydrogen fuel for cooling the air bled from the compressor. The air is bled from the compressor discharge and passes through a heat exchanger where it is cooled by the hydrogen from the fuel tank. The temperature of the hydrogen entering the heat exchanger might be about -200° to -400° F, depending on its use before being piped to the engine. After cooling the air bled from the compressor, the hydrogen in a gaseous state flows to the combustor, where it is burned. The rotor-blade cooling air leaving the heat exchanger is ducted through the inlet struts in front of the compressor, through a hollow shaft, and into the turbine rotor and blades. The stator cooling air, in this case, comes out of the heat exchanger, flows through the

struts in the combustor-inlet diffuser, enters the stator blades at an inner radius, and leaves them at the tips. This type of system is not limited to hydrogen alone, but can be used with any fuel that provides sufficient heat capacity.

The amount of turbine cooling air required for an advanced turbojet engine using an air-cooling system such as this is shown in figure 25. Here again the coolant-flow ratio, or the fraction of the compressor air required for cooling, is plotted against the flight Mach number for a 2500° F engine with a single-stage turbine. The average cooling-air temperature was assumed to be constant at 240° F, and the average blade temperature was 1250° F. The required coolant-flow ratios for altitudes of 80,000, 60,000, and 40,000 feet are shown as well as an assumed condition of climb to 80,000 feet. The discontinuity in the curves occurs because the gas and air supply temperatures are maintained constant. This is in contrast with what occurred in figure 23, where the cooling-air supply temperature was increasing with flight speed. During the climb condition, the pressures in the engine are decreasing, and the coolant-flow ratio increases; at the constant-altitude condition, where the pressure is increasing with flight speed, the coolant-flow ratio decreases. The maximum coolant-flow ratio of 0.075 occurs at a flight Mach number of 2.0 at an altitude of 80,000 feet. This amount of air appears quite reasonable, especially when compared with the 12 to 14 percent required with the ram-air heat exchanger. (Thus it appears that with low cooling-air supply temperature acceptable coolant flow can be obtained for adequate cooling of high-temperature, high-stress engines even at a flight Mach number of 3.5.) The blade configuration, shown on the right in figure 25, used for the calculations of the coolant-flow requirements shown had the cooling effectiveness of a corrugated insert blade with very fine corrugations. Also, the heat-exchanger size required to provide this low-temperature cooling air is such that it could be located over the compressor and would not have to exceed an envelope described by a single-stage turbine.

Experimental Hydrogen-Cooled Turbine

In order to determine if this type of system is a practical way of operating the turbine at elevated temperatures, some full-scale engine tests were made. These tests also provided experimental data for checking the validity of the calculation methods used to determine the cooling-air requirements shown in the previous figures. The tests were conducted in an altitude facility using a J47 engine that was modified with various parts that were readily available. Hydrogen was used as the fuel. A schematic diagram of the setup is shown in figure 26. The fuel is stored as a liquid in large Dewar flasks and is forced through a conventional finned-tube heat exchanger, where it cools the air, and then flows in a gaseous state to the engine. It was burned in standard combustion chambers using modified fuel nozzles. Cooling air at about 60° F from one of

the laboratory systems was used. The cooling air flows through the heat exchanger and then into the turbine rotor through the tail cone. The stator blades were cooled directly by the laboratory air. In the interest of obtaining data at an early date, use was made of existing hardware in order to modify the engine. An air-cooled stator with corrugated insert blades was borrowed from another rig, and the air-cooled turbine rotor was one that had been built for a nonstrategic materials program. The air-cooled rotor blades, which were an early version of the corrugated insert blades, had been fabricated of a material which was about 97-percent iron. For this reason, the average blade metal temperature had to be kept between 900° and 1000° F, instead of the 1250° F temperature chosen for the better materials in the previous figures. The operating rotor-blade metal temperatures and the cooling-air supply temperatures at the base of the blades were obtained with the aid of a rotating thermocouple pickup mounted in the front of the engine.

A view of the turbine looking upstream from the rear of the rotor is shown in figure 27. The air-cooled turbine has a split-disk-type rotor, with the cooling air entering through a central hole in the downstream disk, flowing between the two disks into the blades, and then discharging into the main combustion-gas stream. The insert shows the cooling configuration of the blades. The external holes in the stator casing are the discharge ports for the stator cooling air.

The experimental average rotor-blade temperatures obtained are shown in figure 28. Temperature is plotted against rotor coolant-flow ratio. The top three curves are the average blade temperatures for three turbine-inlet gas temperatures, all substantially above those in current practice. The dashed curve is the cooling-air supply temperature at the base of the rotor blades. The rise in the cooling-air temperature at the low coolant-flow rates is due to the heat addition to the air from its passage through the engine tail cone and the turbine disk. For an average blade temperature of 1000° F, the required coolant-flow rate is 0.06 of the engine air flow for a turbine-inlet temperature of 2100° F. Recently, experimental runs have been made at a turbine-inlet temperature of 2500° F. Although data are not presently available for these tests, they indicate that a cooling system that utilizes the fuel as a heat sink is practical and that turbine-inlet temperatures of 800° to 900° F above those used in present engines may be obtained.

Use has been made of the data in figure 28 as well as for several other turbine-cooling tests to check the accuracy of turbine-cooling calculations. Figure 29 shows a comparison of calculated and measured temperatures for five different cooling-passage configurations over a range of gas temperatures from 1000° to 2100° F. The good agreement with the 45° line indicates that the analytical methods used in the calculated performance presented herein are accurate and reliable.

Closed Cooling System

There are other cooling methods that might offer some advantages in engine performance as well as more effective cooling. In the system shown in figure 24, the cooling air is taken from the cycle at the compressor discharge. The net result of this use of air for cooling is a slight decrease in both pressure and temperature in the exhaust nozzle. An alternate cooling system without these performance penalties is shown in figure 30. This scheme utilizes a closed system consisting of a good heat-transport fluid such as helium for cooling the turbine. This secondary coolant is, in turn, cooled in a heat exchanger by a fuel such as hydrogen. The secondary coolant comes out of the heat exchanger and flows through the rear bearing support and into the turbine rotor through suitable seals. The flow through the rotor blade is assumed to be out through an annulus next to the blade shell, returning through an insert in the blade to the center line of the engine. This flow is perpetuated by the natural pumping forces of the coolant. The secondary coolant then flows into the heat exchanger, where it is cooled by the hydrogen. The stator coolant flows in much the same type of path. It is conceivable that the hydrogen might be used directly in this same type of system, thus eliminating the need for the heat exchanger. The advantages of this system are that a fluid with better heat-transfer properties than air can be used and the effects of cooling losses on engine performance will be less than those which would occur with the direct-air system.

The amount of fuel required to cool the turbine for this closed system is shown in figure 31. The percentage of total fuel flow required to cool a 2500° F single-stage turbine over a range of flight Mach numbers and altitudes is shown. In these calculations the blade temperature was maintained constant at 1250° F, and a 1000° F temperature rise for the hydrogen fuel was assumed. The maximum flow of fuel required for cooling was only about 50 percent of the total. Thus it is evident that there is ample capacity for cooling the turbine to permit the use of high gas temperatures and have capacity left over for the various other cooling problems in the engine and airplane.

Engine Thrust Comparison

By the use of turbine blade cooling combined with the use of the superior cooling capacity of some fuels, high turbine blade design stresses (as much as 50,000 psi) can be attained, and, at the same time, turbine-inlet gas temperatures can be increased from 1500° or 1600° F to as high as 2500° F.

In order to summarize turbine cooling, figure 32 shows the thrust that can be obtained with turbine cooling. The bar graph shows the maximum thrust per pound of air flow attainable at a Mach number of 2.5 for

four nonafterburning engines. As a basis of comparison, the first bar shows the thrust for an uncooled engine with the conventional turbine-inlet temperature of 1500° F. Of course, large thrust gains can be realized in this nonafterburning case by raising the turbine-inlet temperature, as illustrated by the last three bars.

The thrust available depends on the kind of cooling system used. The second bar shows that, with the maximum practical inlet temperature of 2000° F obtainable by cooling the turbine with compressor bleed air which is, in turn, cooled by ram air, thrust is increased about 35 percent over that of the low-turbine-inlet-temperature engine.

By using hydrogen fuel as a coolant, rather than ram air, either through the medium of compressor bleed air or in a closed system, turbine-inlet temperatures up to 2500° F seem possible. With these systems, as shown by the last two bars, thrust gains of well over 100 percent are possible. The compressor bleed system has a slightly lower thrust than the closed system due to the bleed losses.

These thrusts are the thrust per pound of air flow and are purely thermodynamic gains which do not include the gains in air flow per unit frontal area that were discussed previously.

The final result, of course, is the performance obtained when the beneficial effects of high turbine-inlet temperatures are combined with the advantage of higher air flows per unit frontal area.

OVER-ALL PERFORMANCE OF ADVANCED ENGINES

The thrusts with combined high temperatures and high air flows are shown in figure 33. Thrust per unit of engine frontal area and specific fuel consumption are plotted against flight Mach number. In this illustration the frontal area of both the current and advanced engine was assumed to be 12 percent greater than the area at the turbine. This area was chosen because it was felt to be most representative of the area which is associated with engine weight. Two afterburning engines are considered, one a good engine of current design and the other an engine of advanced design. Although the advanced engine has only a small advantage in thrust at low flight Mach numbers, this advantage increases rapidly with Mach number until at Mach 2.5 the thrust per unit area of the advanced engine is more than twice that of the current engine. In addition, the advanced engine will only be about half as long as the current engine.

Of course, the interest in engine performance extends beyond thrust per unit area. Substitution of hydrogen for JP fuel affects specific fuel consumption as shown at the bottom of the slide. The higher heating value results in a 65-percent decrease in specific fuel consumption.

Thus, it is apparent that substantial improvements in engine performance are potentially obtainable. These gains may result from the following changes in engine design: high turbine-inlet temperature, high flow at high flight Mach number, and use of hydrogen as a fuel. In terms of engine weight, which is the variable of primary importance in high-altitude, high-speed applications, the advanced engine would be less than half as heavy as the current engine for the same thrust at a flight Mach number of 2.5.

Although it is obvious that an extensive development effort would be required to produce an engine of this advanced design, it is equally obvious that the potential performance gains would make such an effort well worth while.

ADVANCED TURBOJET ENGINE

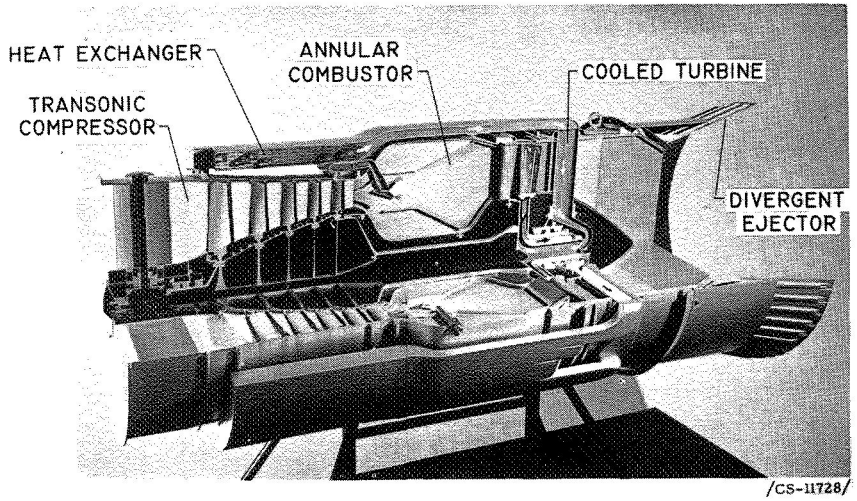

Figure 1

COMPRESSOR AIR FLOW

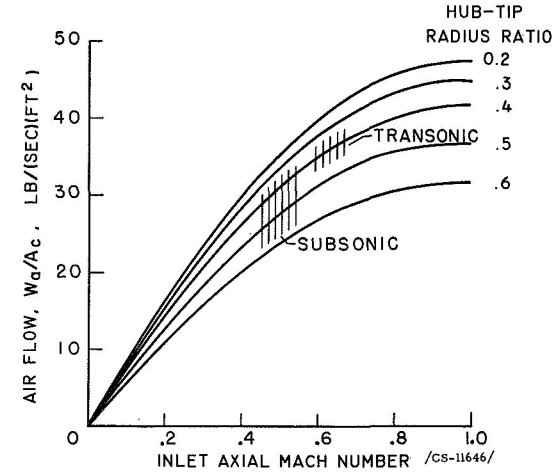

Figure 2

TYPICAL TRANSONIC COMPRESSOR MAP

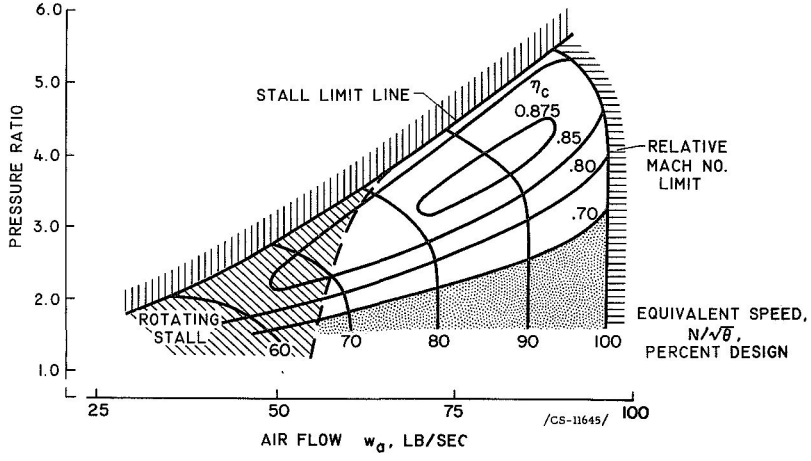

Figure 3

EFFECTS OF INLET FLOW DISTORTION

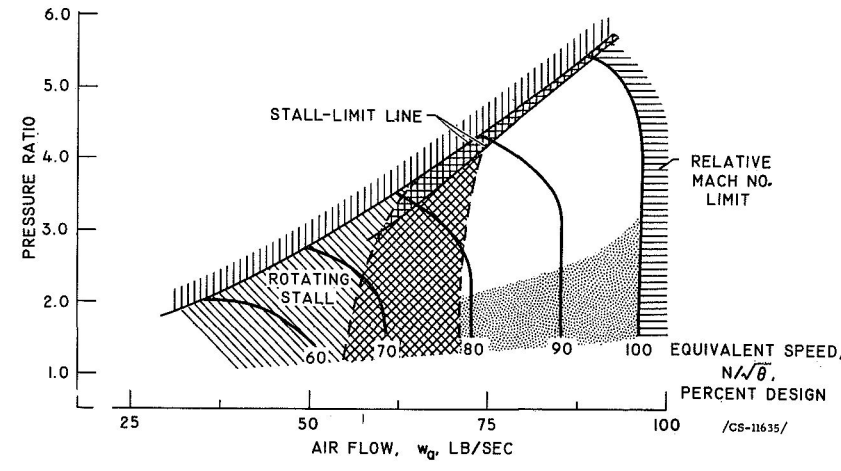

Figure 4

COMPRESSOR OPERATION AT CONSTANT EQUIVALENT SPEED

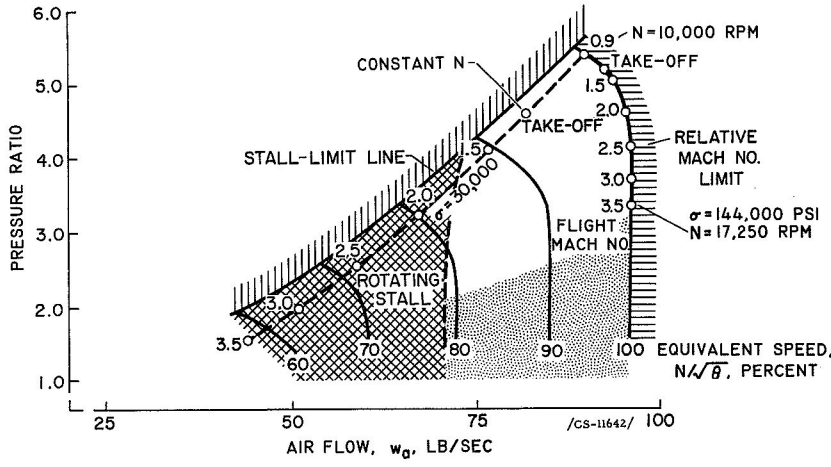

Figure 5

COMPROMISE COMPRESSOR OPERATION

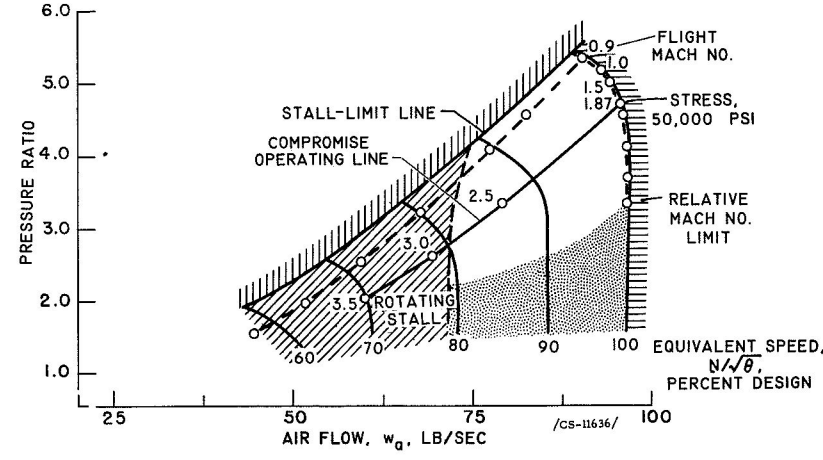

Figure 6

HIGH AIR FLOW AT HIGH FLIGHT MACH NUMBER

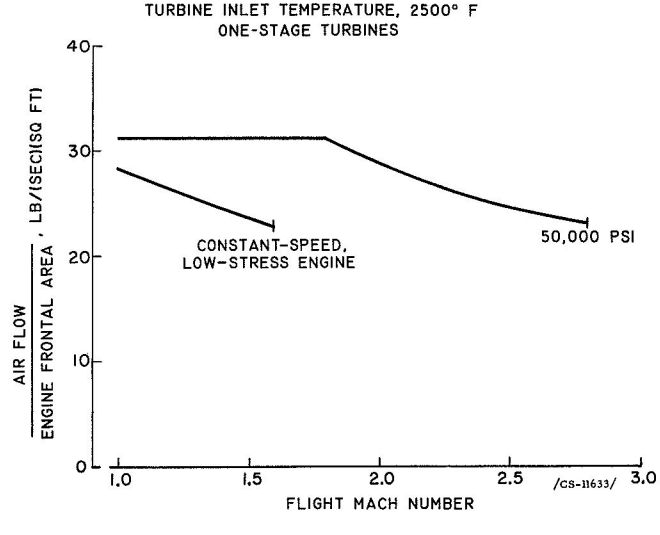

Figure 7

ENGINE SCHEMATIC

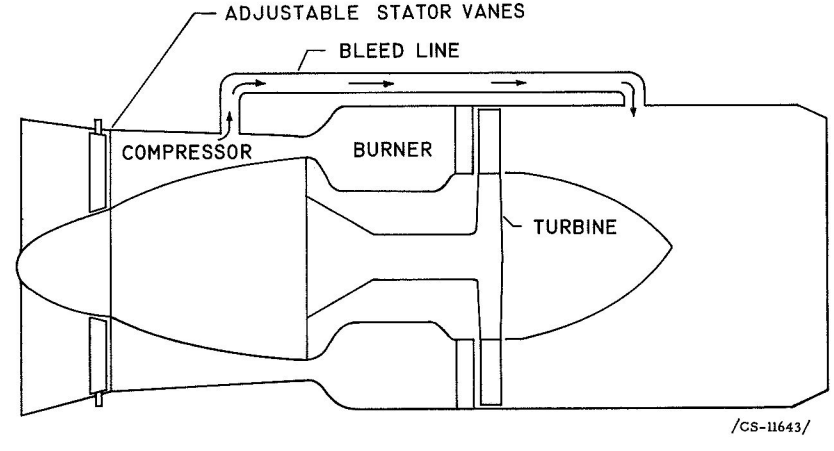

Figure 8

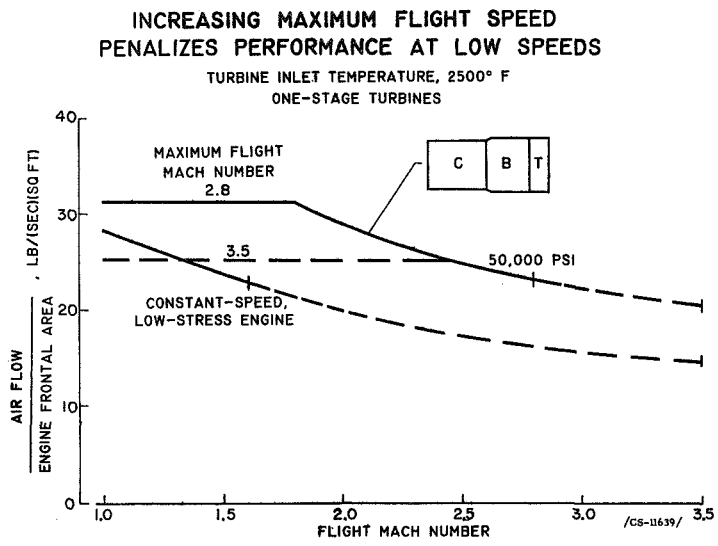

Figure 9

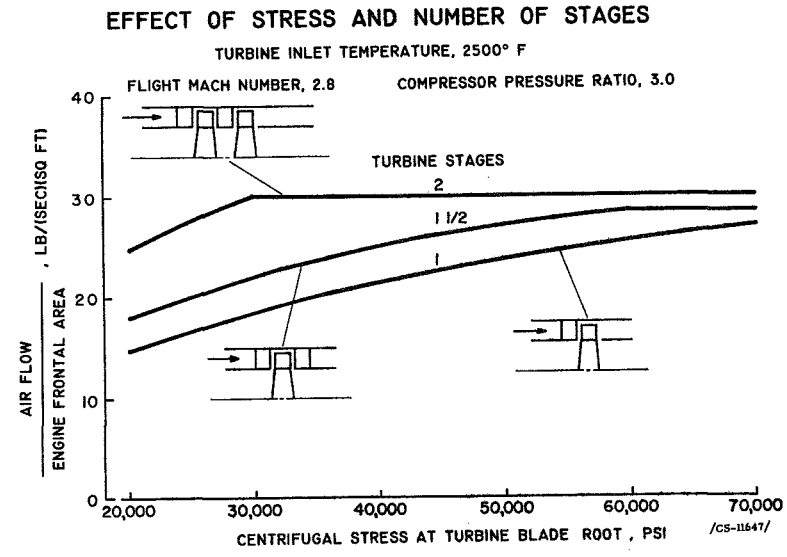

Figure 10

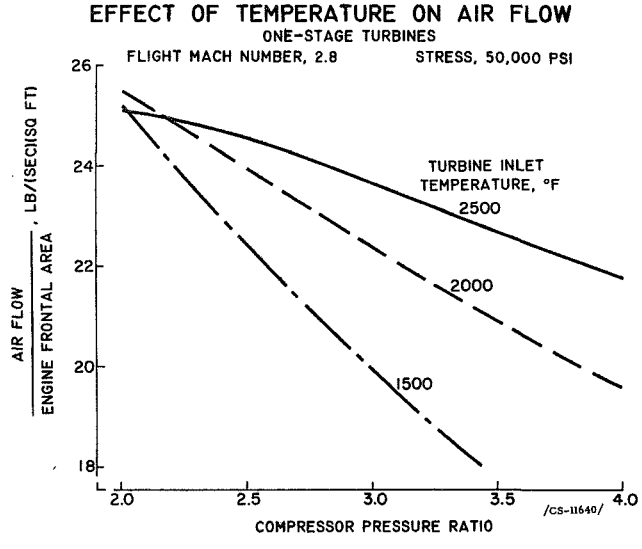

Figure 11

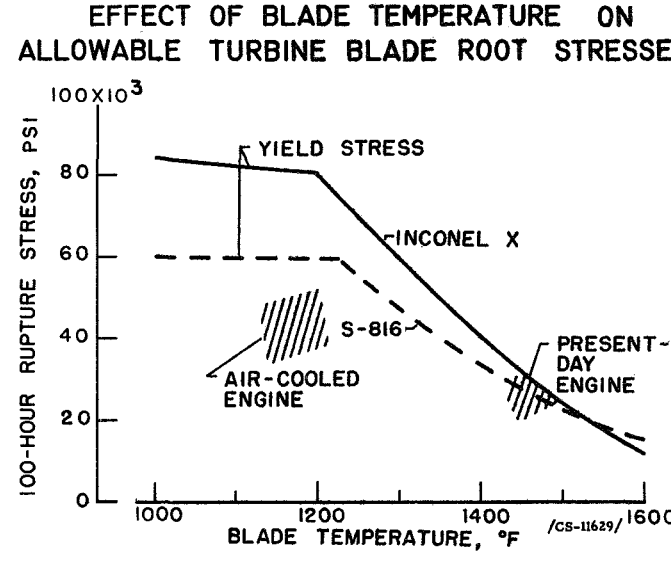

Figure 12

EXPERIMENTAL HIGH-STRESS AIR COOLED BLADE

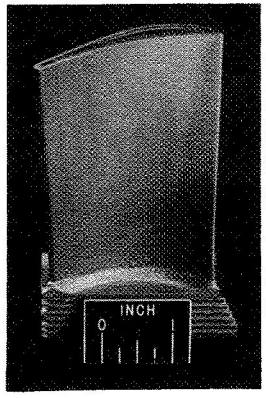

OPERATING CONDITIONS

ROOT STRESS PSI	ROOT TEMPERATURE °F	AVERAGE BLADE TEMPERATURE °F	RUNNING TIME HR
40,000	1050	1250	28
42,000	1100	1300	$\frac{13}{41}$ *

/CS-11627/

*BLADE UNDAMAGED

Figure 13

EFFECT OF TURBINE DESIGN AND FLIGHT MACH NUMBER ON COMBUSTOR REFERENCE VELOCITIES

TURBINE INLET TEMPERATURE, 2500° F ALTITUDES ABOVE 36,000 FEET

FLIGHT MACH NUMBER	COMBUSTOR INLET TEMPERATURE, °F	COMBUSTOR INLET PRESSURE, PSIA	
		50,000 FT	80,000 FT
0.9	280	11.3	2.8
2.0	655	44.3	10.8
3.5	1305	184.2	44.7

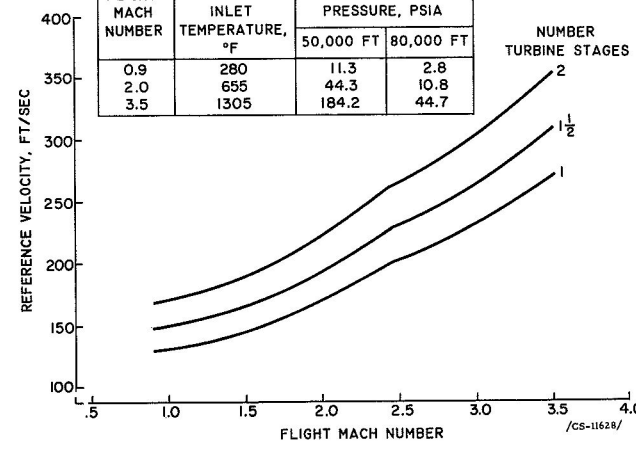

Figure 14

OPERATION OF EXPERIMENTAL COMBUSTOR USING JP FUEL

1-STAGE TURBINE, 80,000 FEET OUTLET TEMPERATURE, 2000° F

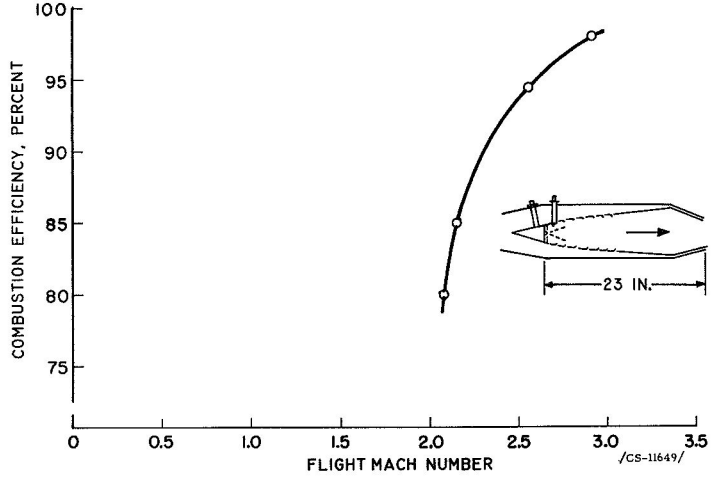

Figure 15

COMPARISON OF PRIMARY COMBUSTORS USING HYDROGEN AND JP FUELS

1-STAGE TURBINE, 80,000 FEET OUTLET TEMPERATURE, 2000° F

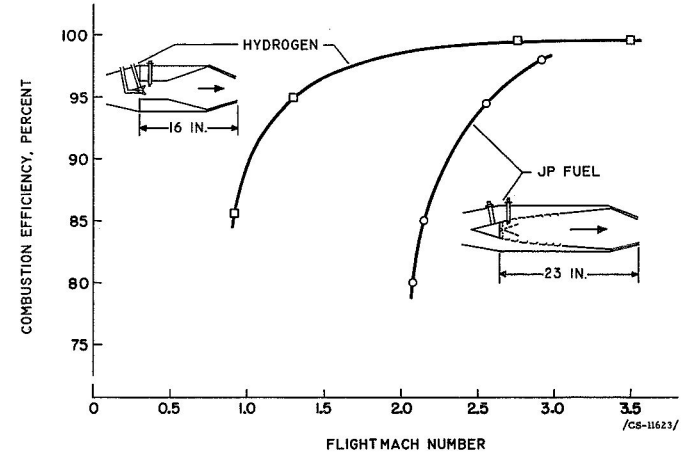

Figure 16

EXPERIMENTAL HYDROGEN-FUELED COMBUSTOR
OUTLET TEMPERATURE, 2000° F

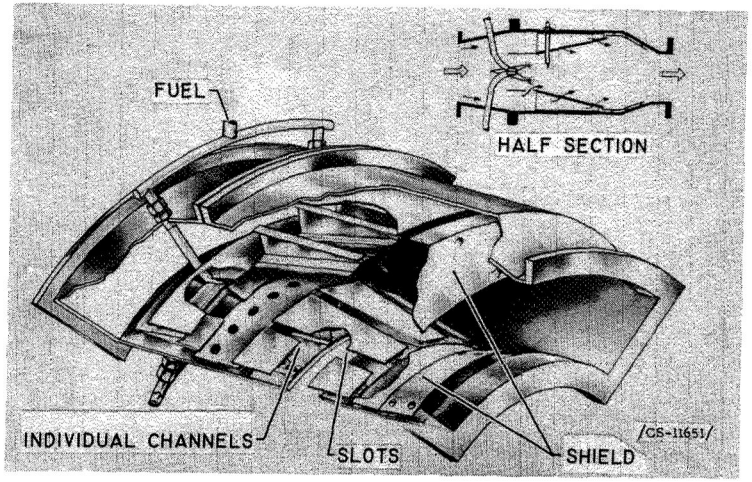

Figure 17

BORON OXIDE FLOW THROUGH TURBINE ROTOR INTO ENGINE TAIL PIPE

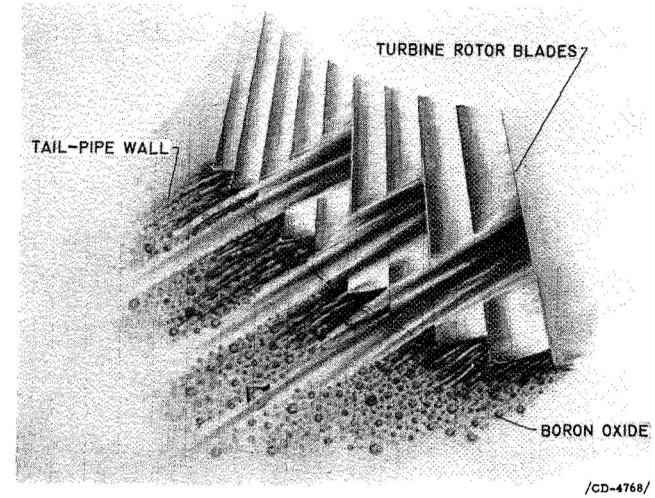

Figure 18

TURBINE EFFICIENCY LOSSES WITH PENTABORANE FUEL

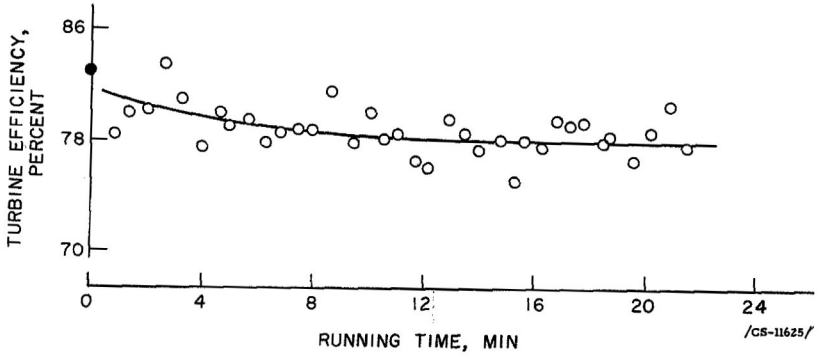

Figure 19

COMPARISON OF AFTERBURNERS USING HYDROGEN AND JP FUELS
2-STAGE TURBINE, 80,000 FEET
OUTLET TEMPERATURE, 3000° F
MAX. AFTERBURNER INLET VELOCITY, 675 FT/SEC

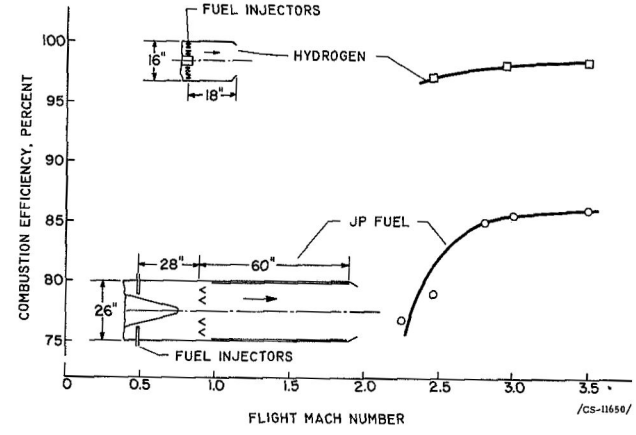

Figure 20

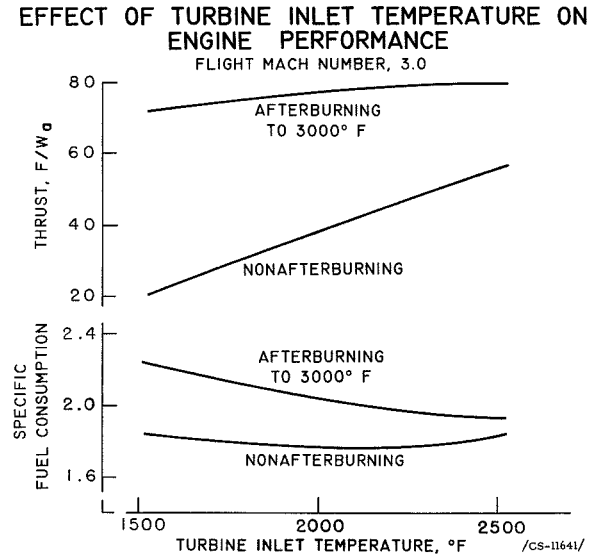

Figure 21

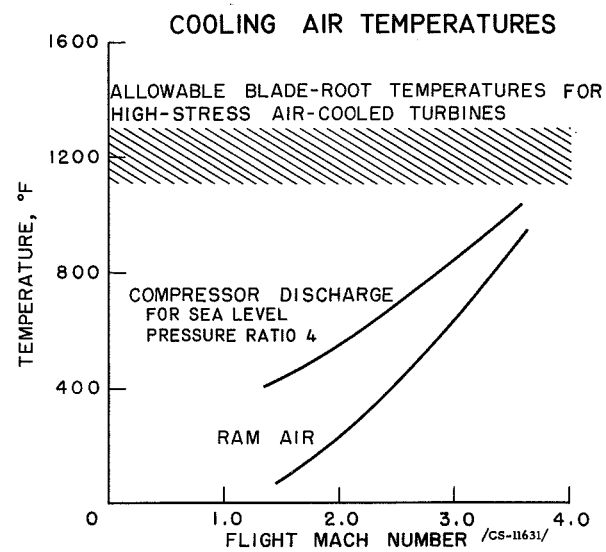

Figure 22

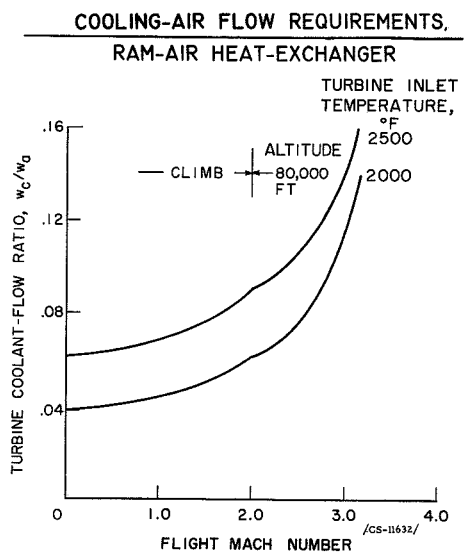

Figure 23

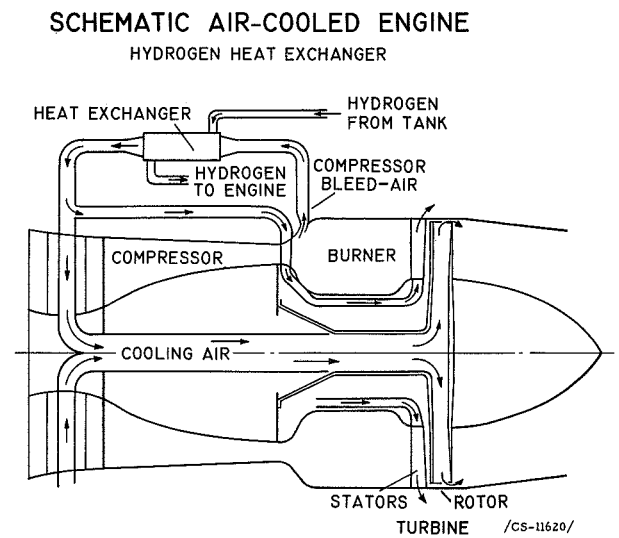

Figure 24

COOLING-AIR REQUIREMENTS WITH HYDROGEN HEAT EXCHANGER

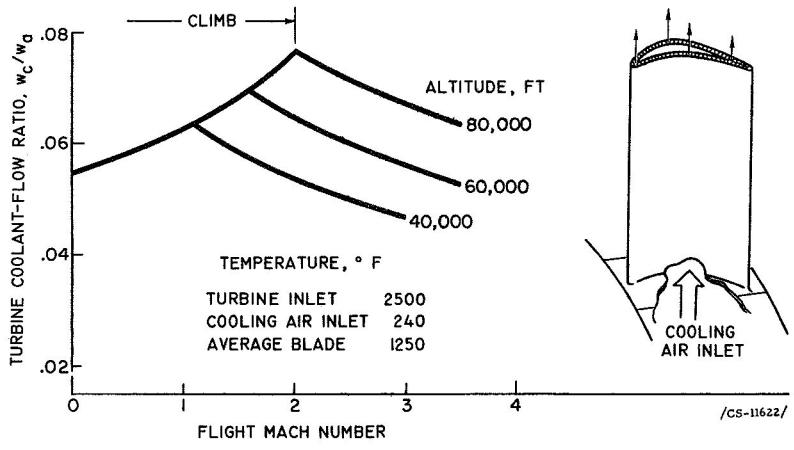

Figure 25

SCHEMATIC EXPERIMENTAL ENGINE TEST SET-UP

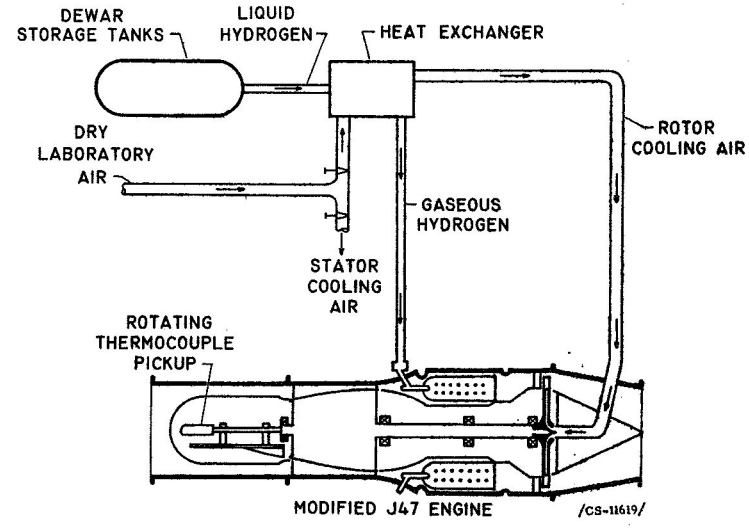

Figure 26

EXPERIMENTAL AIR-COOLED TURBINE

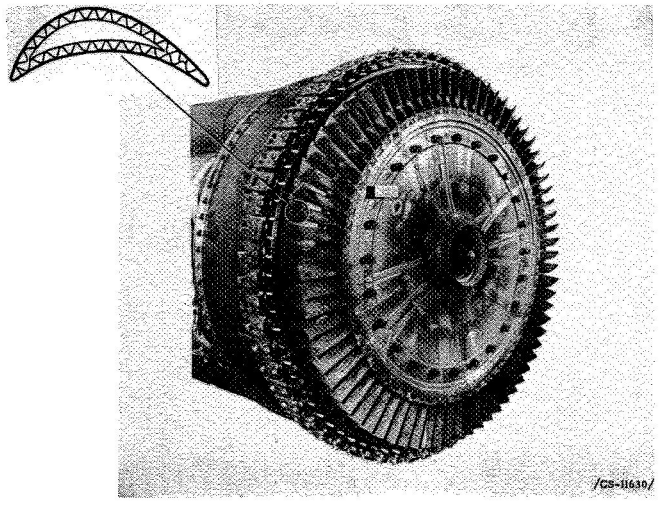

Figure 27

EXPERIMENTAL TURBINE ROTOR BLADE TEMPERATURES USING AIR-TO-HYDROGEN HEAT EXCHANGER

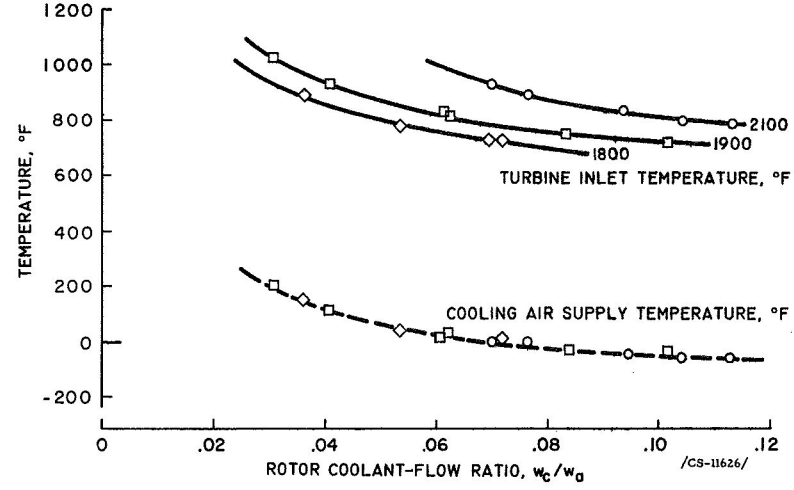

Figure 28

COMPARISON OF CALCULATED AND MEASURED
BLADE TEMPERATURES FOR 5 COOLING CONFIGURATIONS

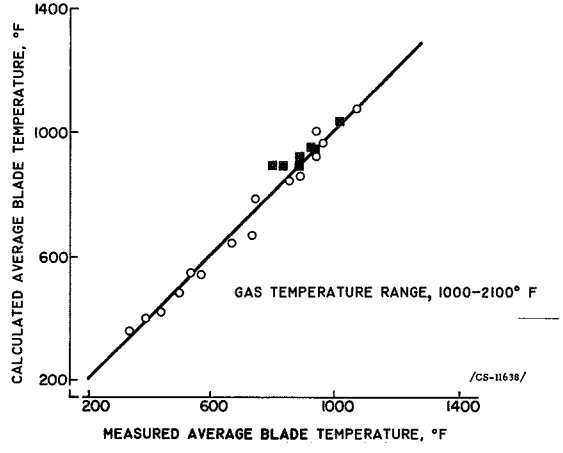

Figure 29

SCHEMATIC COOLED ENGINE
HYDROGEN TO SECONDARY COOLANT HEAT EXCHANGER

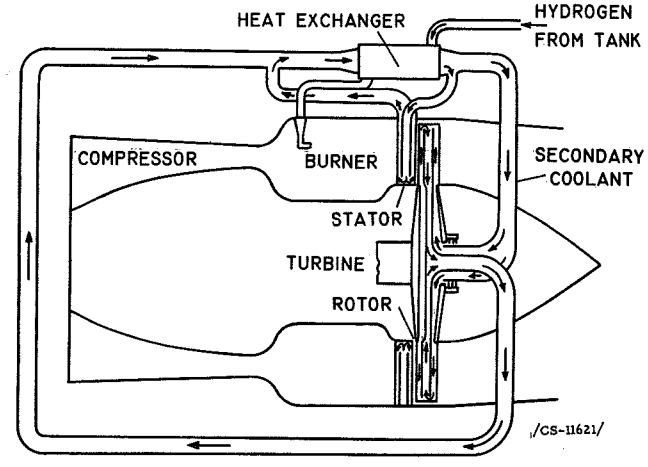

Figure 30

FUEL FLOW REQUIREMENTS FOR TURBINE COOLING

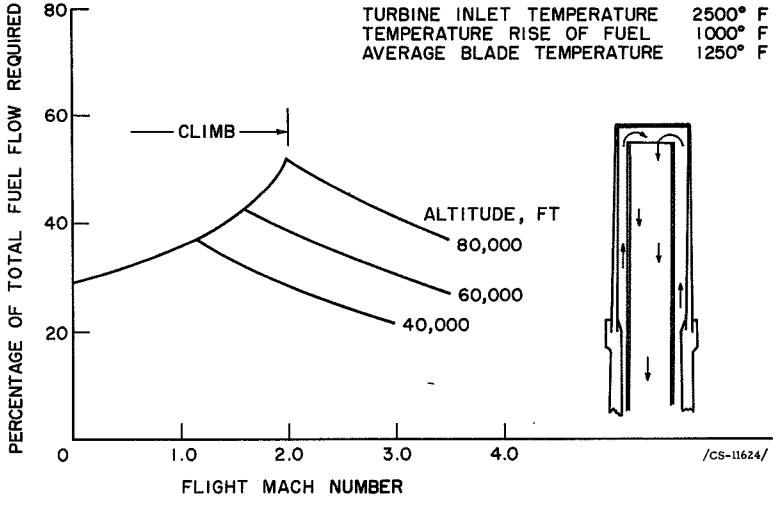

Figure 31

ENGINE PERFORMANCE SUMMARY
NONAFTERBURNING ENGINES
FLIGHT MACH NUMBER, 2.5

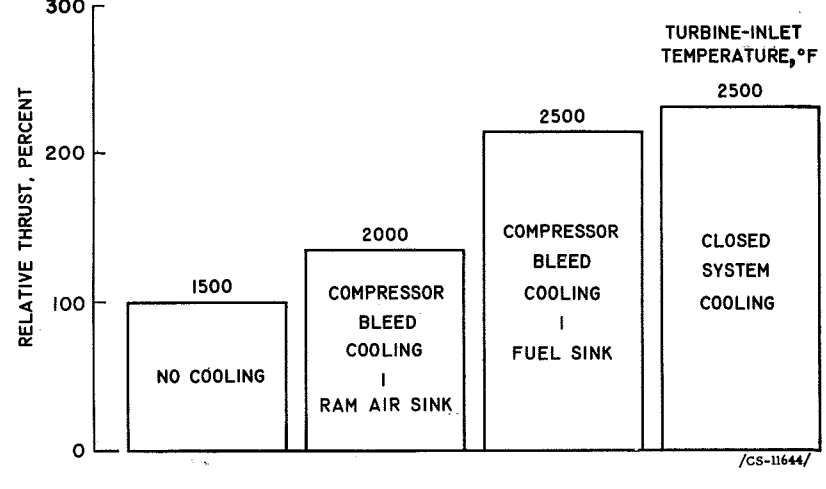

Figure 32

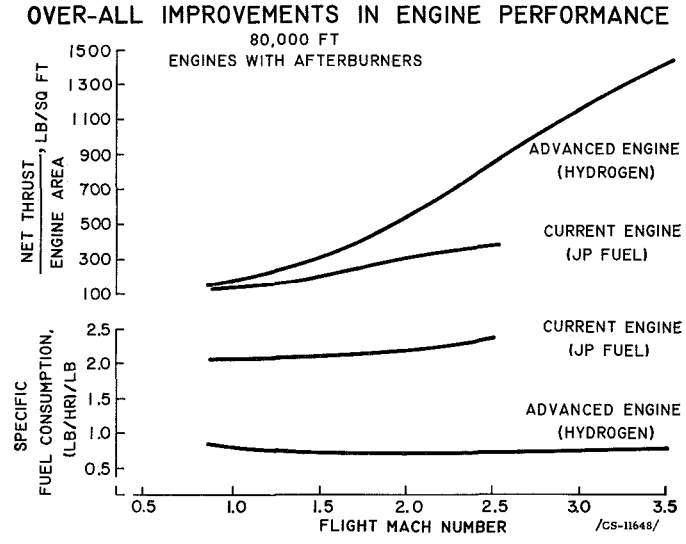
OVER-ALL IMPROVEMENTS IN ENGINE PERFORMANCE
80,000 FT
ENGINES WITH AFTERBURNERS
NET THRUST / ENGINE AREA, LB/SQ FT
1500
1300
1100
900
700
500
300
100
ADVANCED ENGINE (HYDROGEN)
CURRENT ENGINE (JP FUEL)
SPECIFIC FUEL CONSUMPTION, (LB/HR)/LB
2.5
2.0
1.5
1.0
0.5
CURRENT ENGINE (JP FUEL)
ADVANCED ENGINE (HYDROGEN)
0.5
1.0
1.5
2.0
2.5
3.0
3.5
FLIGHT MACH NUMBER
/CS-11648/

Figure 33

3. OVER-ALL TURBOJET SYSTEM AND AIRCRAFT PERFORMANCE

J. Howard Childs, Chairman
Wilson B. Schram
Hugh M. Henneberry
Thaine W. Reynolds
Eldon W. Hall

3. OVER-ALL TURBOJET SYSTEM AND AIRCRAFT PERFORMANCE

INTRODUCTION

The unusual physical and chemical properties of some of the high-energy fuels make them more difficult to handle than conventional jet fuel. The additional complexities and added weight of the aircraft fuel system and the various problems associated with the application of each of these fuels must be taken into account in any over-all evaluation of the merit of a given fuel.

The object of this paper is twofold: First, to examine the fuel-system requirements and some of the problems of application of high-energy fuels; second, to present values of calculated aircraft performance in order to show the relative performances of JP-5 and the high-energy fuels for several different flight missions. The aircraft-performance calculations will draw upon the data presented in this paper on fuel-system weights and the data of the preceding paper on engine design. These calculations will serve to demonstrate the pay-off that is available in terms of flight range, target altitude, and other performance factors of the aircraft as a result of the new developments in engines and in high-energy fuels.

FUEL SYSTEM FOR LIQUID HYDROGEN

Physical Properties of Hydrogen

First, hydrogen fuel will be considered, since it represents the fuel possessing the most unique properties and the properties most widely different from those of JP-5 fuel. Some of the problems associated with the use of liquid hydrogen as a fuel are indicated in figure 1, which shows some of the physical properties of hydrogen. The boiling temperatures are, of course, very low. Because of the large temperature gradient between the surroundings and the liquid in the tank, insulation is required to maintain the heat leak into the tank at a low level.

A second problem associated with hydrogen is the low liquid density. At a pressure of 14.7 pounds per square inch absolute, the saturated liquid has a density of 4.42 pounds per cubic foot, or less than 1/10 the density of JP-5 fuel. Consequently, a large tank volume will be required.

Still another problem associated with hydrogen is indicated by the steep slope of the curve of liquid density against pressure. As the tank pressure increases from 15 to 30 pounds per square inch absolute, the saturated liquid temperature rises 4° F. Accompanying this increase in liquid temperature, the density of the liquid decreases by more than 4 percent. This comparatively large change in liquid density occurs because

the liquid is near its critical temperature. This means that if the fuel tank is filled at a pressure of 1 atmosphere and is then sealed off, allowing the pressure in the tank to build up, the expansion of the liquid would cause a rupture of the tank. To avoid this, there are two obvious possibilities: One is to allow space in the tank in order to provide for expansion of the liquid. The other is to vent the tank so as to maintain constant pressure and prevent liquid expansion. With the vent open, of course, the vapor will escape as rapidly as it is formed in the tank until the engines are started.

With just this brief look at some of the important physical properties of liquid hydrogen, some of the design features that must be employed in the tank for carrying this fuel can be examined.

Aircraft Tank Design

Several different possibilities present themselves for the design of an aircraft tank for liquid hydrogen. One possible tank design is indicated in figure 2. The liquid hydrogen is contained inside of a thin-wall metal tank. The tank will be pressurized because this helps the light-gage tank retain its shape and also provides the fuel pressure necessary for injection into the engine at high-altitude flight conditions. Outside the thin metal wall is a layer of insulation to reduce the heat leak into the tank. The annular space between the outer surface of the insulation and the fuselage will provide additional tank insulation. Insulating materials are available that have sufficient compression strength to support the tank weight plus any acceleration forces on the tank and transmit the resulting loads to the fuselage of the aircraft. One means of supporting the tank would be to use a system of webbing. Of course, many other possibilities exist for the design of a liquid-hydrogen tank, but a more detailed discussion is considered beyond the scope of this paper.

Tank Materials

Metals. - The hydrogen tank of figure 2 is essentially a large-diameter pressure vessel, and in order to keep the metal weight down it must be designed to fairly high stress values. Brittleness is a major concern with structural materials for the low temperature range required here. The nonferrous metals and the 300-series stainless steels are satisfactory in this respect, while plain steel is not. Figure 3 (refs. 1 and 2) shows the yield strengths of 301 and 316 stainless steels, 2024-T aluminum, and monel at temperatures down to the normal liquid-hydrogen boiling point. These curves indicate a marked increase in yield strength at these low temperatures. Yield-strength values of near 150,000 psi can be obtained by a hardened 301-series stainless steel.

The ductility of these alloys in this temperature range may decrease 30 to 40 percent from room-temperature values. The values are still satisfactory, however, and the impact strengths for all these materials have been little affected by this reduction in temperature (refs. 1 and 2).

None of these materials appear to show susceptibility to hydrogen embrittlement at the temperatures and pressures considered here.

Some of the technology developed for the construction of lightweight tanks for long-range rocket missiles can be used effectively here. Large tanks have been fabricated from hardened 301 stainless steel in metal gages near 0.025. Using the 150,000 psi yield-stress value, this metal thickness would provide a fuel tank for one of the supersonic airplanes to be discussed later with a safety factor of 2 at a working pressure of 30 pounds per square inch. The weight of the metal shell alone would be about 8 percent of the fuel weight. For a manned airplane, it might be desirable to increase this safety factor. Doubling it, to 4, would increase the shell weight to about 17 percent of the fuel weight, with a resultant reduction in airplane range of about 6 percent.

Insulation. - The requirements for the insulation are low thermal conductivity, low vapor permeability, low density, and good compressive strength. This combination of properties has led to the consideration of foamed plastics as the materials which best meet all these requirements. Properties of one such material, a typical polystyrene foam, are indicated in figure 4 (ref. 3).

These foams can be made in densities less than $1\frac{1}{2}$ pounds per cubic foot. The physical properties vary with the foam density, the lower-density materials having lower strength and lower thermal conductivity. For foams in the range 1.3 to 2.0 pounds per cubic foot, the compressive strength at room temperature may vary from 10 to 35 pounds per cubic inch. The cell structure of these foams is discontinuous, and, as a result, they have negligible vapor permeability.

Insulation Thickness

Various factors must be considered in selecting the thickness of the fuel-tank insulation. For one thing, the amount of insulation will determine how long the airplane can be stored after fueling without losing too much fuel; the thicker the insulation, the longer the storage time. Also, the rate at which fuel is vaporized in flight must be considered. As discussed in the preceding papers, the fuel should be burned as a vapor in the engine; however, sufficient insulation must be provided so that the fuel does not vaporize in flight faster than the engines use it. Also the fuselage surrounding the tank will be colder than normal, so there may be problems with condensation of moisture and ice formation.

[redacted]

These things call for thicker insulation. On the other hand, if there is more insulation than needed, the aircraft will be penalized, because of added weight and volume required for the tank.

Ground-storage time. - As soon as the aircraft tanks are filled, heat begins to flow from the surroundings into the fuel. This heat must either go into vaporization of a portion of the liquid or into raising the liquid temperature.

If the fuel tanks are filled with liquid hydrogen at its saturation temperature at 1 atmosphere, the liquid will begin to boil unless the tank pressure is allowed to increase. The higher the tank pressure is allowed to rise, the longer will be the time before the liquid begins to boil and fuel is lost by vaporization. This time is called the "no-loss time." After the tank pressure has built up to the design value, no further increase in liquid temperature can be permitted; therefore from that point on, all the heat flow into the tank must be taken up by vaporization of fuel. This fuel vapor must then be vented until the engines are started.

Obviously, as the insulation thickness is increased, the heat flow into the tank is reduced, and so the no-loss time is increased. Figure 5 shows values of the no-loss time for two different fuel-tank sizes with various insulation thicknesses. These tanks are representative sizes for the bomber and fighter airplanes to be discussed later. The configurations for which these calculations were made had a 6-inch annular air space between the insulation and the fuselage. The time values are obtained for an allowed pressure rise to 30 pounds per square inch absolute. The liquid expands as the tank pressure and the liquid temperature increase, and expansion space must be allowed in the tank, as previously noted. Thus, to have a period of time in which no vapor is escaping, the tank cannot be filled.

An alternative procedure that can be followed is to use the same tank size as that required for the foregoing procedure, but more fuel must be added in the tank than is required at take-off in order to fill the expansion space. The extra liquid can then be allowed to evaporate. After the excess liquid fuel has evaporated, the tank vent can be closed as before to let the heat leak into the tank build up pressure. Then there is the same amount of fuel at take-off as in the first case. Figure 6 shows the longer ground-storage time obtained with this procedure. By filling the 8-percent-expansion volume and allowing this extra amount of fuel to vaporize, the storage time on the ground has been increased by a factor of about $2\frac{1}{2}$. The interceptor tank, for example, with 2 inches of insulation, which had $2\frac{1}{2}$ hours of no-loss time, now can stand for over 6 hours before take-off or topping and refueling is required.

[redacted]

Fuselage temperatures of stationary aircraft. - Figure 7 shows some calculated equilibrium fuselage temperatures for a stationary airplane with liquid hydrogen in the fuel tank. As indicated in the sketch, the tank is insulated with a layer of polystyrene foam insulation, and there is a 6-inch air gap between the insulation and the fuselage.

Values of the fuselage temperature are shown for several different thicknesses of insulation. With a 3-inch layer of insulation the fuselage temperature is always about 20° F below the ambient temperature. With 1 inch of insulation this temperature difference is about 40° F. These low skin temperatures, of course, present a problem from condensation of moisture and possible ice formation.

Ice formation on aircraft. - Figure 8 presents values of icing rate for the case where the aircraft are standing on the runway. Rain was assumed because the most severe icing conditions occur when rain is falling. When it is not raining, the high icing rates indicated on this figure will not be encountered because neither water vapor nor fog droplets can contact the aircraft surfaces at a sufficient rate to produce this much ice. Two curves are shown; the upper curve is for a large hydrogen-fueled aircraft, and the lower curve is for a JP-5 fueled aircraft of the same size and configuration. In calculating the icing rate for the hydrogen-fueled aircraft, fuel-tank insulation consisting of a 3-inch layer of polystyrene foam plus a 6-inch air gap was assumed. For the hydrogen-fueled airplane, ice is formed at ambient temperatures up to 52° F. For ambient temperatures below 32° F, there is the familiar case of the freezing rain, and ice is formed on even the conventional airplane. Under freezing-rain conditions, the icing rate on the hydrogen-fueled airplane exceeds that for the conventional airplane by 7.8 pounds per minute. This value is, of course, specific for the particular aircraft size assumed; these calculations are for the case of large bombers. The extension of these icing curves to ambient temperatures below 20° F is indicated by dashed lines; the probability of encountering rainfall at these very low temperatures is not very great. However, rain has been recorded in rare instances at such low ambient temperatures in cases where a sharp inversion in temperature existed near the surface of the earth.

If the aircraft are allowed to stand on the runway in freezing-rain conditions for a period of 2 hours, then the hydrogen-fueled airplane will pick up about 1000 pounds of ice in addition to any ice that would be formed on the conventional aircraft at the same time. Of course, there are means for coping with ice formation while the aircraft are on the runway. For example, sheltering aircraft with large tarpaulins when rain is falling will eliminate the greater part of this ice. However, such schemes as this add to the over-all complexity of the system that is necessary when liquid-hydrogen fuel is used. It may also be possible to live with this problem by taking off soon after filling the fuel tanks on cold rainy days.

Calculations show that once the hydrogen-fueled aircraft are off the runway, the icing problem is no longer important. This is true because the hydrogen-fueled aircraft have such high values of thrust at low altitudes that they can attain high Mach numbers or high altitudes in a very brief period of time.

Fuel vaporization in flight. - Figure 9 shows the ratio of fuel vaporized in the tank to fuel used by the engines for various amounts of tank insulation. The two curves are intended to bracket the probable range of fuel-tank size and shape to be expected with various aircraft types and missions. The fuel-vaporization rate must be maintained between the upper and lower limits indicated on the figure. The upper limit exists at the point where the rate of fuel vaporization from the tanks equals the fuel flow rate to the engines. The lower limit exists because sufficient fuel must be vaporized to maintain tank pressure as liquid fuel is being used from the tank. For a tank pressure of 30 pounds per square inch absolute, the lower limit occurs when the ratio of fuel-vaporization rate to engine fuel flow is 0.035, which is the ratio of density of the vapor to density of the liquid. For the airplanes to be discussed later the thicknesses of insulation required are, in general, smaller from this consideration than would be selected on the basis of good ground-storage requirements.

It perhaps looks peculiar, at first, that the curve for the supersonic plane should be lower than the curve for the subsonic one because of the higher temperatures of the airplane fuselage at high speeds. The ordinate, however, is related to engine fuel flow rate, and the much higher flow rates for the supersonic speeds account for this.

It has been mentioned by the preceding paper that this hydrogen can be used to advantage as a heat sink for both engine and airplane cooling. Actually, the amount of available refrigeration lost by vaporizing fuel in the tank is small, since the latent heat is less than 4 percent of the total enthalpy available in going to 1000° F with the fuel.

Fuselage and insulation temperature in flight. - As the airplane goes to higher speeds the fuselage temperatures of the airplane will increase. The temperatures attained by the fuselage at high Mach numbers might place a restriction on the use of the foamed-plastic insulation. Present temperature limit of this material for continued use is about 200° F. Figure 10 shows the approximate fuselage temperature that would be expected near the fuel tank for different Mach numbers and a flight altitude of 80,000 feet. These temperatures are calculated for an outer-wall emissivity of 0.6. The upper curve shows the recovery temperature. The next lower curve shows the equilibrium fuselage temperature.

Above Mach numbers of about 2.2 the fuselage temperature exceeds the allowable temperature limits of the insulation. However, with the

additional insulation that is provided by the air space between the foam insulation and the fuselage, the surface temperatures of the insulation are considerably below the fuselage temperature. The insulation surface temperature is shown by the bottom two curves for 3-inch and 1-inch layers of insulation.

Figures 9 and 10 show that at higher speeds, the insulation thickness can be less as far as flight requirements are concerned. However, with less insulation, ground-storage time is sacrificed, as shown by figures 5 and 6. Thus, it appears that tank insulation consisting of 1 to 3 inches of polystyrene foam surrounded by an air gap of 6 inches will provide acceptable tank performance on all counts. The main factor determining the desirable insulation thickness for any given case is the required storage time of fuel in the aircraft tank prior to take-off.

Tank Weight

For a tank fabricated of 0.024-inch stainless steel and having a 3-inch layer of polystyrene foam, the over-all weight of the tank shell, the insulation, the bulkheads inside the tank, and the tank-supporting structure amounts to only 15 percent of the fuel weight for a long-range supersonic bomber. This gives a design tank pressure of 30 pounds per square inch absolute with a safety factor of 2. Other organizations have also made analytical studies of the required tank weight (refs. 4 and 5). They too have arrived at a tank weight of about 15 percent of the fuel weight, even though their proposed tank designs were somewhat different from the one presented here.

Fuel Systems for Lower Flight Altitudes

A 30 pounds per square inch absolute pressure in the main fuel tank is only sufficient to supply fuel to the engines at high-altitude flight conditions. As previously mentioned, some additional system must be used to provide a fuel at the higher pressures required during take-off and let-down of the aircraft (and also for cruise, if the flight altitude is not sufficiently high to give combustor pressures well below the 30 lb/sq in. abs tank pressure). One possible technique for accomplishing this is to develop a liquid-hydrogen pump capable of supplying the necessary pressures. The pressure developed by a centrifugal pump is proportional to the density of the fluid to be pumped. Because of the low density of liquid hydrogen, either a high rotational speed or a multistage pump will be required to develop an adequate fuel pressure. Hence, the pump for supplying hydrogen to the engine during the low-altitude portions of the flight will be larger and heavier than JP-5 pumps.

[redacted]

A liquid-hydrogen pump capable of supplying the required flow rates and pressures is not currently available. The development of such a pump poses a difficult problem in obtaining satisfactory seals. Also, cavitation may prove to be a serious problem, since the hydrogen is at its saturation pressure. If a reliable and reasonably lightweight pump can be developed, it appears that this will give the fuel system having least complexity and least over-all weight.

Another fuel system that appears attractive from an over-all weight standpoint is one in which hydrogen is used only for cruise and some other fuel is used for take-off and let-down of the aircraft. For aircraft cruising at sufficiently high altitudes, no liquid-hydrogen pump is required with such a fuel system. In cases where a pump is required for the hydrogen, this pump need only have sufficient capacity to handle the low fuel rates required at altitude conditions. If the fuel used at low altitudes is JP-5 fuel, it will provide only a small heat-sink capacity as mentioned in the preceding paper. So perhaps a better choice would be refrigerated light hydrocarbons (such as propane). Calculations show that light hydrocarbons refrigerated to a temperature near their freezing point will have a large coolant capacity. The preceding paper showed data on the performance of propane in the experimental combustor that was developed for hydrogen. At the higher combustor pressures, the performance with propane was quite satisfactory. To use any fuel other than hydrogen for the lower flight altitudes, a completely separate fuel system would be required, since any fuel remaining in the fuel system would be frozen upon contact with hydrogen.

Pipe Sizes

Some comparative pipe sizes for hydrogen and JP-5 fuel systems are shown in figure 11. For a system in which liquid hydrogen is used only at high altitude and a hydrocarbon is used for take-off and let-down, we would have a dual fuel system with relative pipe sizes for the hydrogen and JP-5 fuel as indicated by figures 11(a) and (c).

For a system using only hydrogen at both high altitude and take-off, the line required to handle the take-off fuel flow rate would have to be somewhat larger as indicated in figure 11(b). The hydrogen lines would be vacuum-jacketed or insulated in some manner to keep the heat leak into them at a low value. The larger hydrogen line (fig. 11(b)) is also about the size that would be required to handle the high-altitude hydrogen fuel flow if it were all in the vapor phase.

The comparisons are, of course, only relative, and are shown here only to indicate that in spite of the higher volume flow rates of hydrogen involved, the size requirements for the hydrogen system should present no difficulties.

[redacted]

Now there will undoubtedly be problems with controls, heat exchangers, and other fuel-system components that have not been discussed. An experimental investigation of some of these problems is being started at the Lewis laboratory.

FUEL SYSTEMS FOR OTHER FUELS

Up to now only the hydrogen fuel system has been considered and comparisons have been made between the hydrogen fuel system and the one for JP-5 fuel. As pointed out at the beginning of the discussion, hydrogen has been given detailed consideration because it is the fuel that differs most markedly from JP-5. Now the fuel-system requirements for the other fuels of interest will be considered. These include EDB, pentaborane, and diborane among the high-energy fuels; and JP-5 and the light hydrocarbons, among the more conventional fuels.

EDB and JP-5 Fuels

For EDB, the ultimate fuel that is forthcoming from Project Zip, the required fuel system may be no different from that for JP-5 fuel. To date, there has not been sufficient quantity of this material to permit a detailed determination of its properties. However, data that are available indicate that this fuel may be quite similar in most of its handling properties to ordinary JP-5 fuel, and so the EDB fuel system may be quite similar to that for JP-5 fuel.

This is not meant to imply that there should be no fuel-system design problems for EDB, however. With both EDB and JP-5 difficulties can be expected due to fuel decomposition and the formation of gummy materials in the fuel lines. The available data on thermal stability of commercial grades of EDB indicate that this fuel will be more prone to cause trouble than conventional jet fuel, and jet fuel is already giving trouble, as mentioned in a preceding paper.

In at least one production turbojet engine, the formation of carbonaceous and gummy materials is currently causing clogging of filters and fuel injectors. Fuel temperatures in the neighborhood of 300° F, which are encountered in the engine fuel system, are apparently high enough to produce this fuel decomposition. Of course, the exact temperature at which fuel decomposition becomes troublesome will vary with the properties of the particular jet-fuel blend. These high fuel temperatures are partly the result of current fuel-system design. The quantity of fuel handled by the fuel pump remains constant for a constant engine speed. So as altitude is increased and engine fuel flow decreases, a large amount of fuel is recycled. Line friction and pump work are therefore greater than necessary.

Improvements in fuel quality control and in fuel-system design may possibly eliminate this problem for JP-5 and EDB at low supersonic speeds. However, it appears that more drastic measures will be required as flight speeds are increased. As flight Mach number is increased, the problem will become more severe because of the aerodynamic heating of fuel in the aircraft tanks. For example, at a flight Mach number of 2.5 at 60,000 feet, the fuel in uninsulated tanks will attain temperatures over 300° F near the end of a 2-hour flight. Refrigeration of the fuel prior to loading into aircraft tanks will help. The addition of volatile components to the fuel that will vaporize and cool down the remaining fuel will also help. However, if part of the fuel is vaporized, it becomes necessary to somehow pump these vapors into the engines. To supply these fuel vapors to the engines is much more difficult than for the case of hydrogen-fueled aircraft. This is because the aircraft designed to use these more dense fuels are also designed to cruise at lower flight altitudes. This means that the pressures in the combustors are higher than for hydrogen-fueled planes. Therefore, either a high fuel-tank pressure or a pump for handling vapor will be required to feed any vaporized fuel to the engines.

Still another possibility for coping with the fuel aerodynamic heating (and the one that appears most promising at first glance) is to insulate the fuel tanks. A quiescent air gap between the tank wall and the aircraft skin will provide sufficient tank insulation at flight Mach numbers at least as high as 2.5 for EDB and JP-5 fuels.

Regardless of exactly what means are employed to cope with fuel aerodynamic heating, the fuel system for JP-5 and EDB must take on at least a portion of the complexity previously outlined as being necessary for hydrogen fuel.

Pentaborane

For pentaborane, radically different fuel-handling techniques must be employed from those used for JP-5 fuel because pentaborane is extremely toxic, will ignite spontaneously when spilled, and can also react violently with water, alcohol, and other oxygen-containing substances. Great care must therefore be taken to have the fuel tanks clean and free of moisture before filling with this fuel. Pentaborane is quite volatile; it has a vapor pressure of about 15 pounds per square inch at 140° F. In addition, the problem of fuel decomposition is worse with pentaborane than with EDB.

Diborane and Light Hydrocarbons

The fuels EDB, pentaborane, and JP-5 have very little cooling capacity, and liquefied gases such as diborane and the light hydrocarbons

therefore show promise as fuels. The liquefied gases would have to be stored in the tanks at low temperatures. Although the tank temperatures would not be as low as for hydrogen, the temperature would nevertheless be low enough to require a great many of the fuel-system design features previously outlined for hydrogen.

AIRCRAFT PERFORMANCE CALCULATIONS

The discussion up to this point has served to point out the design requirements for aircraft fuel systems and the problems that arise with the aircraft themselves when high-energy fuels are used. The discussion did not indicate all the details of fuel-system design. However, a sufficient study has been made to permit a rough evaluation of the required size and weight of the various fuel-system components.

By drawing on this information and on the data relating to engine design that were presented in the preceding paper, there is the necessary information to permit an estimate of the performance of aircraft employing high-energy fuels. The remainder of this paper will deal with these aircraft performance calculations. Several flight missions have been considered in the analysis.

Supersonic Interceptor

Configuration. - The interceptor airplanes are exemplified by the models shown in figures 12 and 13. They are fairly conventional supersonic designs, having a straight wing with an aspect ratio of 3 and slender fuselages with an over-all fineness ratio of 12. The wings are only $3\frac{1}{2}$ percent thick, and all of the fuel is carried in the fuselage. Both models represent interceptors with a gross weight of 25,000 pounds capable of combat at Mach numbers from 2.5 to 3.0. The smaller model (fig. 12) represents a JP-5 airplane capable of a combat ceiling of just over 60,000 feet. Wing loading for this interceptor is 125 pounds per square foot. An EDB airplane would look similar to this model because the density of EDB and JP-5 are nearly the same, so that fuselage size would be unchanged.

The larger interceptor model (fig. 13) represents a hydrogen-fueled airplane with fuel tank, insulation, and structural assumptions that represent, as nearly as possible, the state of the art brought to light in this and previous papers. It is intended to exploit the performance possibilities made available by the unique properties of the hydrogen fuel. Combat Mach number is 2.5 as it was for the JP-5 airplanes, but combat ceiling is over 80,000 feet for this airplane. The wing loading was reduced to 70 pounds per square foot, in keeping with this extremely high ceiling.

The engines assumed for these two airplanes were similar in all respects except size. The engines have a cooled turbine with an inlet temperature of 2040° F, a sea-level compressor pressure ratio of 7, and an afterburner with a maximum temperature of 3340° F. The engine incorporated many of the advanced design concepts discussed by the preceding paper. For the JP-5 interceptor with a ceiling near 60,000 feet, two engines with a compressor diameter of 21 inches would be adequate. For the hydrogen interceptor with its 80,000-foot ceiling, two 28-inch engines would be required. Because long burner lengths are required for JP-5 fuel both in the primary combustor and the afterburner, the JP-5 nacelles have a much higher fineness ratio than the nacelles for the hydrogen airplane.

These two models bring to light the geometrical similarity between the airplanes which is possible even with fuels of widely different properties. Except for size, the hydrogen airplane looks almost exactly like its JP-5 or EDB counterpart. Because of the increase in altitude, more wing area is needed. But along with the increase in wing size came a corresponding increase in fuselage size necessary because of the low-density fuel that is stowed entirely in the fuselage in these supersonic airplanes. Also, the increase in altitude requires an increase in engine size; so the airplane is larger in all respects, but with the same gross weight and the same relative proportions. Of course, the weight distribution of the two airplanes is very different. Structural weight is 35 percent of gross for the small JP-5 airplane and fuel weight is 40 percent. For the hydrogen-fueled airplane, structure weight is up to 45 percent, and the ratio of fuel weight to gross weight is down to 20 percent. The two airplanes look alike, so that from the aerodynamic standpoint, the hydrogen-fueled airplane represents no radical departure from conventional airplanes.

Flight plan. - Figure 14 shows a typical flight plan selected for the interceptors represented by these models. The airplane takes off from a short runway, accelerates to Mach 0.9 at sea level, then climbs to its cruise condition in about 3 minutes. This cruise altitude was chosen to give maximum radius, and in general was below the combat altitude as indicated here. However, for flight plans where the combat altitude is very low, cruise altitude may actually be above the combat altitude. Cruise out at Mach 2.5 is along a Brequet path. At the end of cruise the airplane climbs to the combat point. It combats for 5 minutes at Mach 2.5. This is followed by cruise back at a Mach number of 2.5 and reduced altitude. The airplane lets down near the base and lands with a fuel reserve equal to 5 percent of its take-off fuel load.

This flight plan is quite arbitrary, and many others could have been chosen. The flight plan illustrated in figure 14 was selected because it provides a convenient yardstick by which engine and fuel comparisons can be made. Also, the subsequent discussion will show the effect of

variations in the principal flight-plan variables in order to extend the comparison of the results to other flight plans. Because cruise is generally at a lower altitude, high combustor pressures will be encountered during cruise. In making calculations the availability of a hydrogen pump to supply these pressures was assumed.

Effect of turbine-inlet temperature. - Figure 15 shows total radius against turbine-inlet temperatures for both afterburning and nonafterburning engines. The fuel is hydrogen. Two curves are shown for the afterburning engine. The lower solid curve represents engines with an afterburner weight W_{AB} of 30 percent of the dry engine weight W_e. This is fairly typical of present-day JP-5 afterburners, which are some 5 to 6 feet long. The upper curve represents a weight increase of only 10 percent for the afterburning engine and is probably the best that could be hoped for with the extremely short afterburners that may be possible with hydrogen fuel. In subsequent discussions a value of 20-percent additional weight will be used as a logical estimate of what this number should be for hydrogen afterburners. A 20-percent afterburning engine is represented at 2040° F turbine temperature by the circle in figure 15.

Figure 15 shows that high turbine-inlet temperatures are desirable, especially for the nonafterburning engine. So the choice of an engine for the interceptor will lean toward the high turbine-inlet temperatures and therefore will involve turbine cooling, which was discussed in some detail in the previous paper. The nonafterburning engine with a 2540° F turbine gives approximately the same range as the afterburning engine with 2040° F turbine temperature and a 20-percent afterburner weight. A choice between the 2040° afterburning engine and the 2540° nonafterburning engine would have to be based on ease of development, suitability for other airplanes, and other factors that have not been considered here. For the present interceptor studies the engine represented by the circle symbol was arbitrarily chosen. Subsequent trends will be discussed in terms of this engine, using an afterburner weight of 20 percent for hydrogen and EDB fuels and 30 percent for JP-5 fuel.

Effect of flight Mach number. - The effect of flight Mach number on combat radius for three different fuels using the afterburning engines just described is presented in figure 16. As in the previous figure, combat is for 5 minutes at 80,000 feet. For this figure, the cruise out and back was assumed at the same Mach number as combat; therefore, the abscissa refers both to cruise and combat. From figure 16 it appears that a Mach number of 2.5 is a good point for the turbojet engines, and this is true regardless of the fuel under consideration. At 80,000 feet, the pressure in the afterburner is about 1/4 atmosphere at this lowest Mach number, 1.5. EDB and hydrogen will probably burn satisfactorily at this condition, but JP-5 fuel will need some special provisions. It was assumed that tail-pipe size and weight were increased

to reduce afterburner velocity to 450 feet per second for the JP-5 fuel. Even with this velocity, afterburner combustion efficiency would be only 75 percent. Afterburner velocity was 550 to 600 feet per second for the EDB and hydrogen curves, and afterburner efficiency was 90 percent for these fuels.

For the middle curve, it was assumed that EDB was burned in both the primary combustor and the tail pipe. At present, this fuel produces deposits of boron oxide in the turbine and tail pipe, which will cause engine performance to deteriorate. In the calculations, however, no effect on engine performance was assumed because of the deposition of solid products. Also, in obtaining the EDB curve, equilibrium expansion was assumed through the turbine and exhaust nozzle. That is, it was assumed that the composition and phase of the exhaust products were in equilibrium at all temperatures. This may also prove to be an optimistic assumption since the true case may be closer to frozen composition during expansion through the turbine and exhaust nozzle. To show what effect this might have on the calculations, one point for frozen expansion is shown by the circle symbol at a Mach number of 2.5. The nature of the expansion process may have considerable effect on the performance to be expected from this fuel. For this case the radius decreased over 7 percent. Even though these optimistic assumptions were made for EDB, hydrogen still appears to good advantage. At 80,000 feet, hydrogen provides a radius about 110 percent above JP-5. The radius for EDB is about 55 percent above the radius for JP-5.

These comparisons are considerably altered when other combat altitudes are considered.

Effect of combat altitude. - Figure 17 shows interceptor radius as a function of combat altitude for a Mach number of 2.5 and for the three fuels considered in the calculations. The advantage hydrogen enjoys at 80,000 feet dwindles as altitude is reduced. At 60,000 feet, the range for EDB exceeds the range for hydrogen. Again, it was assumed that engine performance was unaffected by deposits of boron oxide that may be encountered with EDB, and also equilibrium expansion in the EDB engine was assumed. Above 80,000 feet, of course, hydrogen's advantage continues to grow. Maximum combat altitude possible with the EDB and JP-5 fuels is about 90,000 feet, and it is about 95,000 feet for the hydrogen-fueled interceptor.

At the low altitudes, it may be surprising to note that hydrogen does well in view of the drag penalties associated with its low density. But this is combat altitude, and the interceptor was allowed to cruise out at the altitude that gave greatest radius. In the case of hydrogen, the cruise altitude was above the combat altitude for this part of the curve. The same thing was true to a lesser extent for the other fuels. For instance, at a combat altitude of 40,000 feet, the hydrogen interceptor cruises out and back at 63,000 feet, and the EDB and JP-5 interceptors cruise out and back at 56,000 feet. Thus the hydrogen is severely

penalized for its low density only during the relatively brief combat maneuver, and its performance therefore does not fall as rapidly as might be expected.

Take-off thrust. - The data of figure 18 are intended to give an indication of the very large thrust available for take-off and climb in these airplanes. When an airplane is designed to fly at extreme altitudes, it always has more than adequate take-off performance. The thrust to gross weight ratio at take-off is shown for the interceptors designed to combat at a Mach number of 2.5 and at the altitudes shown on the abscissa. With a thrust-weight ratio greater than 1, vertical take-off schemes can be considered, and this is possible for all the aircraft represented on this figure. Actually in the airplane calculations conventional take-off was assumed and the weight of a conventional landing gear was allowed. However, the data of figure 18 invite speculation as to possible vertical take-off schemes.

Curves are shown for both afterburning engines and nonafterburning engines. In take-off performance the nonafterburning engines show a marked advantage, although the low-speed performance of the afterburning engines is still more than adequate. For a combat altitude of 80,000 feet the nonafterburning engines provide a thrust-weight ratio of 1.85, and the afterburning engines give 1.4. The reason nonafterburning engines appear to better advantage here lies in the response of the two engines to changes in flight Mach number. A given amount of thrust must be provided at the combat condition by either engine, and since afterburning engine thrust drops more rapidly with decreasing Mach number it ends up with lower thrust at the low speed condition shown here. Thrust does not drop rapidly for combat altitudes below 65,000 feet because cruise altitude does not change in this region, as was pointed out in the discussion of figure 17.

Supersonic Bomber

Configuration. - The next airplane to be considered is a supersonic bomber, and it is represented by the model shown in figure 19. This model is intended to represent a hydrogen-fueled airplane capable of arriving over the target at a Mach number of 2.5 and an altitude of 80,000 feet. The gross weight is 150,000 pounds and carries a pay load of 10,000 pounds and fixed equipment weight of 5000 pounds. It is similar in many respects to the interceptor just discussed. It has a thin straight wing with an aspect ratio of 3 and a long slender fuselage to achieve low drag at supersonic speeds. Six engines are used in this model, two in each of the inboard nacelles. For nonafterburning engines, represented on the model, a compressor diameter of 40 inches would be required for each of the six engines. The engines assumed had a turbine-inlet temperature of 2540° F and a sea-level compressor pressure ratio of 7.

[redacted]

Flight plan. - The flight plan selected for this airplane is shown in figure 20. The bomber takes off from base, accelerates to 0.9 Mach number, and then begins its climb to altitude. The airplane arrives at its initial cruise point, Mach 2.5, and an altitude a little below target altitude in about 3 minutes. From here it cruises along a Breguet path at Mach 2.5 to the target and back again. It lets down over the base and lands with a 5-percent fuel reserve. Note that almost the entire flight is conducted at, or near, the airplane ceiling. This is in contrast to the interceptor flight plan, which called for cruise at a lower altitude and only brief combat near the airplane ceiling. Again, this flight plan is quite arbitrary, and many others might have been chosen. The purpose of analyzing this one is to establish relative performance of engines and fuels as was done for the interceptor; and the effects of the major flight plan variables will be examined again.

For flights involving low altitudes, high combustion-chamber pressures will be encountered; and for these conditions, the availability of a satisfactory hydrogen fuel pump will be assumed. For some of the higher cruise altitudes to be discussed in subsequent figures, no cruise fuel pump would be needed in the airplane.

Effect of turbine-inlet temperature. - The basis for an engine selection is shown in figure 21. This figure shows bomber radius against turbine-inlet temperature for afterburning and nonafterburning engines. The fuel is hydrogen. Again, 10 and 30 percent of dry engine weight represent the limits within which the afterburner weight may be expected to fall. Figure 21 is similar to figure 15 for the interceptor, with a steep slope on the nonafterburner curve and a much flatter slope on the afterburning curves. In the bomber, however, the nonafterburning engine appears to better advantage because of the different flight plan. The interceptor flight plan was well suited to the afterburning engine because the afterburner was used for maximum thrust only for the rather brief combat maneuver at extreme altitude. Therefore, the high specific fuel consumption when employing full afterburning was of little consequence. In this bomber, on the other hand, virtually the entire flight is conducted near the airplane ceiling, and this type of flight is better suited to a nonafterburning engine whose full thrust specific fuel consumption is lower than that of an afterburning engine. Whereas the nonafterburning engine did not show a range advantage at any turbine-inlet temperature for the interceptor, here it shows a slight advantage at 2540° F. The 2540° F nonafterburning engine shows considerable advantage over the 2040° F afterburning engine. As before, a 2040° F afterburning engine with an afterburner weight 20 percent of the dry engine weight is represented by the circle.

For hydrogen fuel, the 2540° F nonafterburning engine was selected for the analysis to be presented in subsequent figures. Either of two engine types could be used. One of these two engine types has a one-stage turbine with 50,000-pound stress and a sea-level compressor

[redacted]

pressure ratio of about 4. The same flight radius was obtained with a two-stage turbine with 40,000-pound stress and a sea-level pressure ratio of 7.

Although figure 21 applies only to hydrogen fuel, performance with JP-5 and EDB will be investigated. The previous paper has emphasized the difficulties involved in achieving a turbine-inlet temperature of 2540° F with the more dense fuels because of their inadequate heat-sink capacity. In considering either JP-5 or EDB, therefore, the turbine-inlet temperature was limited to 2040° F. In fact, the afterburning engine with a 20-percent afterburner weight for EDB and the same engine with a 30-percent afterburner weight for JP-5 will be used. It is similar to the engine used in the interceptor, and has a sea-level compressor pressure ratio of 7.

Effect of flight Mach number. - Figure 22 shows the effect of flight Mach number on the radius of the supersonic bomber for three fuels. The JP-5 and EDB curves were calculated for a 2040° F afterburning engine, and the hydrogen curve was calculated for a 2540° F nonafterburning engine. A Mach number of 2.5 appears well suited to the bomber as it did for the fighter. Mach number has little effect on the comparison between the three fuels. Here again, with EDB no deterioration was assumed in engine performance due to deposition of boron oxide in the engine, and equilibrium expansion of the exhaust products was also assumed. The flight radius with hydrogen is about 125 percent above that for JP-5 fuel. The radius with EDB is about 30 percent greater than for JP-5. Hydrogen looks a little better here than it did in the interceptor because cruise altitude is higher and because it has better engines than the EDB and JP-5 fuels. In the interceptor, all three fuels were calculated with the same engine.

Effect of target altitude. - The effect of target altitude is shown for the three fuels in figure 23. This is for a Mach number of 2.5. Again hydrogen is superior at very high altitudes, but EDB is able to compete with it below 55,000 feet. Best altitude for the hydrogen fuel is 65,000 feet where a radius of 1800 nautical miles is shown. Maximum radius for the EDB is about 1500 miles, and maximum for the JP-5 fuel is about 1000 nautical miles. These results are all for a gross weight of 150,000 pounds and a pay-load weight of 10,000 pounds.

The supersonic-bomber radius with hydrogen drops off rapidly at altitudes below 65,000 feet. This is in contrast to the picture for the interceptor. However, the interceptor actually cruised out at 60,000 to 65,000 feet and only descended for a brief period of combat at the lower altitudes. In contrast, this bomber flies the entire mission at or near the target altitude. Thus, the radius is greatly reduced with hydrogen at the lower altitude because of the low fuel density. From this, it is evident that design altitude for the Mach 2.5 hydrogen-fueled bomber should always be above 65,000 feet.

[redacted]

The maximum radius obtained for this superior bomber was 1800 nautical miles at an altitude of 65,000 feet with hydrogen fuel. The question arises as to whether this radius can be increased by increasing airplane size.

Effect of aircraft size. - Figure 24 presents flight radius against airplane gross weight for the three fuels. These calculations were made for a Mach number of 2.5 and a target altitude of 80,000 feet. Increases in radius are not great for gross weights larger than 150,000 pounds. Of course, this depends on the assumed pay load and fixed weight. If the pay-load weight (10,000 lb) and fixed equipment weight (5000 lb) were doubled, it would be necessary to increase the gross weight probably to about 300,000 pounds from the 150,000 pounds in order to obtain the same radius.

Figure 24 shows that airplane size has little effect on the relative performance of the three fuels. EDB is about 30 percent better than JP-5 throughout, and hydrogen is 125 percent better.

Take-off thrust. - For this bomber, the thrust at take-off is more than adequate because of the large engines used to attain the high flight altitudes. In fact, for the hydrogen-fueled bomber, take-off thrust to gross-weight ratios greater than 1.0 are possible for all target altitudes in excess of 75,000 feet.

Subsonic Aircraft

The performance of supersonic bombers and interceptors designed for high-altitude operation has been examined. A flight radius much in excess of 1500 nautical miles for operation at high altitudes was not obtained with these supersonic aircraft. With the new developments in lightweight engines, higher altitudes can also be attained at subsonic speeds. It is to be expected, of course, that a much greater radius can be attained at subsonic speeds. In order to fly subsonically, however, it will be necessary to fly at much higher altitudes than now appear feasible if the mission is to be at all successful. Unless major advances are made in airplane structures, these altitudes cannot be achieved without new design concepts and principles. At high altitudes low wing loadings will be needed, and the airplane wing becomes the major structural item. Consequently, thick wings will be needed to reduce the wing structural weight. It will be necessary to design for low load factors, and so low-altitude operation will be severely restricted. With the low wing loading, take-off and landing speeds will be low, which might allow the use of a lighter landing gear. Climb speeds would also be limited so as to keep the aerodynamic loads to a minimum. After doing all these things, perhaps it might be better to consider this not so much as an airplane but more as a powered glider. These, however, are the features needed in order to fly at extremely high altitudes at subsonic speeds.

[redacted]

Configuration. - A model of such a subsonic airplane designed to use hydrogen as the fuel is shown in figure 25. This airplane, like the supersonic bomber, weighs 150,000 pounds and has a target altitude of 80,000 feet. The fixed equipment plus pay load totals 15,000 pounds. The principal features are, of course, the low wing loading and high wing aspect ratio, which result in a wing span of 345 feet. Wing loading is 15 pounds per square foot, and the aspect ratio is 12. The improvement in lift-drag ratio that results from the high aspect ratio and low wing loading more than compensates the increase in wing weight. The lift-drag ratio is 30. The structure of this airplane weighs 43 percent of the airplane gross weight. The engine weight is 17 percent and fuel weight is 26 percent of the gross weight. Part of the cruise fuel is carried in pressurized tanks in the wing. The maximum thickness of the wing at the root is over 5 feet.

The average wing thickness was assumed to be 12 percent. In addition, the design lift coefficient at cruise is 0.55. These factors tend to limit the maximum flight Mach number to avoid high drag. Even with the sweep of over 25° that was assumed for this airplane, it is limited to a maximum Mach number of 0.75.

Effect of airplane size. - Figure 26 shows the radius plotted against gross weight for airplanes using the three fuels. The target altitude for these curves is 80,000 feet. At this or higher altitudes, hydrogen clearly has the advantage. With a gross weight of 150,000 pounds, a radius of about 4300 miles is indicated. This is the performance of the particular airplane shown in figure 25. The radii indicated for EDB and JP-5 are 2900 and 2300 miles, respectively. Increasing the gross weight from 150,000 to 300,000 pounds increases the radius with hydrogen fuel from 4300 to nearly 5000 miles. Of course, changes in weight of fixed equipment plus pay load from the assumed 15,000 pounds would require a corresponding change in required gross weight for the same radius.

Engine characteristics. - At 80,000-foot target altitude, best performance was obtained with turbine-inlet temperatures that do not require turbine cooling. Turbine-inlet temperature with all fuels was selected at 1540° F. Transonic compressors having high air flows were assumed. The higher efficiency of the engines without afterburners more than compensates for the decrease in total engine weight of engines with afterburners so that best range is obtained without afterburners at a target altitude of 80,000 feet. At higher altitudes, however, the radius would be improved with afterburning. Rated sea-level pressure ratio is 7. Bare engine specific weight at sea level is 0.22.

Engine performance with all fuels is severely penalized at the high altitudes because of the very low Reynolds numbers in the engine compressor. However, since large engines are required at high altitudes, this

effect is reduced to some extent. At a target altitude of 80,000 feet, using four engines as illustrated on the airplane in figure 25, the compressor tip diameter of each engine is 47 inches. The engines (like the rest of the airplane) were assumed to be designed for operation at 80,000 feet. For example, compressor first-row-blade chords were assumed to be 8 inches in order to minimize Reynolds number effects.

The take-off thrust of the airplane designed for 80,000 feet is over 2/3 of the take-off gross weight. Even the subsonic airplane that is designed for high-altitude flight will have more than adequate take-off performance.

CONCLUSIONS

For liquid hydrogen, despite its unusual physical properties, it appears possible to design an aircraft tank that will have an over-all weight of about 15 percent of the fuel weight. To obtain a practical fuel system for liquid hydrogen, various fuel-system components must be developed. For some of these components, there is a good background of experience with similar equipment. Some of the other components, such as the pump for handling this low-density liquid, the heat exchangers, and the fuel control represent a fairly marked departure from past experience. Nevertheless, there appear to be no fundamental limitations preventing the attainment of a satisfactory fuel system for liquid hydrogen. The problems that must be overcome appear to be those that succumb to straightforward engineering development.

The estimates of airplane performance using high-energy fuels and the new developments in turbojet engines lead to the following conclusions:

For all the airplanes considered, the supersonic interceptor, the supersonic bomber, and the subsonic bomber, the best flight radius is obtained with hydrogen for altitudes above about 60,000 feet. For lower altitudes, EDB provides a flight radius that is equal to, or above, the radius for hydrogen. EDB provides a radius about 30 percent greater than JP-5 at most flight conditions. For the interceptor, it was interesting to learn that the radius with hydrogen was only about 5 to 6 percent below the radius for EDB at combat altitudes down to 40,000 feet. This is true because it is possible for the hydrogen-fueled interceptor to cruise out at its optimum altitude and descend to lower altitudes for combat.

The subsonic hydrogen-fueled airplane can attain a flight radius of 4000 to 5000 nautical miles at an altitude of 80,000 feet. Hydrogen is the only chemical fuel permitting us to even approach such a long radius at this high altitude.

All the high-altitude aircraft considered in the analysis had adequate take-off thrust. Consequently, it was not necessary to compromise engine design in any way to provide good take-off performance.

In calculating aircraft performance with the high-energy fuels, it was assumed that satisfactory fuel systems and engines will be available for these fuels. At the present time, however, turbojet engines are adversely affected by boron oxide deposits when operating with the boron hydride fuels. Also, several fuel-system components have yet to be developed for liquid hydrogen. Additional research is therefore required in order to attain in practice the aircraft performance indicated by the calculated curves.

REFERENCES

1. Kropschot, R. H., Parkerson, C. R., O'Donel, J., and Crum, M. G.: Low Temperature Tensile Testing Equipment and Results (300°-20° K). Rep. 2708, U.S. Dept. Commerce, Nat. Bur. Standards, July 1, 1953. (NBS Proj. 0306-20-2667.)

2. Anon.: Stainless Steel Handbook. Allegheny Ludlum Steel Corp., 1951.

3. Hanson, William B.: Proceedings of the 1954 Cryogenic Engineering Conference. Rep. 3517, U.S. Dept. Commerce, Nat. Bur. Standards, Feb. 1955.

4. Anon.: Design Study of Liquid Hydrogen Tankage for Internal Installation in Aircraft. RN No. 292, Summers Gyroscope Co., Feb. 1955. (Contract No. AF33(616)-2702, Proj. 5-(3-3084), Task No. 30271.)

5. Isakson, V., et al.: Design Study for Liquid Parahydrogen Internal Fuel Tanks. Eng. Rep. 1420, Beech Aircraft Corp., Jan. 26, 1955. (WADC Contract AF33(616)-2685, Proj. 5-(3-3084), Task No. 30271.)

PROPERTIES OF LIQUID HYDROGEN

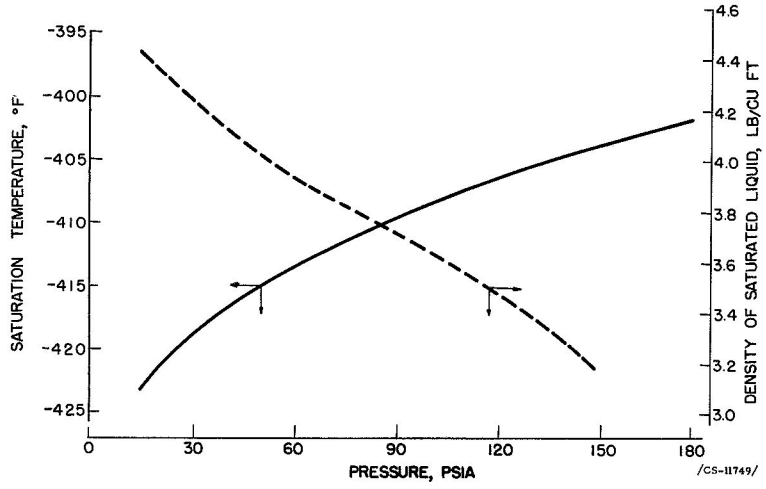

Figure 1

LIQUID-HYDROGEN FUEL TANK

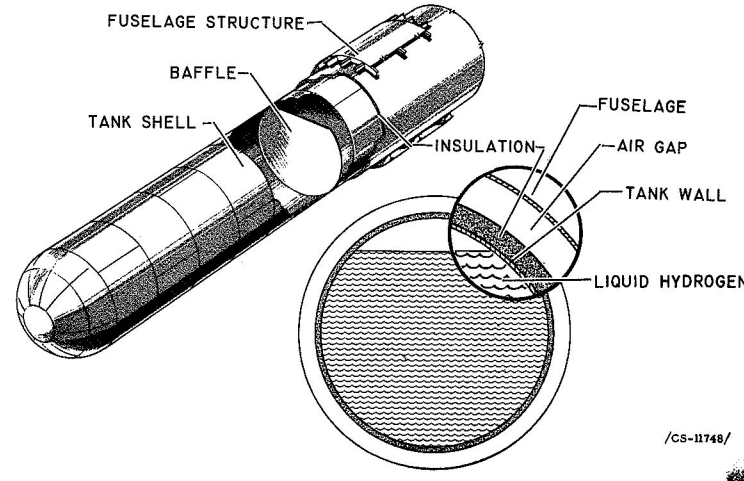

Figure 2

YIELD STRENGTHS OF SEVERAL ALLOYS AT LOW TEMPERATURES

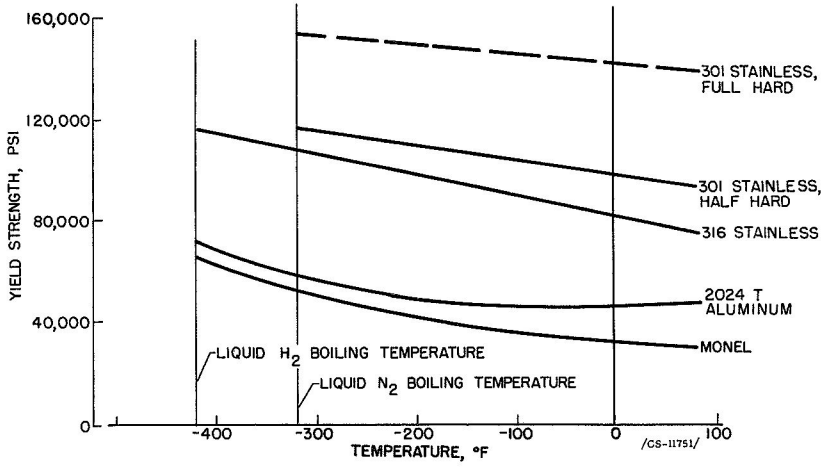

Figure 3

PROPERTIES OF A POLYSTYRENE FOAM

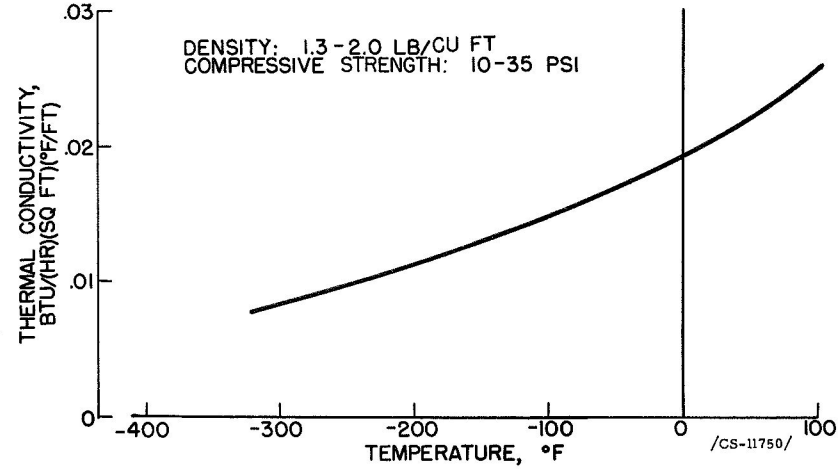

Figure 4

NO-LOSS TIMES FOR LIQUID-HYDROGEN FUELED AIRCRAFT

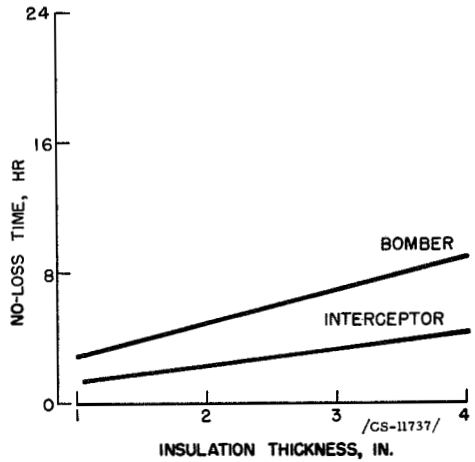

Figure 5

GROUND STORAGE TIME FOR LIQUID-HYDROGEN FUELED AIRCRAFT

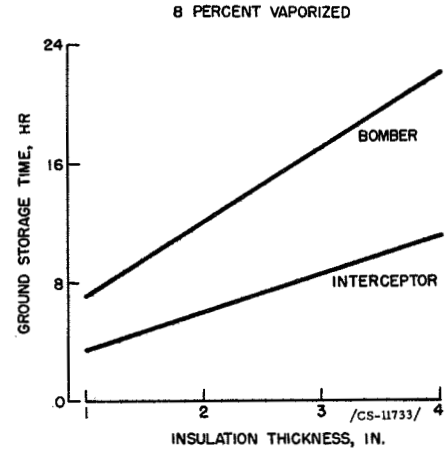

Figure 6

SKIN TEMPERATURES FOR STATIONARY LIQUID-HYDROGEN FUELED AIRCRAFT

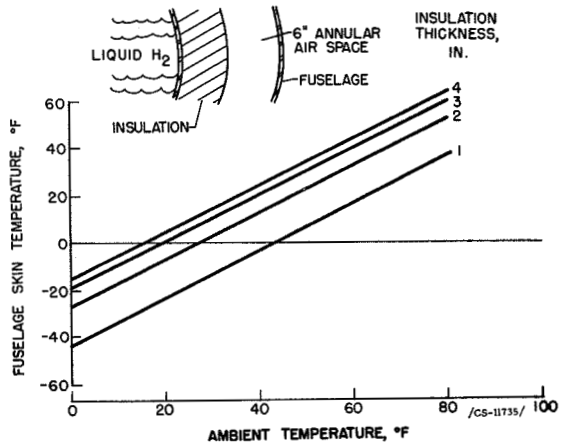

Figure 7

ICING ON STATIONARY AIRCRAFT

(WITH RAINFALL)

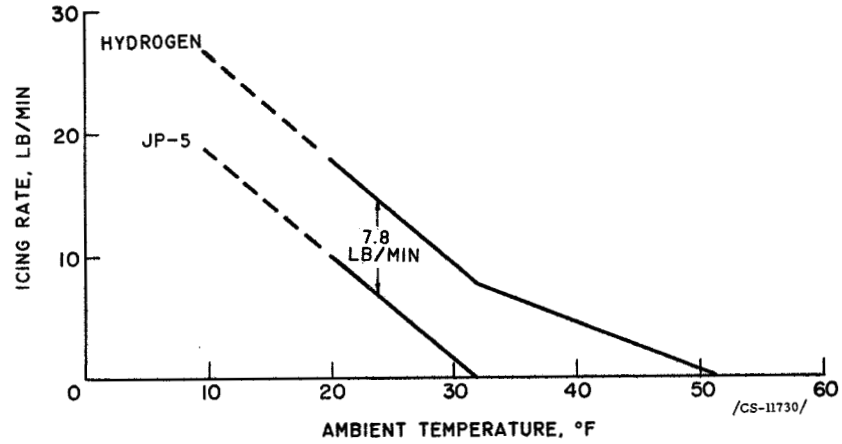

Figure 8

FUEL VAPORIZATION DURING FLIGHT

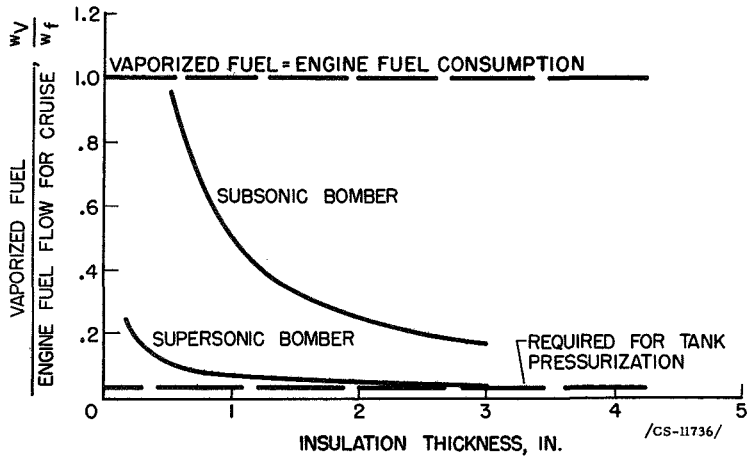

Figure 9

EQUILIBRIUM FUSELAGE AND INSULATION TEMPERATURES

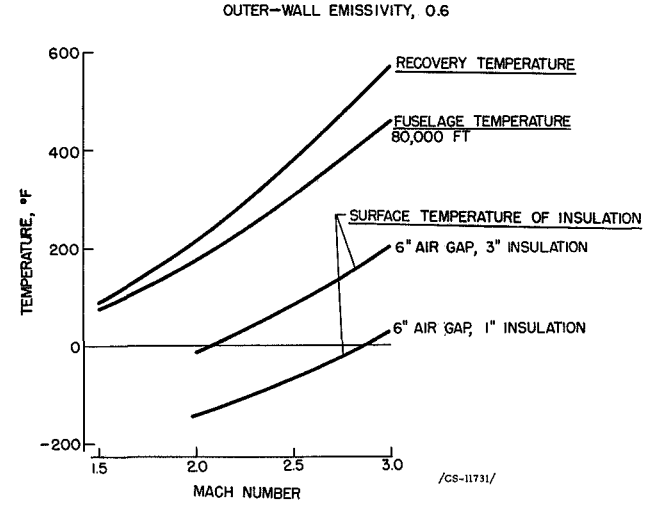

Figure 10

FUEL LINES FOR JP-5 AND HYDROGEN FUEL SYSTEMS

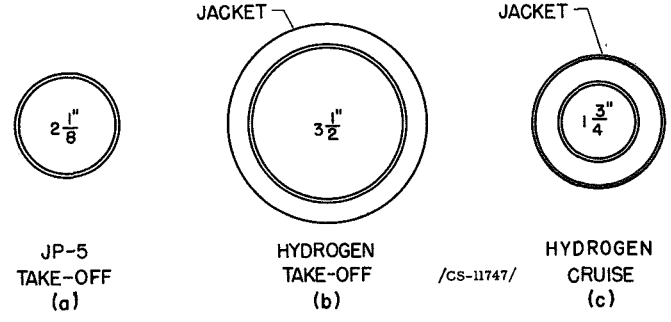

Figure 11

SUPERSONIC INTERCEPTOR MODEL
JP-5 FUEL
(FUSELAGE LENGTH, 63.6 FT)

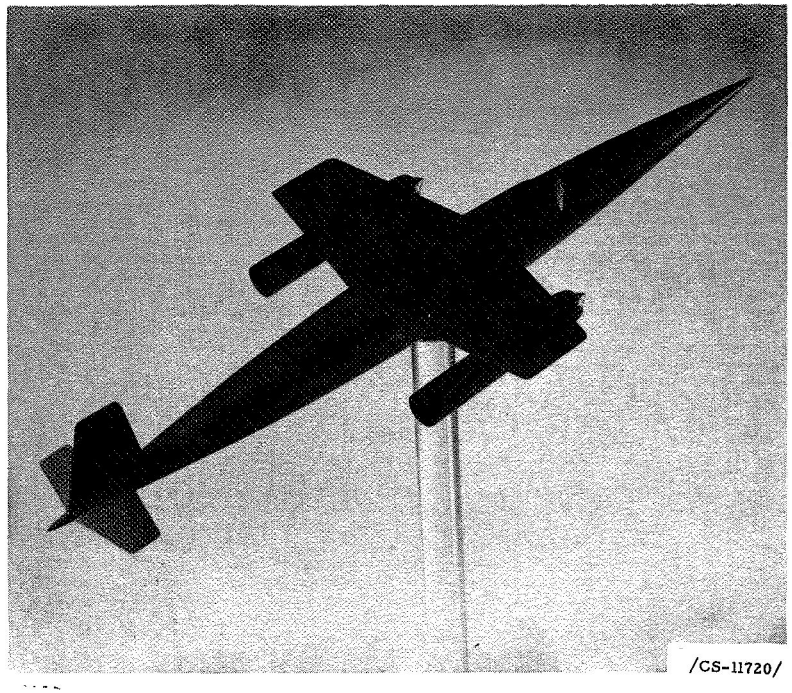

Figure 12

SUPERSONIC INTERCEPTOR MODEL
HYDROGEN FUEL
(FUSELAGE LENGTH, 93.2 FT)

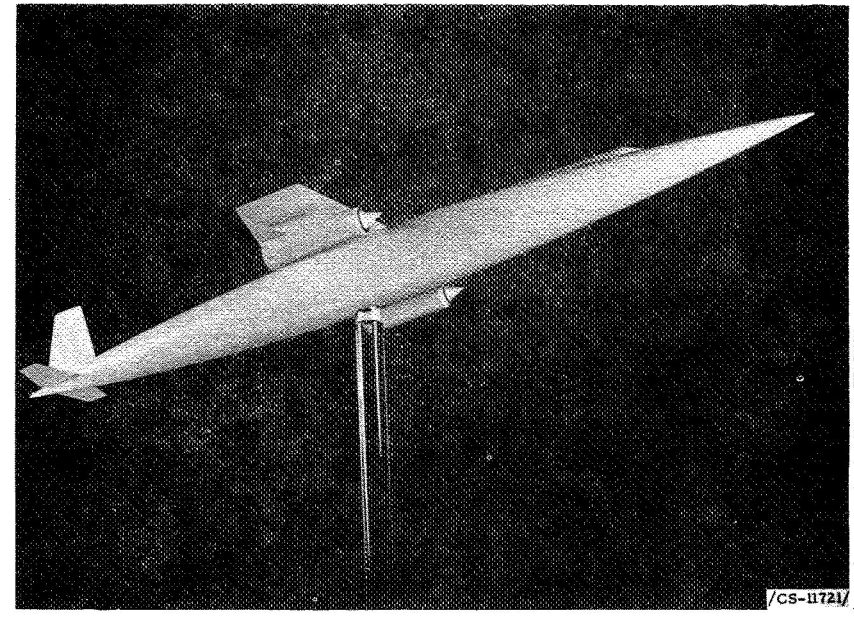

Figure 13

SUPERSONIC INTERCEPTOR FLIGHT PLAN

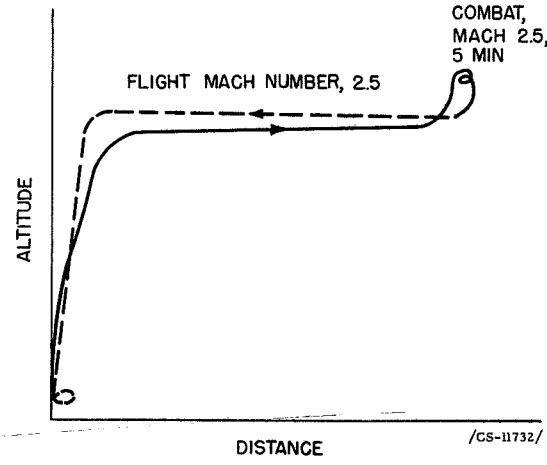

Figure 14

EFFECT OF TURBINE-INLET TEMPERATURE ON RADIUS OF SUPERSONIC INTERCEPTOR

HYDROGEN, MACH 2.5 AND 80,000 FT; GROSS WEIGHT, 25,000 LB

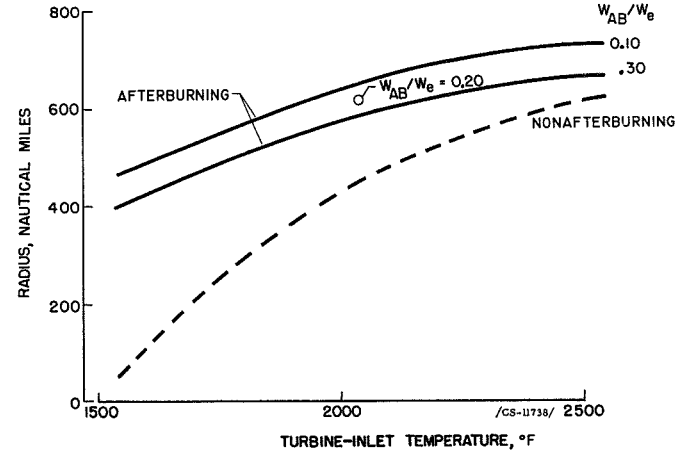

Figure 15

EFFECT OF MACH NUMBER ON RADIUS OF SUPERSONIC INTERCEPTOR

COMBAT, 80,000 FT; GROSS WEIGHT, 25,000 LB

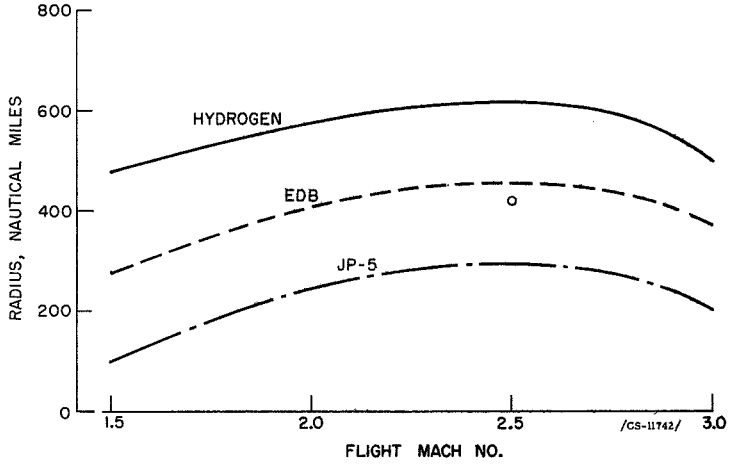

Figure 16

EFFECT OF COMBAT ALTITUDE ON RADIUS OF SUPERSONIC INTERCEPTOR

MACH NUMBER, 2.5 GROSS WEIGHT, 25,000 LB

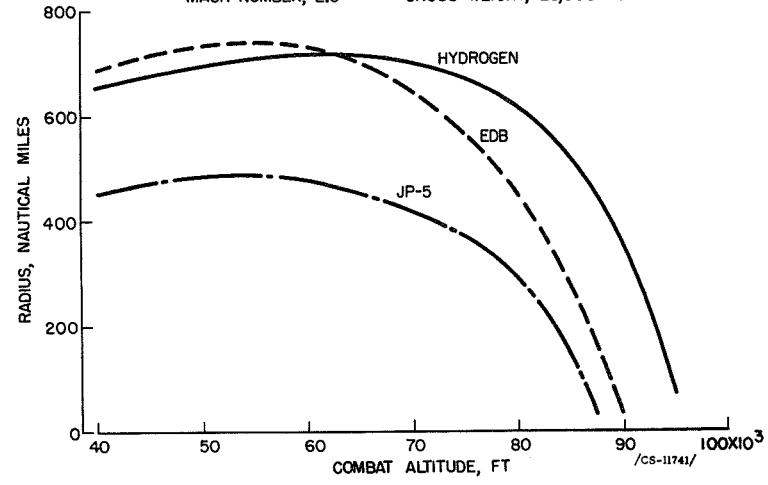

Figure 17

EFFECT OF COMBAT ALTITUDE ON TAKE-OFF THRUST OF SUPERSONIC INTERCEPTOR

MACH 2.5

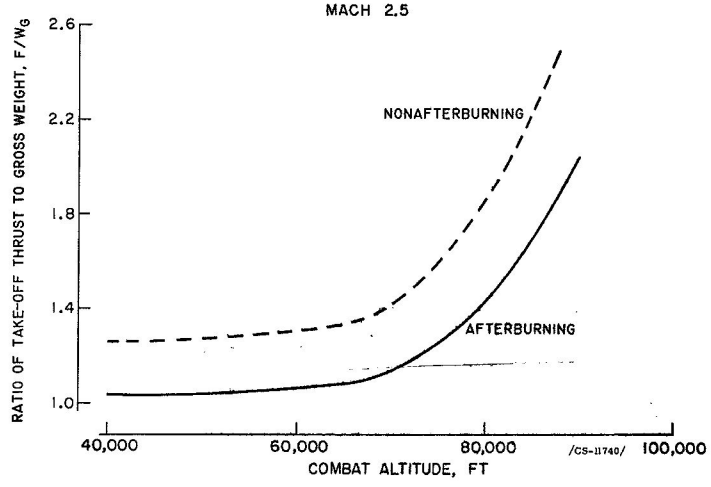

Figure 18

SUPERSONIC BOMBER MODEL

HYDROGEN FUEL

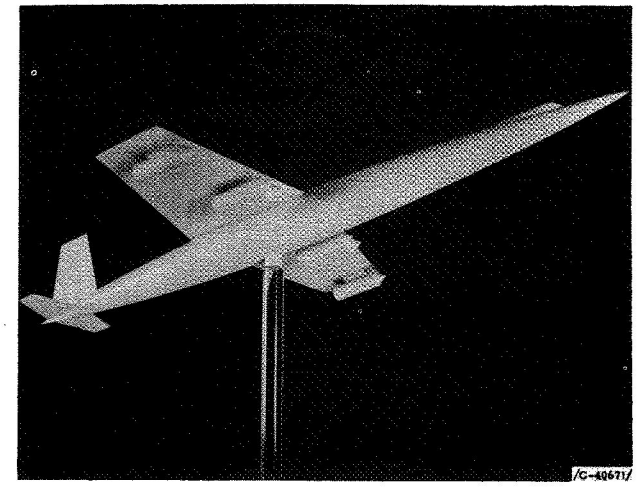

Figure 19

SUPERSONIC BOMBER FLIGHT PLAN

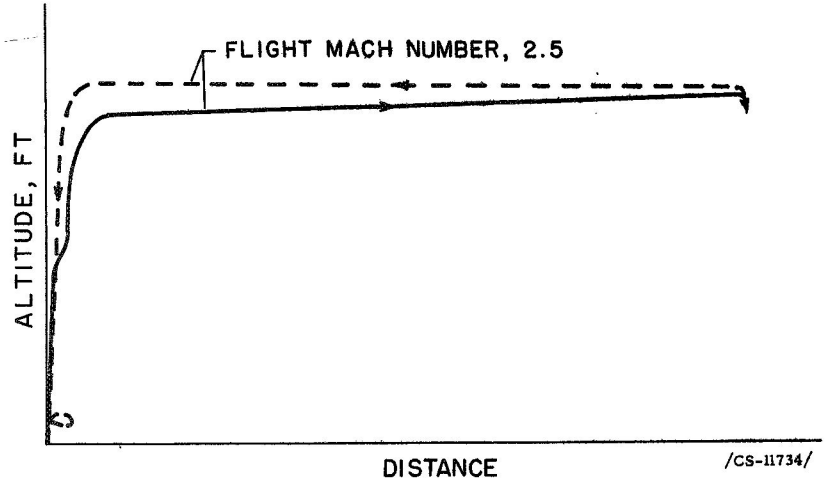

Figure 20

EFFECT OF TURBINE-INLET TEMPERATURE ON RADIUS OF SUPERSONIC BOMBER

HYDROGEN MACH 2.5 AND 80,000 FT

GROSS WEIGHT 150,000 LB PAYLOAD 10,000 LB

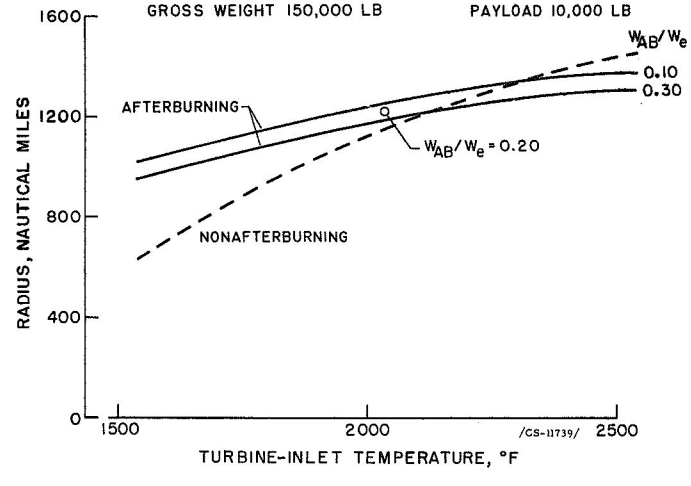

Figure 21

EFFECT OF MACH NUMBER ON RADIUS OF SUPERSONIC BOMBER

TARGET ALTITUDE, 80,000 FT GROSS WT, 150,000 LB

PAYLOAD, 10,000 LB

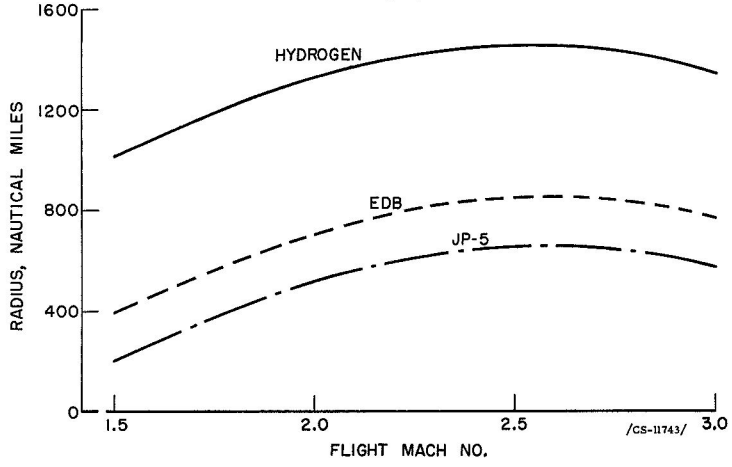

Figure 22

EFFECT OF TARGET ALTITUDE ON RADIUS OF SUPERSONIC BOMBER

MACH NUMBER, 2.5

GROSS WEIGHT, 150,000 LB PAYLOAD 10,000 LB

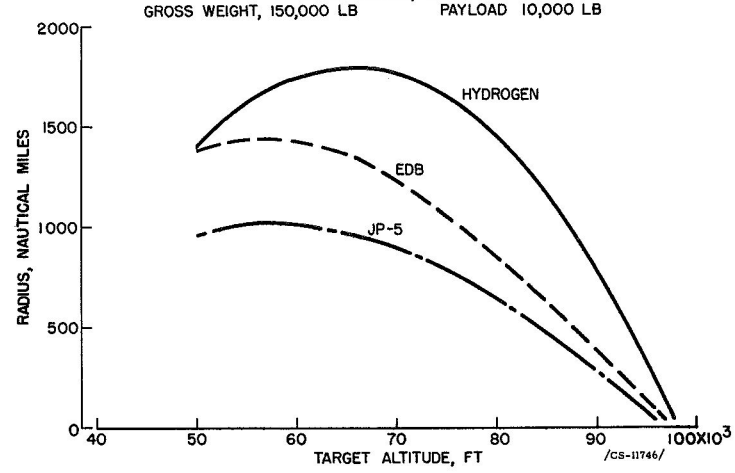

Figure 23

EFFECT OF GROSS WEIGHT ON RADIUS OF SUPERSONIC BOMBER

MACH 2.5 TARGET ALTITUDE 80,000 FT

PAYLOAD 10,000 LB

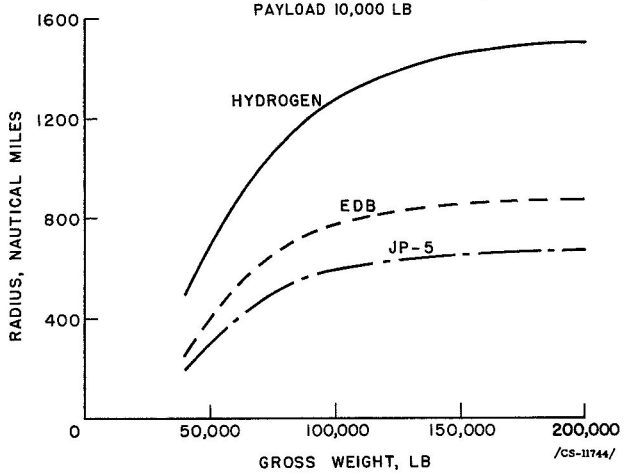

Figure 24

SUBSONIC AIRPLANE MODEL

HYDROGEN FUEL

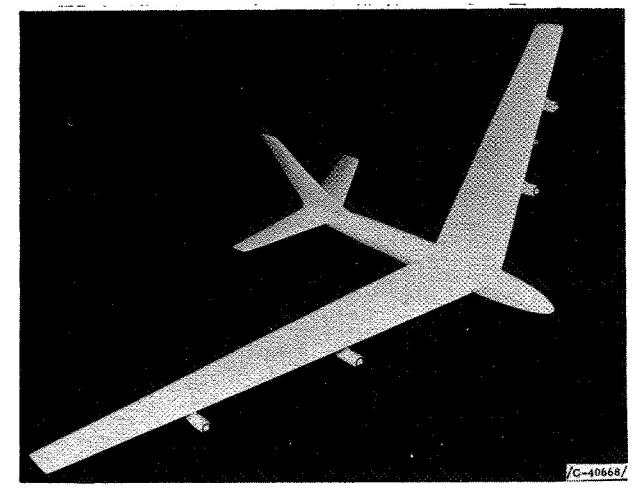

Figure 25

EFFECT OF GROSS WEIGHT ON RADIUS OF SUBSONIC AIRPLANE

TARGET ALTITUDE, 80,000 FT; FLIGHT MACH NUMBER, 0.75

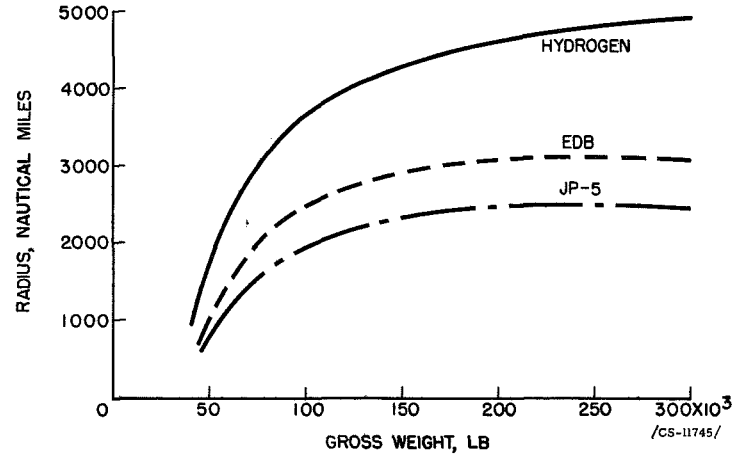

Figure 26

4. RAM-JET ENGINE AND MISSILE PERFORMANCE

Seymour C. Himmel, Chairman
Clarence B. Cohen
Richard J. Weber
Warren D. Rayle
Leonard K. Tower

4. RAM-JET ENGINE AND MISSILE PERFORMANCE

INTRODUCTION

The preceding papers have discussed the application of the turbojet engine to several types of aircraft. In these discussions, the desirability of using high-energy fuels was brought out and some of the problems associated with the application of these fuels were considered. The ram-jet engine and its application to long-range supersonic missiles are discussed herein. In this process, an evaluation of missile capabilities when high-energy fuels are used is made.

Trends differing from those obtained in the turbojet-powered aircraft analyses are to be expected in the present study because of the quite different mission being considered. A missile is required to make but one flight without return; no crew is required; therefore no provision need be made for them and their associated equipment. In addition, a completely different engine is to be employed. The differences between the ram jet and the turbojet that are of major importance in a performance analysis are as follows:

(1) The ram jet is comparatively a light engine, weighing only about one-third as much as an advanced turbojet such as those described in the preceding papers.

(2) The combustor-outlet temperature is not limited by a turbine.

(3) The ram jet, lacking a mechanical compressor, must rely solely on the diffuser to compress the air entering the combustor.

(4) The ram jet, of course, produces no thrust at static conditions and therefore auxiliary boosters are required to bring the missile up to its operating flight conditions.

In this paper, the various factors affecting missile range will be examined first. In this process current engine performance capabilities will be established. Although the propulsion system is the primary consideration of this paper, the engine and airframe are so closely interrelated at the high flight speeds and altitudes considered for missiles that considerable attention must be given to structural and aerodynamic factors. Second, the range increases that can be anticipated from improved engine components will be inspected. Finally, the gains to be had from the use of high-energy fuels will be shown by presenting experimental data on the combustion of these fuels in ram-jet engines and by presenting results of missile-range analyses using these fuels.

All of the analytical work presented is based on a class of missile configurations that is considered reasonable according to present-day

design practices, although not necessarily an optimum design. In this manner, the effects of fuel type, engine design point, and flight conditions can be examined on a common basis. Changes in configuration or detailed assumptions may shift the absolute values of the results presented, but, in general, the trends obtained are expected to persist.

ASSUMPTIONS

Configuration. - The missile configuration assumed for the analysis is shown in figure 1, which is a photograph of a model built to illustrate the principal features. The missile fuselage is a long, slender body with a fineness ratio of 12. The delta wing chosen has an aspect ratio of 2.0 and a thickness-chord ratio of 0.025. The empennage was assumed to have a total projected area equal to one-third that of the wing. The fuselage and the horizontal tail surfaces were assumed to contribute no lift to the configuration. The structure was designed for a normal load factor of 2.0 and an axial load factor of 5.0. There are two engines suspended from the wing in nacelles, one on each side of the fuselage. This configuration is not considered the best that could be designed, but it is expected to yield reasonably good lift-drag ratios by present standards.

Two rocket boosters fueled by gasoline and liquid oxygen are assumed. Their weight varies with the altitude and speed to which the missile is boosted; in all the cases considered, their total gross weight was greater than that of the missile itself. The combined gross weight of missile and boosters was generally assumed to be 200,000 pounds.

Flight path. - The flight path assumed for the missiles is shown in figure 2 where flight altitude is plotted as a function of distance. The missile is boosted to its initial cruise altitude and flight Mach number by the rockets, at which point they exhaust their fuel and are separated. The ram-jet engines then take over and cruise out to the target along a Breguet flight path, that is, the Mach number and lift-drag ratio remain constant and the engine always operates at its design point. However, the altitude increases as the fuel is used.

RESULTS AND DISCUSSION

The range equation for the ram-jet missile is the same as that used for the turbojet airplane in the preceding papers, namely, the Breguet equation

$$R = \eta_e \, h_c \, \frac{L}{D} \ln \frac{W_g}{W_s + W_e + W_p}$$

where

R range

η_e over-all engine efficiency

h_c heating value of fuel

L/D missile lift-drag ratio

W_g missile gross weight

W_s structural weight

W_p payload weight

W_e installed engine weight

As written, this equation applies to the missile alone after the boosters have brought it up to its initial flight conditions. In the present analysis, the payload weight was taken as fixed at 7000 pounds. As has been seen for the airplanes considered in the preceding paper, all the terms in this equation, except for the heating value of the fuel and, of course, the payload weight, are dependent upon the flight speed and altitude which do not appear explicitly. In addition, the fuels which determine the heating value to be used vary greatly in their densities, a ratio of 10 to 1. This large variation in density will have a major effect on the volumes required and hence on structural weights. These interrelations combine to produce optima of flight conditions, engine and missile design that are different for each fuel. The sensitivities of the range to the various terms in the equation will be considered subsequently.

Weights

Engine weight. - The ram-jet weight is relatively low, which would imply that changes in weight-per-unit-frontal-area would not be important since the engine weight is only a small part of the missile weight. Relative range plotted against engine weight for a constant engine efficiency is shown in figure 3. These results are for a family of JP-5 fueled missiles designed for a flight Mach number of 4.0. The weight change considered is that due to improvements in mechanical design, that is, changes in the actual physical hardware, not in the cycle. The results indicate that the weight is not very important for low altitudes, but also show that as the altitude increases the necessary

[redacted]

increase in relative engine size accentuates the importance of engine weight. At 110,000 feet, only a 4-percent reduction in engine weight is required to extend the range 1 percent; whereas, at 70,000 feet, the ratio is 16 to 1. These trends are the same for all the fuels considered.

Structural weight. - In the term called "structural weight" W_s not only the weights of wing and fuselage have been included but also the weights of fuel tanks, instruments, and controls. Of these terms, only one, the wing weight, varies greatly when design altitude is changed. The reason is obvious; as altitude increases the air density decreases and a larger wing is required to support the missile. Required engine weight also increases with design altitude. Thus, the sum of these two terms, engine and wing weights, represents the major effect of design altitude on weight apportionment. This term, engine-plus-wing weight divided by missile gross weight, is plotted as a function of altitude for a hydrogen-fueled Mach 4.0 missile family with a fixed missile-plus-booster gross weight of 200,000 pounds (fig. 4). At the high design altitudes, the sum of wing and engine weights is increasing very rapidly. This sum would be increasing even faster except for another factor which becomes important at these altitudes.

This factor is the missile skin temperature. At the high flight speeds under consideration, the skin friction can cause appreciable heating of the missile surface and the greater the temperature the heavier the required missile structure. The extent of this heating is also a function of altitude as can be seen in figure 5 where the average equilibrium skin temperature is shown as a function of altitude for three Mach numbers. (For this figure an arbitrary length of 30 ft was assumed.) The temperature of the skin is the result of a balance of the heat flow in through the boundary layer and the heat radiated from the surface. The emissivity of the surface is an important factor in determining the equilibrium temperature. The horizontal dash-dot lines show the temperatures that would be reached if the emissivity were zero, that is, the recovery temperatures. The solid lines show the temperature of the surface if an emissivity of 0.6 is assumed. At Mach 4, for example, with an emissivity of 0.6, the skin temperature would be 870° F at 70,000 feet but would drop to 680° if the altitude were increased to 100,000 feet. Thus, skin temperatures can be reduced by designing for higher altitudes, or, for that matter, by flying more slowly.

There are two other ways by which lower skin temperatures can be achieved: (1) by increasing the emissivity and (2) by achieving a laminar rather than a turbulent boundary layer on the missile surface. The emissivity might be raised as high as 0.9 by special treatment of the surface. This might drop the temperature 80° to 100° as illustrated by the dashed curve for Mach 5.0. The gains associated with

[redacted]

laminar boundary layers can be seen by comparing the left- with the right-hand portions of figure 5. At Mach 4.0 and 100,000 feet the skin temperatures drop from 680° F with a turbulent boundary layer to 490° with a laminar layer, even with an emissivity of 0.6. These gains are, of course, only of academic interest unless these laminar layers can be achieved. This will be discussed in the section "Boundary-layer effects."

Thus, increasing design altitude requires heavier engines and wings despite the lighter structures that the lower temperatures permit.

Lift-Drag Ratio

Design altitude has a direct effect on the usable lift-drag ratio which affects the range directly as can be seen from the range equation. The performance of a family of hydrogen-fueled missiles flying at Mach 4.0 is shown in figure 6. The effect of design altitude on lift-drag ratio is shown in the upper curve. The lift-drag ratios shown are those that produce maximum range for each altitude. This requires a compromise between wing weight and fuel weight. Thus the lift-drag ratios given are somewhat less than the maximum that the wing could produce.

Lift-drag ratio increases at first with altitude, then reaches a maximum and declines. The initial rise is the result of the increase of wing size relative to the fuselage. This increase of wing size is required by the reduction in air density as design altitude is increased. If this increase of wing size with altitude were continued, a point would be reached at which all of the missile weight would be required for wing, leaving no weight for fuel. In order to avoid this, the wing size must be restricted; then, in order to obtain the necessary lift, the wing must be flown at higher angles of attack. This increases the drag, resulting in lower lift-drag ratios.

The variation of range with design altitude is shown in figure 6. At high altitudes, high lift-drag ratios are obtained but, as shown in figure 4, large and heavy engines and wings are required. At the lower altitudes, the engines and wings are light but the lift-drag ratios are also lower. Therefore, the maximum range is obtained at some intermediate altitude; in this case, 95,000 feet.

Boundary-layer effects. - When the effects of altitude are considered, the lift-drag ratio and, therefore, the range is greatly affected by the nature of the boundary layer. For example, for the case under consideration, an increase of about $2\frac{1}{2}$ in the lift-drag ratio will result if a laminar boundary layer is achieved.

This result is primarily due to the reduced skin friction drag. The magnitude of the possible reductions can be noted from figure 7, where the average skin-friction coefficients, computed for the

equilibrium temperatures previously mentioned, are plotted for both laminar and turbulent boundary layers. At a Mach number of 4.0 and an altitude of 100,000 feet, for example, the laminar skin friction is only about one-quarter that of the turbulent. At lower altitudes this reduction is even greater if laminar layers are achieved.

Unfortunately, the exact Reynolds number at which transition from laminar to turbulent boundary layers occurs is not as yet very well defined. However, some indications as to the present status can be given. For uncooled boundary layers at moderate Mach numbers, transition Reynolds numbers of only 2 to 3 million seem reasonable. On the other hand, there is a strong favorable effect of high Mach number and surface cooling. For example, the NACA Ames laboratory has measured values of transition Reynolds number as high as 16 million at Mach 7. This was for an extremely rough skin cooled to slightly less than twice the free-stream static temperature. With a smooth surface, free-flight tests conducted by the Lewis laboratory have yielded values as high as 32 million at Mach 3.7. This latter result was obtained with a blunted cone and reflects the following additional reason for optimism: It has been proposed that, at supersonic speeds, blunting of leading edges will prolong the existence of a laminar layer by virtue of the reduction in local Reynolds number that occurs. This reduction results from the total-pressure loss through the bow wave from the leading edge. Figure 8 shows the ratio of the free stream to the local Reynolds number plotted against Mach number for a blunted slender cone. Transition of the boundary layer is hoped to be essentially dependent on the local Reynolds number. In this event, this ratio represents the possible extension of the laminar layer. This is now being investigated experimentally. The single point on the figure shows the result for a blunted-lip hollow cylinder for which nearly the same theoretical curve applies.

Considering these effects, transition Reynolds numbers of the order of 10 to 20 million for the speed range of interest for ram-jet missiles seem reasonable. To put this in terms of length, at Mach 4 and 100,000 feet altitude, a transition Reynolds number of 20 million means that a laminar run of 50 feet could be achieved. At 60,000 feet only about 6 feet of laminar layer would result. Thus, at the high altitudes at which these ram-jet missiles would fly there would be reason to expect a significant extent of laminar layers even with moderate transition Reynolds numbers. However, because of the uncertainty that still remains, the present analysis has been restricted to turbulent layers, except at certain points where the improvements possible, if laminar boundary layers can be achieved, are indicated.

Advanced configurations. - A reduced skin-friction drag can contribute most to lift-drag ratio for a configuration which has the least relative pressure drag. An example of a configuration that may in the future appreciably exceed present standards is illustrated in figure 9.

This configuration is currently being investigated at the NACA Ames laboratory. It consists basically of a half-cone fuselage under a refinement of a flat delta wing. The configuration is designed to take advantage of the interacting flow fields from the fuselage and body. Perhaps the most striking feature is its simplicity. Some estimated lift-drag ratios for this type of configuration, compared with those of the configurations considered in the present paper, are shown in figure 10 plotted as a function of Mach number for both laminar and turbulent boundary layers. For either type, the effect of Mach number is small as compared with the possible gains in going from a turbulent to a laminar layer. The advantage of the Ames design is especially large for the laminar layers because with its low pressure drag it can benefit the most from low skin-friction drags. Preliminary tests of this high-efficiency model indicate that the theoretical predictions are valid. Therefore, with further development of this type of configuration, much greater ranges of flight at supersonic speeds may be anticipated. Perhaps this configuration could even be applied to manned flight as well as missiles.

Engine Performance

The next term to be considered in the range equation is the engine efficiency. For good engine performance a ram jet should fly at high speed. The variation of maximum over-all efficiency of the ram-jet engine is shown as a function of flight Mach number in figure 11. These efficiencies are of the order of 40\ to 50 percent which makes the ram jet the most efficient of all air-breathing heat engines. Engine over-all efficiency increases with flight Mach number, maximizing in the vicinity of Mach 6. However, it is somewhat better to fly at speeds slower than those giving the greatest engine efficiency because, as seen in figure 10, better lift-drag ratios are attainable at lower speeds. Also, and even more important, is the fact designing for the lower speeds yields lower structural temperatures that permit lighter structures to be built. Thus these terms, engine efficiency on one hand and lift-drag ratio and structural temperatures on the other, have opposite requirements as far as flight speed is concerned. Obviously, some best-compromise design-flight speed exists.

High engine efficiency may be obtained in other ways besides flying at high speeds. These ways have to do with the components of the engine and their individual performances. These components shall be examined to determine possible improvements. More important, the effect of each improvement in a component efficiency on range shall be evaluated. In some cases, one or two points in component efficiency is not always worth this effort, since the net effect on range may be quite small.

[redacted]

Diffuser. - The diffuser is the first engine component to be discussed. Basically, the diffuser is just a device to compress the air entering the combustion chamber. Naturally, its efficiency is of major interest. Unfortunately, throughout the years, engine designers have grown into the habit of indicating the diffuser efficiency in terms of the pressure recovery, which is defined as the ratio of the total pressure delivered by the diffuser to that of the free stream. The word "unfortunate" is used because at the very high flight Mach numbers now being considered, the pressure recovery can become quite a misleading number. The reasoning behind the foregoing statement is given below.

In a ram jet, the high-pressure air from the diffuser enters the combustor where fuel is added and burned. Expansion of the hot gases then takes place through an exhaust nozzle to produce thrust. This means that the effects of pressure losses in the diffuser are present at the exhaust nozzle when the expected pressure ratio is not obtained. The importance of this loss is indicated on figure 12, which shows the relative jet thrust produced by a series of exhaust nozzles designed for various pressure ratios. At each Mach number, these pressure ratios vary directly with pressure recovery. If there were no pressure losses anywhere in the engine, the available pressure ratio across the nozzle is that shown by the circles. These correspond to the maximum thrust condition at each flight Mach number.

When the diffuser is inefficient, this maximum amount of pressure is not made available to the nozzle, which, of course, reduces the thrust produced. Pressure recovery is quite important at low Mach numbers, such as 3, but, relatively, not as important at higher Mach numbers. Also, at low Mach numbers, good pressure recovery decreases the required size of the combustion chamber, which reduces the engine frontal area. However, at high Mach numbers, the combustion chamber is already smaller than the inlet, so that further reductions do not affect the frontal area.

These arguments lead to the conclusion that pressure recovery is not, in itself, a very satisfactory criterion to use for diffusers operating in the region of flight Mach numbers considered in the present paper. Instead, a related parameter is preferred, the kinetic-energy efficiency of the diffuser.

This term is defined in figure 13. A simple ram-jet engine is illustrated. The air enters at the left and slows down while passing through the diffuser, thus raising the pressure. If the air is merely expanded back to its original ambient pressure through a frictionless nozzle without any burning in the combustor and if the diffuser were perfect, the jet velocity produced would be equal to the velocity of the entering air. However, because there are losses in the diffuser, the exit velocity is always somewhat less than the initial velocity; the square of this velocity ratio is defined as the kinetic-energy efficiency.

[redacted]

The importance of this parameter is evident from the fact that a 1-percent increase in kinetic-energy efficiency generally results in about a 2-percent increase in over-all engine efficiency. This in turn would result in a 2-percent increase in missile range.

The kinetic-energy efficiency is plotted as a function of pressure recovery for several flight Mach numbers in figure 14. Just as an example, a pressure recovery of 0.15 would ordinarily be considered to be very poor indeed, but the figure shows that at a Mach number of 6 this value corresponds to an efficiency of 90 percent which is actually quite good.

The lower dashed curve on the figure shows the performance of the simple normal-shock type of diffuser. At all but the lowest Mach numbers, it is very inefficient. The experimental data points on the upper dashed curve show the performance that has been obtained with highly refined inlet designs. At high Mach numbers the pressure recovery falls off rapidly, but the efficiency is above 90 percent even up to Mach 5.0. It has already been mentioned that a 1-percent increase in efficiency will result in approximately 2-percent increase in range. But efficiencies are already so high that relatively little room remains for future improvement in this respect.

One other point might be mentioned about diffusers that does not appear explicitly on the figure. Diffusers giving the highest efficiencies often have large nacelle drags associated with them. In many cases, it may be desirable from a range standpoint to deliberately surrender some efficiency in order to reduce these drags.

The preceding discussion should not be interpreted to mean that good pressure recovery is not desired. It is desired, but the determining factor is what is considered good. A value of pressure recovery that is considered poor at low Mach numbers would be called good at a high Mach number. Another factor is that the pressure recovery determines the pressure level in the engine. And high pressures are desirable for good combustion efficiency.

Combustor. - The importance of good combustion efficiency is apparent from the figure 15. The left-hand figure shows relative range plotted against combustion efficiency. A change in combustion efficiency affects the range in direct proportion. An efficiency of 90 percent was used in the cpmputations for the present paper. This is a very reasonable value, as will be established later in this paper.

Flameholders are normally required for good combustion efficiency. The loss in range caused by flameholder pressure loss is indicated by the figure on the right. Relative range is plotted against pressure loss in terms of q, the dynamic head of the stream approaching the flameholder. At Mach 4 considerable flameholder pressure loss can be

tolerated. At lower flight Mach numbers the flameholder pressure loss becomes more important as was the case with diffuser pressure recovery.

In some cases, the increased pressure loss accompanying additional flameholding action is more than outweighted by improved combustion efficiency. For example, in one test an increase of one q in flameholder pressure loss was accompanied by an 8-percent improvement in combustion efficiency.

Another factor influencing combustor performance is the velocity profile of the air stream entering the combustor. Very irregular profiles, that is velocity distributions containing both high- and low-velocity air, are not desirable. They reduce the combustion efficiency and also increase combustor pressure losses. The addition of screens upstream of the combustor will often improve poor velocity distributions. The pressure losses across the screens may be more than compensated for by the increased combustion efficiency. With hydrocarbon fuels, another method for correcting the effects of a bad profile is possible. This method is to burn stoichiometrically in the most uniform part of the flow. The combustion products mix with the rest of the air before it enters the exhaust nozzle.

Exhaust nozzles. - The exhaust nozzle is the final engine component whose performance can affect the over-all engine efficiency. In figure 16, relative range is plotted as a function of the exhaust-nozzle velocity coefficient. Range is quite sensitive to this parameter; a 1-percent increase in velocity coefficient results in more than a 3-percent increase in range. However, velocity coefficients ranging from 0.960 to 0.975 have been obtained experimentally with many nozzle designs. This seems to leave little room for any major range improvements.

High-Energy Fuels

The components of ram-jet engines have been examined and the possible improvements in engine performance have been ascertained. Each of the improvements alone offers relatively small range increases; but, if they can be compounded, reasonably large improvements in range can result. This will require great effort to obtain, however. In any event no major break-through in missile range capabilities is apparent; unless, of course, laminar boundary layers or the higher lift-drag ratios that appear possible with advanced aerodynamic configurations such as the Ames configuration can be achieved.

If these improvements are not considered, the only possible means for improving range lies in the one remaining term in the range equation, namely, the heat of combustion of the fuel. There are a number of possible fuels with heating values considerably in excess of those

of hydrocarbons. The density of these fuels is a factor of major importance because the ram-jet missile is composed largely of fuel.

Combustor tests. - A question to consider before analyzing missile performance with high-energy fuels is how well and how easily these fuels will burn at the conditions that will be encountered in ram-jet combustors. The amount of experimental data on the combustion of these fuels cannot be compared with the vast quantity accumulated for hydrocarbon combustion in the past decade; but, recently quite a bit of data on the combustion of high-energy fuels in ram-jet combustors have been obtained at the NACA Lewis laboratory.

Numerous tests using quite an assortment of combustor hardware, ram-jet engines, and facilities have been carried out. For example, with pentaborane, there are data from direct-connect installations, from flight tests of a 9.75-inch ram jet, and from free-jet tests of a 48-inch ram jet.

The combustor developed during the direct-connect tests and used for the flight tests of the 9.75-inch ram jet is shown in figure 17. Its fuel injector is a set of radial bars which fits between the elements on the right. The direct-connect tests showed that the pentaborane burned about as well without flameholders. So the V-gutter elements on the right were probably not needed to stabilize the flame. They did serve another and entirely different purpose; they accelerated the air flowing by the fuel injectors. Thus the pentaborane emerging from the bars was immediately blasted by a high-velocity air stream. This helped to mix the fuel and air and also served to prevent the flame from seating on the fuel injectors. The results obtained from the flight tests of this design indicated combustion efficiencies of over 90 percent.

The combustor used in the free-jet tests of the 48-inch ram jet is shown in figure 18. The flameholding action is negligible. The principal components are the fuel injectors, radial tubes of insulated double-walled construction to shield the fuel from the hot air stream. With this unit, the data shown on figure 19 were obtained. Two tests were made at a simulated altitude of about 80,000 feet and a Mach number of 2.75. For the first test, the combustion efficiencies were between 85 and 90 percent, decreasing with increasing equivalence ratio. Here the combustor was 8 feet from fuel injectors to exahaust nozzle. The second test, at slightly different flow conditions, yielded efficiencies from 80 to 87 percent with a 6-foot combustor length.

Hydrogen has also been tested in various units. Figure 20 illustrates a ram-jet combustor (16-inch diameter) designed for hydrogen fuel. No flameholder was used; the fuel was simply injected through annular fuel-bar segments. The combustor length from fuel injector to exhaust nozzle was only 28 inches. (The radial elements shown just downstream of the exhaust nozzle are water sprays to cool the exhaust gases during the tests.)

[redacted]

Results obtained from this combustor are given in figure 21. Combustion efficiency is shown as a function of equivalence ratio for two pressure levels. The combustion was quite efficient; at an equivalence ratio of 0.8, efficiencies of 94 and 97 percent were obtained at the two pressure levels. The location of the peak efficiencies is not especially significant, since burners generally can be designed to exhibit peak efficiency at any equivalence ratio desired.

Data of this type that have been obtained with high-energy fuels are summarized in figure 22 which shows the inlet conditions under which the data were taken on a pressure-temperature map and notes the peak efficiencies achieved. The inlet conditions of interest for the ram-jet missiles are in the right half of the figure where contours of flight Mach number and altitude are plotted. All the experimental data are at combustor-inlet temperatures somewhat lower than those that would exist in the missile engines. However, there seems no reason to suppose that increasing temperature should do anything but increase the combustion efficiency. The data indicate that with the experience now available, combustors can be designed to burn the high-energy fuels at efficiencies of 90 percent or higher in the general region of interest. For example, with a temperature of 40° F and a pressure of 4 pounds per square inch absolute, pentaborane was burned at an efficiency of 95 percent. Diborane yielded 95 percent efficiency at an inlet temperature of 290° F and a pressure of 8 pounds per square inch absolute. The only fuel, EDB, for which no data are shown has been available in amounts too small for such tests. Experiments with blends of EDB and JP-5, however, show that its behavior compares favorably with that of pentaborane.

3982

Combustor design principles. - From many tests similar to those previously mentioned, guiding criteria have been determined for the design of ram-jet combustors for high-energy fuels. Some of these design principles are as follows:

COMBUSTOR DESIGN PRINCIPLES FOR FUELS OF THREE TYPES

Hydrocarbon (JP-5)	Boron hydrides	Hydrogen
Stratify flow to burn near stoichiometric	Distribute fuel uniformly with total air	Use large number injection points for uniform mixing
Stabilize flame with large flameholder	Little flameholding action required	Little flameholding action required
Design can reduce effects of bad profile	Flat velocity profile advantageous	Flat velocity profile advantageous
Careful provision for ignition is necessary	Ignition no problem	Easily ignited
	Oxide deposits may be problem	Very short combustor may be used

[redacted]

JP-5 is included as representative of the hydrocarbons. For the boron hydrides, most of the data were obtained with pentaborane, but the design principles should be expected to apply to the other fuels of this class.

The fuel injection and distribution: With hydrocarbons, the greatest efficiency can be obtained by stratifying the engine air flow. That is, the fuel is mixed with just a part of the engine air, so that local combustion is at nearly stoichiometric fuel-air ratios. With pentaborane, the best results have been obtained by distributing the fuel uniformly with the total air, regardless of the over-all equivalence ratio. With hydrogen (injected as a gas) a large number of injection points has been found to provide the best results.

Stabilizing the flame: With hydrocarbons, a flameholder blocking a considerable portion of the combustor area is required. This may, of course, be less true as the inlet temperatures become very high. For pentaborane, research thus far has indicated that the combustion is equally efficient with or without a flameholder. With hydrogen, again the contribution of the flameholder seems negligible.

Inlet-air velocity profile: For hydrocarbons the flow stratification permits the combustor design to partly compensate for nonuniform profiles. With the other fuels, because of their high reactivity, good combustion efficiency can be achieved even with relatively poor velocity. If uniform velocity profiles are obtained, short combustors can be utilized with these fuels.

Ignition: Igniting the hydrocarbon fuels may be quite difficult, since the air velocities will be high and the static pressures quite low. Of the boron-hydrides, pentaborane or diborane will probably ignite spontaneously; the hydrogen will ignite readily.

Experimental results with hydrogen fuel have also indicated that combustor lengths much shorter than required for hydrocarbons may be used.

The great reactivity of the boron fuels and also of the hydrogen may lead to special problems. The flames are not clinging to flameholders to avoid being swept downstream - they are apt to propagate right up to the fuel injectors. If local regions of low air velocity exist, the fuel injectors may even become surrounded by flame; in this event, even if the injectors do not melt completely, their performance is apt to be affected. In the case of the boron fuels, especially, there is danger of oxide forming on the fuel nozzles and, also, the fuel decomposing inside the fuel line because of the heat.

Actually, these two factors, oxide deposition and thermal decomposition are problems in their own right. Obviously, any large accumulation

of oxide on the combustor or exhaust nozzle may appreciably affect the engine performance. With the ram jet, at least, the problem seems less severe than with the turbojet. Insufficient data are available to evaluate properly the problem at the flight speeds and altitudes of interest.

Thermal decomposition is a problem for the boron fuels, and also for the hydrocarbons. If these fuels are overheated, they break down. The residues contain both solid and gummy substances which may complicate both handling and combustion of the material.

Tankage problem. - From the previous discussions, apparently no major difficulties are to be expected in operating engines on these high-energy fuels. The combustion problem, if anything, should be simpler than with the usual hydrocarbons.

A problem which still remains is that of excessive heating of the fuel while in the tanks. This is of particular importance for the ramjet missile because, at the Mach numbers to be encountered, the skin of the wing and fuselage may be heated up to as high as 800° or 900° F. At the same time, it is necessary to keep the fuel from vaporizing faster than the engines are using it. Otherwise, extra vapor would have to be dumped overboard to keep the pressure from building up until it burst the tanks. The fuel that has the lowest boiling point is hydrogen. Therefore, if vaporization can be restricted, the worst boiling problem will have been eliminated.

The assumed missile configuration shown in figure 23 contains two fuel tanks in the fuselage with the central area occupied by the pay load. The tank construction is basically the same as with the turbojet airplane and so the same technique can be employed for insulating; that is, the fuselage is converted into an oversized thermos bottle by venting the space around the tanks to the atmosphere to reduce convection and polishing or silvering the inside of the skin to reduce radiation. Venting to the atmosphere is especially effective for the missile because the flight altitudes will be so high that a vacuum is approached around the tanks. The question then arises of how effective these design principles are in cutting down the heat transfer to the tanks with hydrogen. The calculations show that, in order to absorb all the heat that leaks through into the tanks, about 2000 pounds of fuel per hour must be vaporized. Actually, the engines use about 20,000 pounds an hour, so that a factor of safety of about 10 results. Some of this extra cooling capacity of the fuel will undoubtedly be necessary to cool local hot spots such as the leading edges of the wings or the engines.

Trouble may still be encountered, however, just sitting on the ground waiting for take-off after the tanks have been filled. As with the turbojet airplane, the tanks were insulated to extend this no-loss time. The present analysis indicates that 1 inch of insulation would

enable the hydrogen-fueled ram-jet missiles to remain on the ground for 2 hours before any fuel is lost through boiling off. This insulation costs less than about 3 percent in range. Thus, there are apparently no unsolvable problems with the fuel tanks, whether JP-5 or any of the high-energy fuels are used.

Missile Performance

The range equation has been discussed; and the combination and interrelation of engine performance, structural weights, and aerodynamics in the design of a good missile have been pointed out. As for the engine itself, high component efficiencies are concluded to be a necessity for long ranges; however, the efficiencies obtainable today (at least in the laboratory) are so high that future component improvements can not be expected to greatly increase missile ranges.

New aerodynamic developments, such as the Ames configuration, appear very promising, especially if laminar boundary layers can be maintained. However, the emphasis herein is placed upon what can be done from the propulsion systems approach. For missiles propelled by ram-jet engines, one is led almost by process of elimination into considering the advantages of fuels other than the usual hydrocarbon type.

A number of high-energy fuels have been proposed and it was concluded that there are probably no insurmountable obstacles to their use, as far as storing in fuel tanks and burning in the engines are concerned.

With this as a foundation, some calculated performance of the over-all missile system can now be presented.

Effect of combustion temperature. - In the past, hydrocarbons have been the only fuels intensively considered for long-range missile applications. Figure 24 shows the ranges of a whole family of missiles using JP-5, each with a missile-plus-booster gross weight of 200,000 pounds. The independent variable is the engine combustion temperature. At each temperature and Mach number, a new missile has been designed with the combination of engine size, wing loading, and flight altitude that yields the best range.

If the temperature is too low, the engine does not develop much thrust. Range is lost because the engines that are required become big and heavy. On the other hand, too high a temperature may reduce the engine size but the over-all engine efficiency also drops off and again range is lost. The temperatures for greatest range increase with flight speed. The maximum range obtained is about 5400 nautical miles, which comes at a Mach number between 3.5 and 4.0.

[redacted]

Effect of gross weight. - One way to improve the range of hydrocarbon-fueled missiles is to increase the size of the missile. This is shown in figure 25 which gives range as a function of missile-plus-booster gross weight for a JP-5 missile. This method of extending range is definitely expensive. For example, increasing missile-plus-booster gross weight from 200,000 to 250,000 pounds raises the range by only 250 miles, less than 5 percent.

Evidently, high-energy fuels are a more promising way to achieve longer range for the same gross weight (or, conversely, to obtain the same range with lower gross weights). This is illustrated by figure 26 in which curves have been added showing the range possible with hydrogen and pentaborane. Two points are also spotted on the figure for EDB and diborane. Hydrogen has, of course, the highest heating value but is penalized severely by its low density, so that the resulting range is somewhat less than that with the boron hydrides. However, all four high-energy fuels provide considerably more range than JP-5 at the same missile-plus-booster gross weight.

A point to keep in mind when gross weight is mentioned is the different amounts of fuel contained in the missiles even when the gross weight of the missile is the same. This is emphasized on figure 27, which shows the percent of fuel contained in ram-jet missiles designed for JP-5, for pentaborane, and for hydrogen. About 70 percent of the JP-5 missile weight is initially fuel; whereas, for the other missiles, the fuel weight is a smaller proportion. This is due, of course, to the larger structure required to contain the less dense fuel.

Since the fuel-to-gross weight ratio is seen to vary from one fuel to the next, the results are certainly affected by the criterion used to compare various missiles. The figures, generally, present the range obtainable with a fixed weight of the missile plus booster. Either, missile gross weight or empty weight or even cost (which would have taken into account the presently high cost of most high-energy fuels) could have been used. At any rate, it is hoped that similar trends would have been found even if one of the other criteria had been used besides fixed missile-plus-booster gross weight.

Effect of flight Mach number. - The different fuels have been compared in the preceding discussion at a single Mach number. A more general picture is given by figure 28, which shows maximum missile range as a function of flight Mach number for the various fuels. The best speed for all the missiles considered is in the region of Mach 3.5 to 4.0, with pentaborane yielding the longest ranges. Single points have been included for diborane and EDB. Including the effects of both heating value and density, diborane gives about the same performance as pentaborane, and EDB is between pentaborane and hydrogen.

[redacted]

The shaded region indicates the variation in range of the pentaborane missiles depending on whether there is frozen or equilibrium expansion in the nozzle. Similar variations would also occur for the diborane and EDB points. But in any case, the differences are quite small for the conditions of interest.

All fuels are compared on this figure at the same combustion efficiency. However, as already discussed, the high-energy fuels might reasonably be expected to burn more efficiently and so demonstrate even greater superiority over JP-5.

The results of the third panel indicated that for the turbojet bomber, at high altitudes, maximum range was obtained with hydrogen used as the fuel. Even when the bombers were designed and flown at the optimum altitudes for each fuel, hydrogen still gave the longest ranges although its margin of superiority was reduced. This is not the case for the ram-jet missile. The reason for this is related to the generally higher fuel-to-gross weight ratios for the missiles. More fuel can be carried by the missiles because lighter engines are used and components such as landing gear can be omitted. But because so much of the total weight is fuel, the performance of the missile is more severely affected when a low-density fuel is used. The structure enclosing all this fuel gets much larger and heavier, which penalizes the missile designed for hydrogen. This same argument explans why the hydrogen missile starts to improve at the very high flight Mach numbers. Aerodynamic heating requires a heavier structure for flight in this region so that there is less room for fuel. And when there is not much fuel carried, the low density of hydrogen is not so much of a problem, which is similar to the case of the turbojet bomber at low Mach numbers.

The optimum altitudes that were used to obtain the ranges illustrated in figure 28 are shown in figure 29. The altitudes at the start of cruise are given at the left; the optimum altitudes increase with flight Mach number and are highest for the least dense fuel. (The reasons for this have been given in the preceding papers.) Initial cruise altitude is probably not so important as the altitude at which the missile nears its target. The flight path (fig. 2) showed a gradual increase in altitude as fuel was consumed. The optimum altitudes over the target are shown on the right. The JP-5 missile, which initially has 60 to 70 percent of its weight in fuel, increases about 25,000 feet in altitude. The hydrogen missile is initially only about 45 percent fuel and gains less than 15,000 feet during flight. It still has the highest final altitude, however.

Effect of design altitude. - The maximum range obtainable at each Mach number and the optimum altitudes yielding those ranges are shown in figures 28 and 29. Figure 30 illustrates, specifically, the effect on range of variations in initial-design-cruise altitude for the hydrogen missile family at a Mach number of 5. The range drops substantially

if the missile is designed for the wrong altitude, as shown by the lower curve which assumes a turbulent boundary layer. However, if the Reynolds number is decreased by going to higher than "normal" altitudes, it may be possible to achieve a considerable extent of laminar boundary layer and the associated greatly increased range. For example, the upper curve indicates the range that can be expected with laminar layers over the entire airframe. As previously stated, predicting the conditions under which transition occurs from turbulent to laminar layers is a very inexact science as yet. However, the shaded area illustrates the probable gains that would result for transition Reynolds numbers of the order of 10 to 20 million. Both longer ranges and higher flight altitudes apparently are distinct possibilities because of this boundary-layer effect.

Selection of design flight conditions. - The effect of flight Mach number on missile range for the different fuels has been discussed and the design altitude been shown to be of major importance. It might be interesting to take a slightly different approach to the comparison of the different fuels and flight conditions than that already presented.

The best JP-5 missile presented had a range of 5400 nautical miles for the standard missile-plus-booster gross weight of 200,000 pounds. In order to achieve this range, it was necessary to design for one particular flight speed and altitude. If this range is adequate would there be any advantage in going to high-energy fuels?

Of course, instead of using the longer ranges, the weight of the missile could be substantially reduced (fig. 26).

Another alternative is to employ the greater potential of the high-energy fuels in order to fly either faster or higher, both of which are desirable for tactical purposes. In other words, the designer is no longer so restricted in his selection of cruising Mach number and altitude. This is shown in figure 31 where final cruise altitude is plotted against flight Mach number. The contours represent the extremes in altitude and Mach number for which the missiles can be designed and still fly 5400 miles with a total gross weight of 200,000 pounds. The single point in the center is for the JP-5 missile. If either the flight speed or altitude of the JP-5 missile is changed, this range can no longer be achieved. This single point can be expanded into the comparatively large area within the inner ring if hydrogen fuel is used. Any combination of design speed and altitude within this area will result in ranges of 5400 miles or more. Similarly, any point within the outer ring will result in ranges of more than 5400 miles for the pentaborane missiles.

Thus, with either pentaborane or hydrogen, considerably more freedom in the missile designs can be tolerated than with JP-5 fuel.

CONCLUDING REMARKS

The analysis showed that with conventional hydrocarbon fuels there are some gains in engine performance to be had by improving engine components but nothing of what might be considered major proportions. With regards to propulsion systems, the greatest field of exploitation that remains exists in the realm of high-energy fuels. The high combustion performance theoretically possible has been experimentally established for such fuels. With the use of these fuels, the range could be appreciably increased for a given missile-plus-gross weight or, conversely, gross weight could be decreased for a given range. Or, what may be an equally important consideration, it is possible to design a missile that can fly higher and faster to accomplish the same mission. The boron hydrides and hydrogen are very competitive in this connection, both giving fairly wide latitude in the selection of flight conditions for a given range.

Another possible way of improving missile capabilities is the achievement of laminar boundary layers. Here again the high-energy fuels and their ability to fly high and fast offer the best possiblity of getting into the flight regime where laminar boundary layers may prevail - this may permit even greater freedom in the selection of design flight conditions.

If the promising aerodynamic characteristics of missile designs such as the Ames configuration are added, an entirely new vista of possible missile performance has been opened to the designer. In fact, if each of these effects can be simply compounded, the range now possible could probably be doubled.

All of these are relatively new fields for exploration, and they offer an interesting and important challenge for future research.

RAM-JET MISSILE

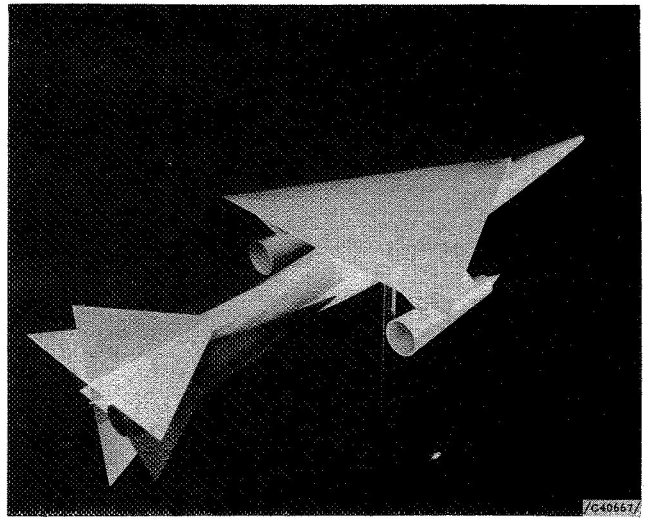

Figure 1

MISSILE FLIGHT PATH

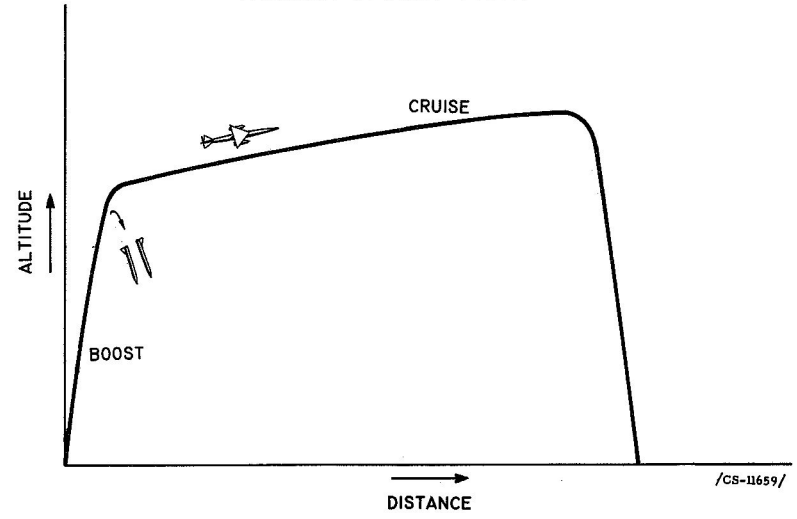

Figure 2

EFFECT OF ENGINE WEIGHT ON RANGE
AT CONSTANT ENGINE EFFICIENCY

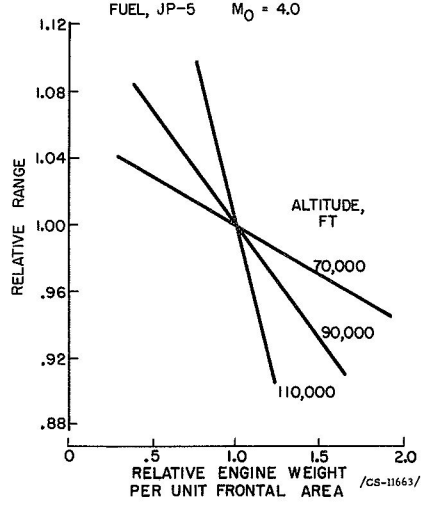

Figure 3

EFFECT OF ALTITUDE ON SUM OF
WING AND ENGINE WEIGHTS

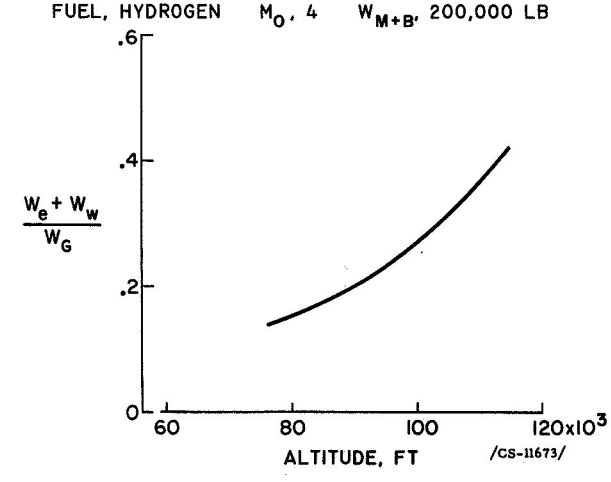

Figure 4

AVERAGE RADIATION EQUILIBRIUM SKIN TEMPERATURES

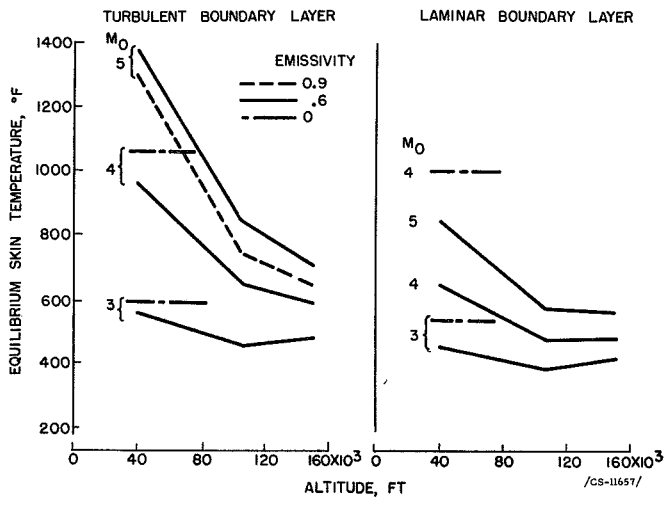

Figure 5

EFFECT OF ALTITUDE ON MISSILE PERFORMANCE

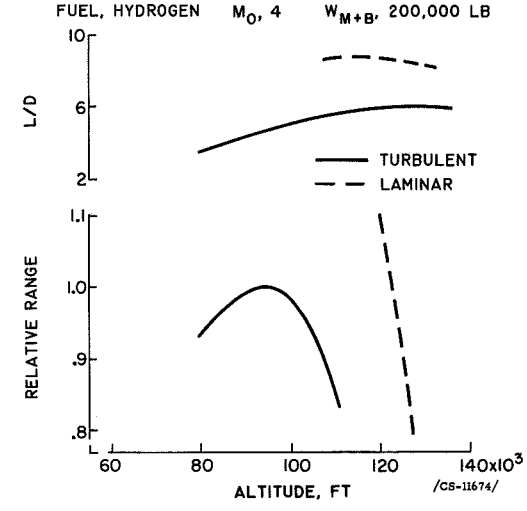

Figure 6

AVERAGE SKIN FRICTION COEFFICIENTS

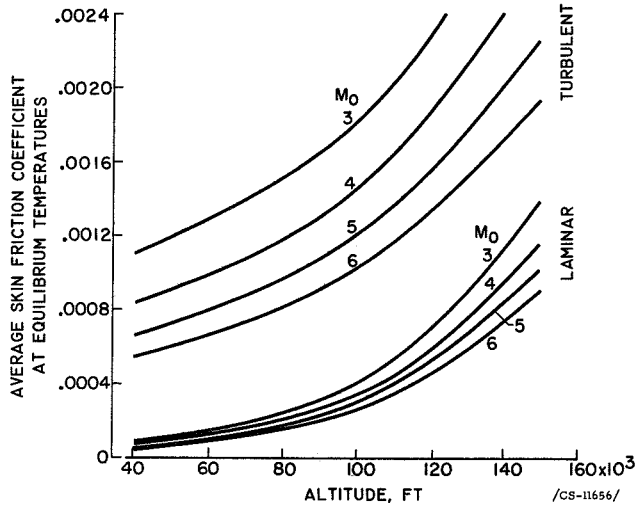

Figure 7

EFFECT OF LEADING EDGE BLUNTING ON REYNOLDS NUMBER

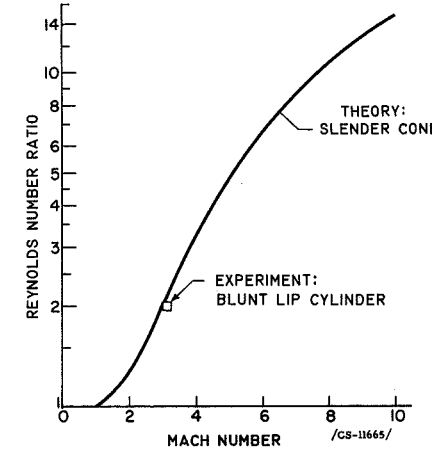

Figure 8

ADVANCED MISSILE CONFIGURATION

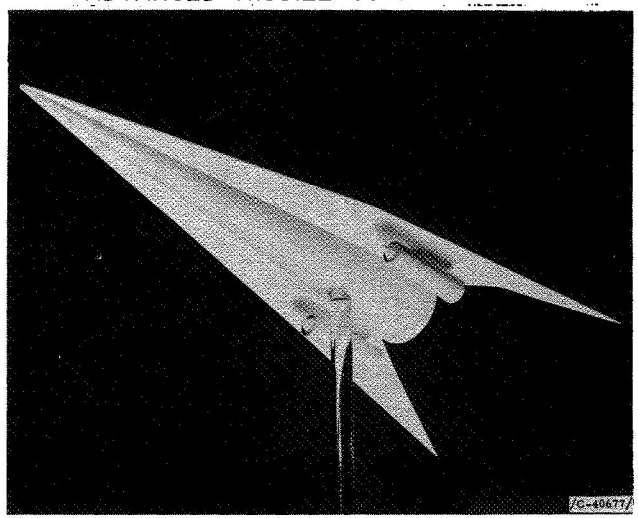

Figure 9

MAXIMUM MISSILE LIFT-DRAG RATIOS

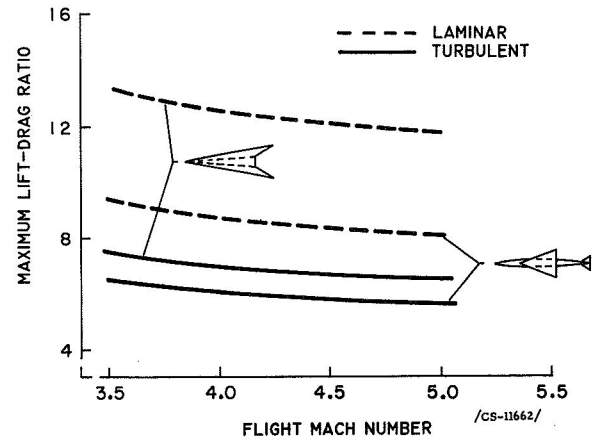

Figure 10

MAXIMUM OVER-ALL EFFICIENCIES OF RAM-JET ENGINE

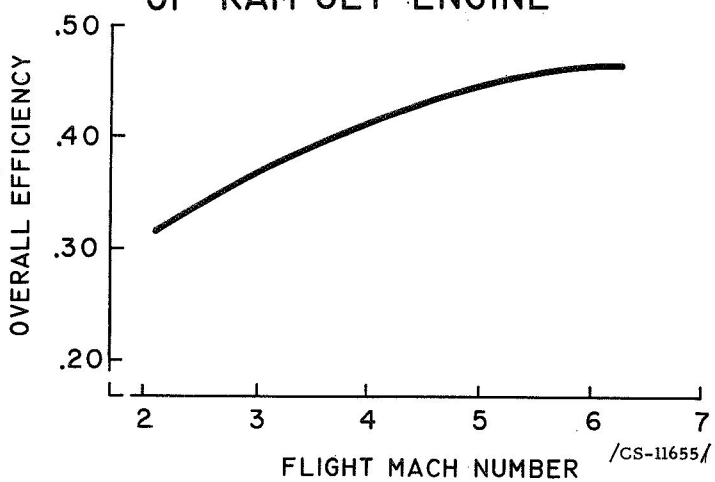

Figure 11

JET THRUST OF RAM-JET ENGINE

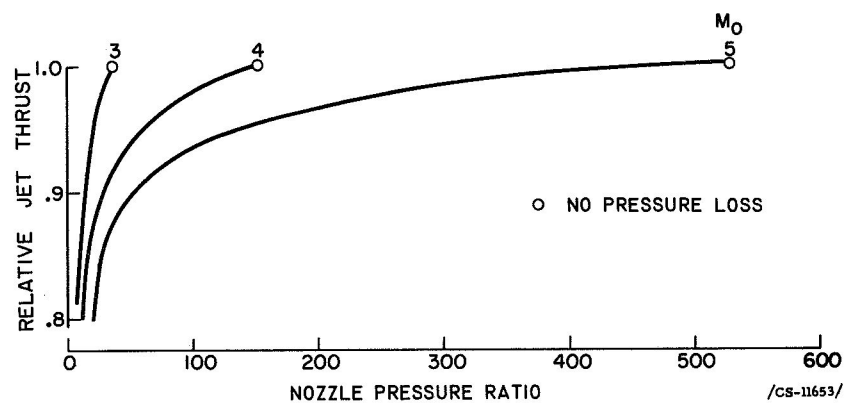

Figure 12

KINETIC-ENERGY EFFICIENCY

$$\eta_{KE} = \frac{\text{KINETIC ENERGY OUT}}{\text{KINETIC ENERGY IN}} = \left(\frac{V_{out}}{V_{in}}\right)^2$$

/CS-11654/

Figure 13

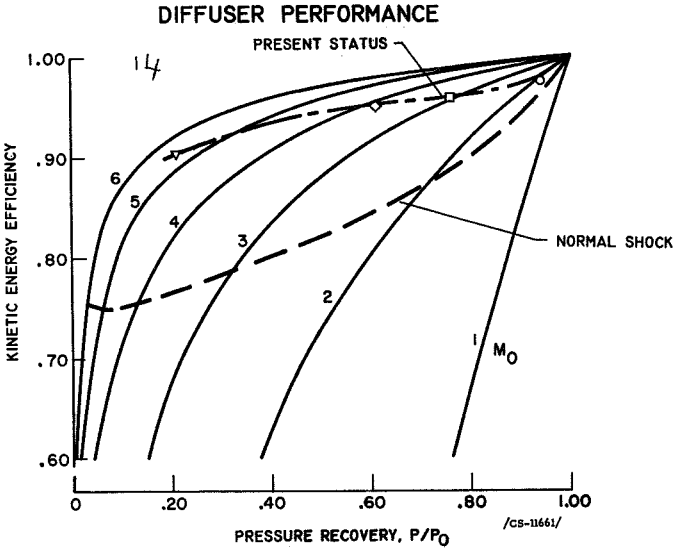

Figure 14

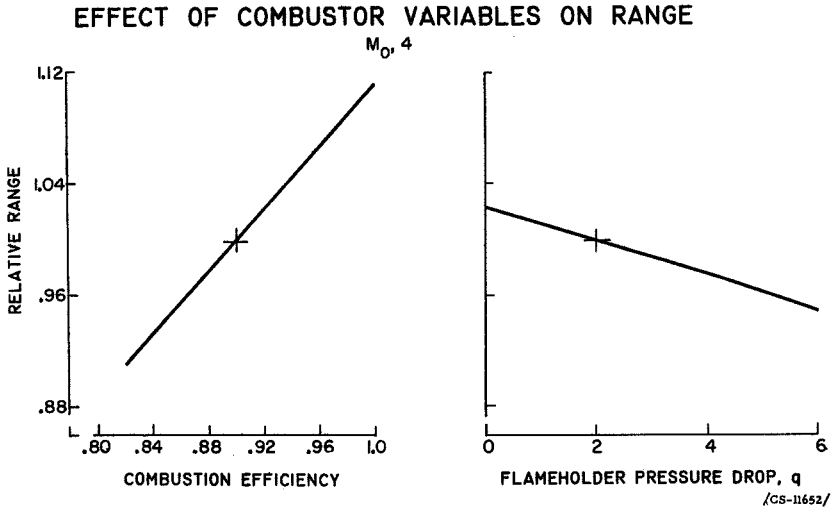

Figure 15

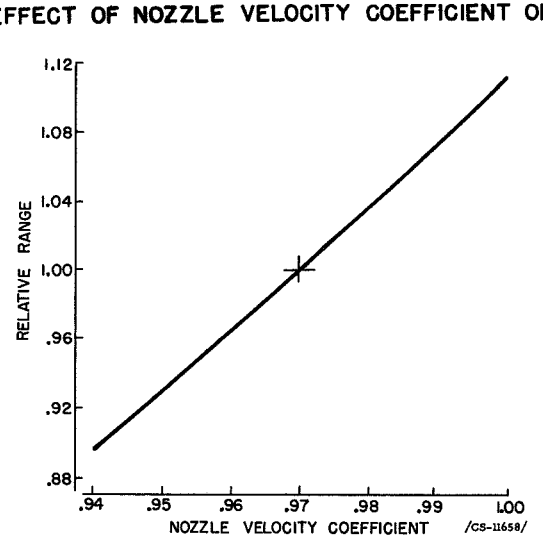

Figure 16

PENTABORANE COMBUSTOR FOR 9.75-INCH RAM JET

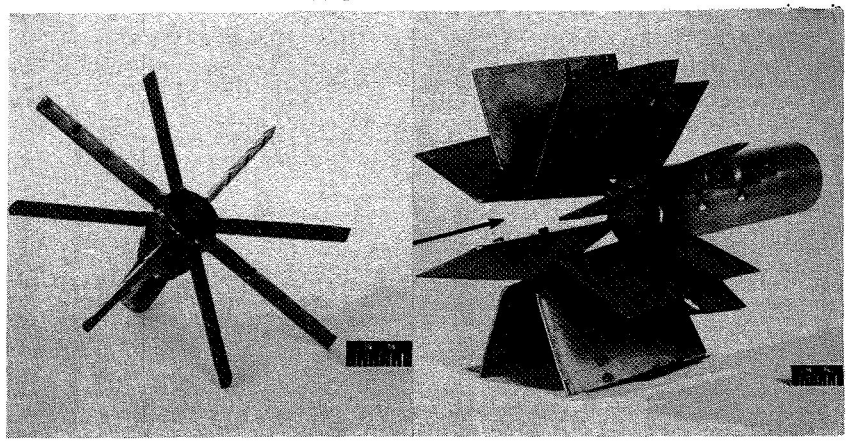

FUEL INJECTOR AIR ACCELERATOR /CS-11660/

Figure 17

PENTABORANE COMBUSTOR FOR 48-INCH RAM JET

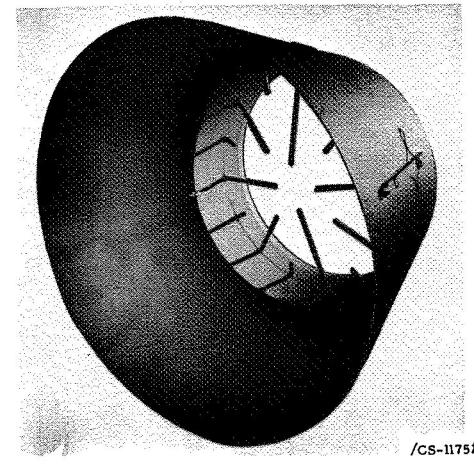

/CS-11754/

Figure 18

PERFORMANCE OF 48-INCH RAM JET ENGINE WITH PENTABORANE FUEL

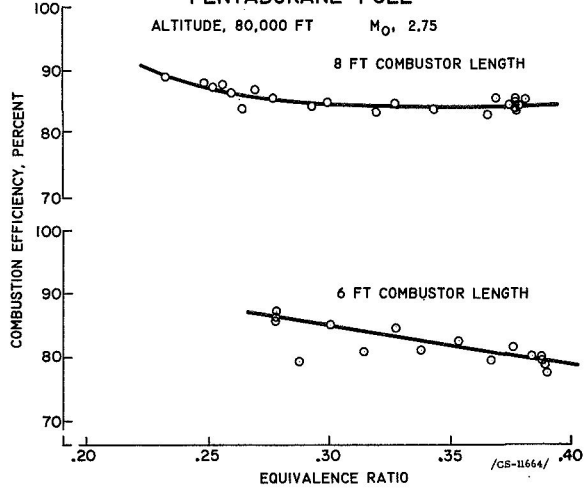

Figure 19

COMBUSTOR FOR 16-INCH RAM JET USING HYDROGEN FUEL

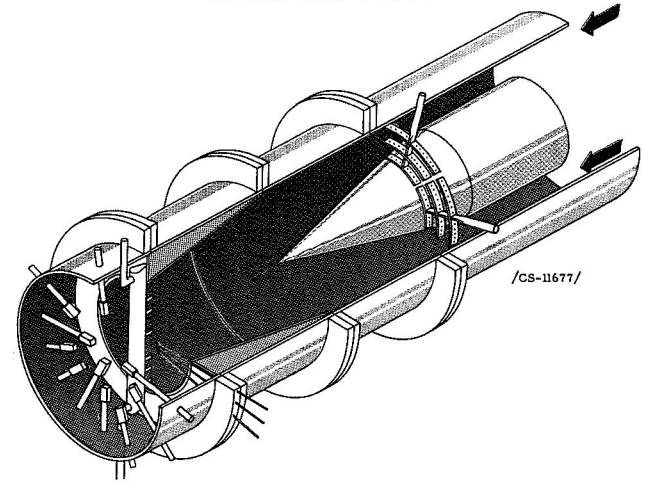

Figure 20

PERFORMANCE OF HYDROGEN FUEL
IN 16-INCH RAM JET ENGINE

COMBUSTOR LENGTH, 28 INCHES

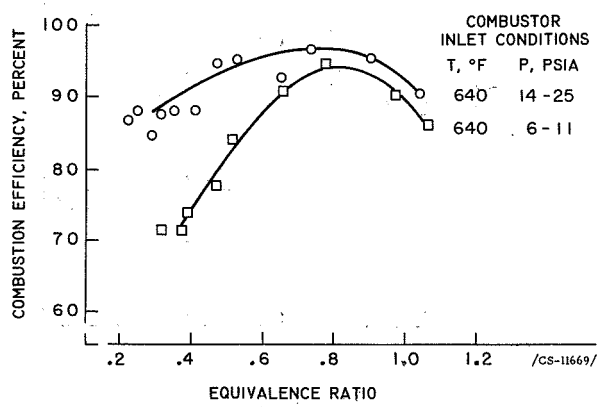

Figure 21

MEASURED COMBUSTION EFFICIENCIES

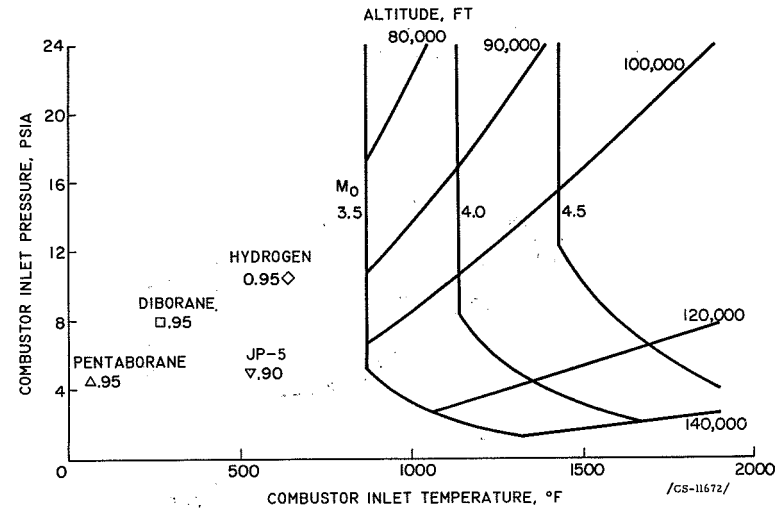

Figure 22

FUEL-TANK CONFIGURATION

RAM-JET MISSILE

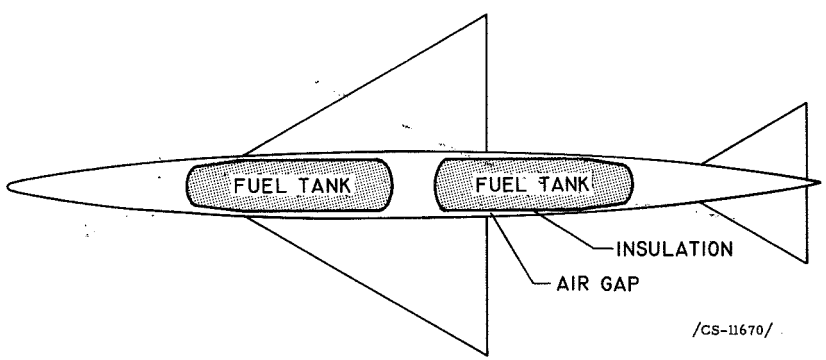

Figure 23

EFFECT OF COMBUSTION TEMPERATURE ON RANGE

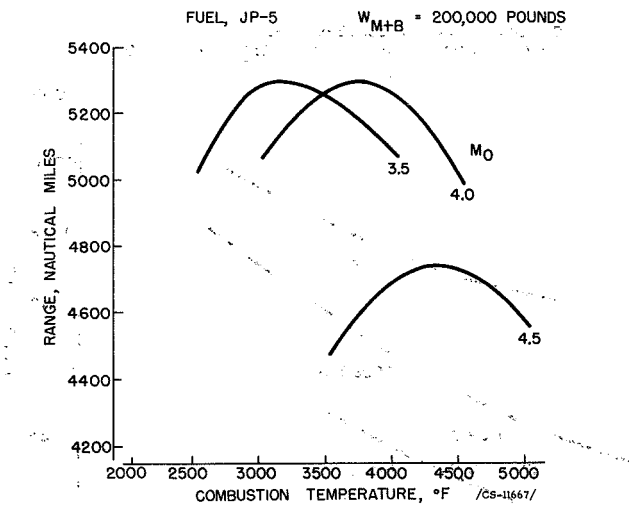

Figure 24

EFFECT OF MISSILE-PLUS-BOOSTER GROSS WEIGHT ON RANGE

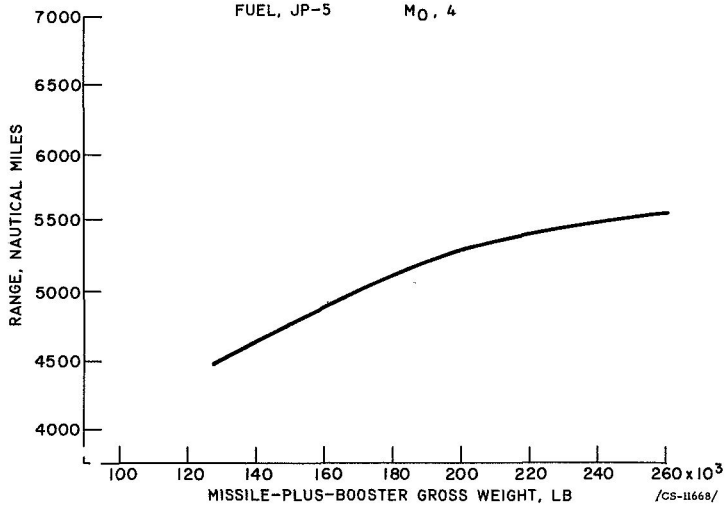

Figure 25

EFFECT OF MISSILE-PLUS-BOOSTER GROSS WEIGHT ON RANGE

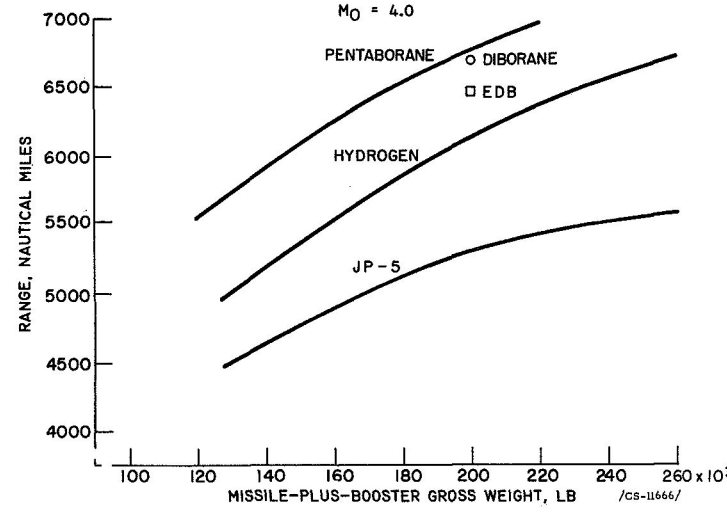

Figure 26

MISSILE WEIGHT DISTRIBUTION

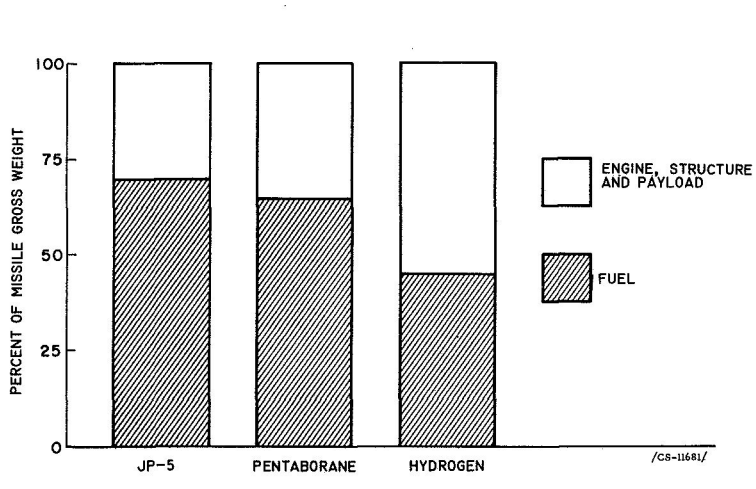

Figure 27

EFFECT OF FLIGHT MACH NUMBER ON RANGE

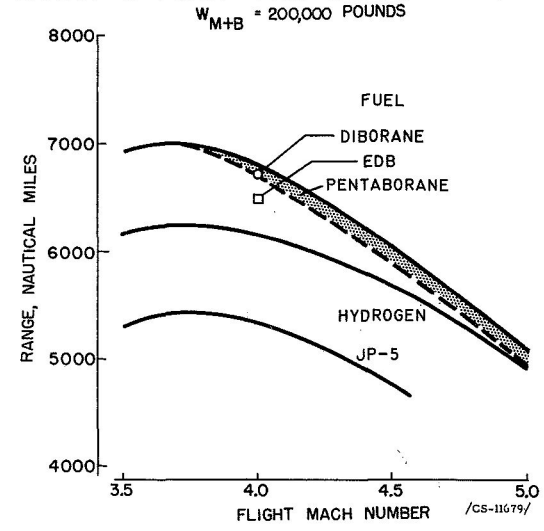

Figure 28

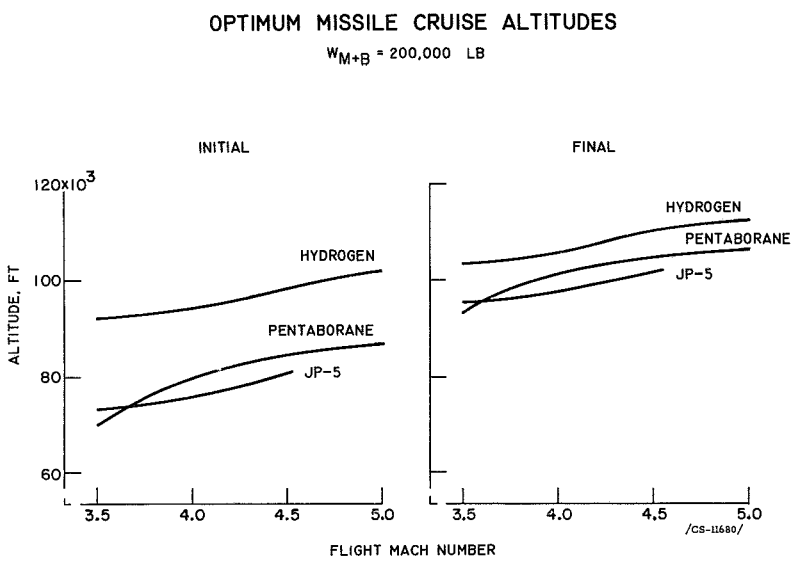

Figure 29

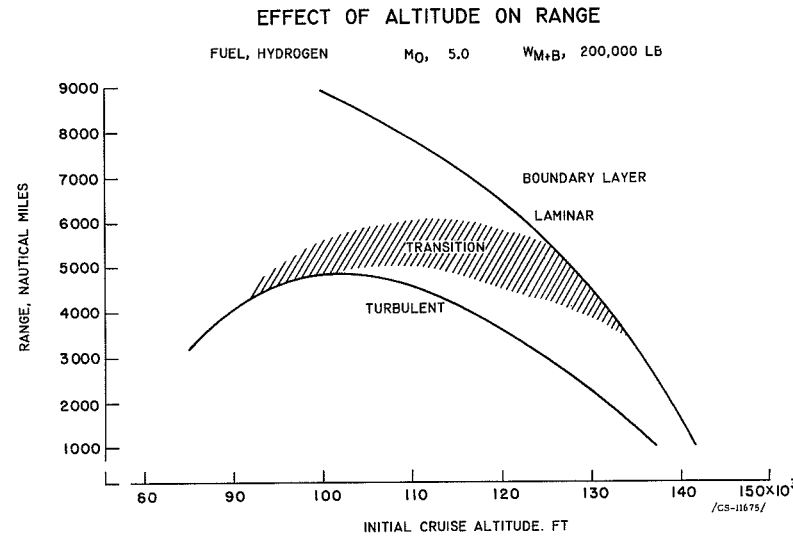

Figure 30

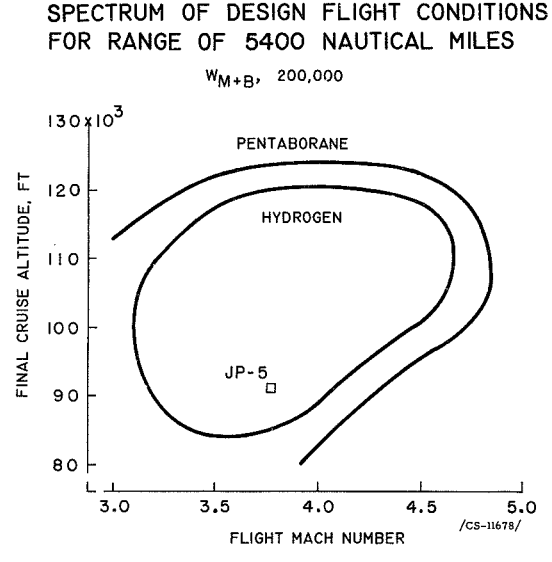

Figure 31